JIMMA UNIVERSITY

SCHOOL OF GRADUATE STUDIES

JIMMA INSTITUTE OF TECHNOLOGY

FACULTY OF CIVIL AND ENVIROMENTAL ENGINEERING

STRUCTURAL ENGINEERING STREAM

Evaluation of Shear Capacity Prediction of Concrete Beam without Transverse Reinforcement

A Thesis Submitted to School of Graduate Studies of Jimma University in Partial Fulfillment of the Requirements for the Degree of Masters of Science in Structural Engineering

By

ADDISU LATA CHEMEDA

AUGUST, 2020

JIMMA, ETHIOPIA

JIMMA UNIVERSITY

SCHOOL OF GRADUATE STUDIES

JIMMA INSTITUTE OF TECHNOLOGY

FACULTY OF CIVIL AND ENVIROMENTAL ENGINEERING

STRUCTURAL ENGINEERING STREAM

Evaluation of Shear Capacity Prediction of Concrete Beam without Transverse Reinforcement

A Thesis Submitted to School of Graduate Studies of Jimma University in Partial Fulfillment of the Requirements for the Degree of Masters of Science in Structural Engineering

By

ADDISU LATA CHEMEDA

Main Advisor: Temesgen Wondimu (PhD)

Co advisor: Asanti Keno (MSc)

AUGUST, 2020

JIMMA, ETHIOPIA

DECLARATION OF THESIS

I assure that this thesis is my original work and has not been presented for any Degree in other Universities.

Thesis submitted by

Addisu Lata Chemeda _____ 04/08/20

Signature Date

Approved by advisors

Main advisor:

Temesgen Wondimu (PhD) _____ 06/08/20

Signature Date

Co-advisor:

Asanti Keno (MSc) _____ 21/08/20

Signature Date

JIMMA UNIVERSITY

SCHOOL OF GRADUATE STUDIES

JIMMA INSTITUTE OF TECHNOLOGY

FACULTY OF CIVIL AND ENVIROMENTAL ENGINEERING

STRUCTURAL ENGINEERING STREAM

Evaluation of Shear Capacity Prediction of Concrete Beam without Transverse Reinforcement

A Thesis Submitted to School of Graduate Studies of Jimma University in Partial Fulfillment of the Requirements for the Degree of Masters of Science in Structural Engineering

By

ADDISU LATA CHEMEDA

JIMMA INSTITUTE OF TECHNOLOGY

Temesgen Wondimu (PhD)	_____	_____
(Main Advisor)	Signature	Date
Asanti Keno (MSc)	_____	_____
(Co-advisor)	Signature	Date

Approved by board of Examiners

_____	_____	_____
(External Examiner)	Signature	Date
_____	_____	_____
(Internal Examiner)	Signature	Date
_____	_____	_____
(Chairman)	Signature	Date

ACKNOWLEDGEMENT

My first gratitude goes to Almighty God who is with me starting from my undreamed to come to this earth till this time and be forever in all direction.

Secondly, my special and grateful is to my main advisor Temesgen Wondimu (PhD) and co-advisor Asanti Keno (MSc) who are making me confidential by investing their valuable advice and guidance on me to doing this thesis.

Also, I would like to express my gratitude to my families specially my wife Ibsitu Fite, and my friends for their sharing their idea, concept and even who are in my life in my entire career.

Finally, my special thanks go to Jimma institute of Technology for facilitating this program which helps me for upgrading my profession.

ABSTRACT

Unlike other failure modes like flexural failure, almost no warning occurs for structures at the onset of failing in shear. Therefore, it is important to evaluate the accuracy of the determination the shear capacity of reinforced concrete beams by different design standards. This study evaluates the accuracy of some of the equations proposed by different codes of standard. Moreover, in order to gain an understanding of how different parameters, such as concrete strength, shear span-to-depth ratio and amount of longitudinal reinforcement affects the shear resistance of concrete beams without transverse reinforcement.

For this purpose fifty-six reinforced rectangular concrete beams without transverse reinforcement have been selected from different experimental studies by other researchers taking into account longitudinal reinforcement, compressive strength of concrete and shear span to depth ratio. The experiment result is used to evaluate the accuracy of the prediction of some building codes, i.e., ACI 318-14, 2011,Eurocode 2, 2004, Zsutty, 1971, and Niwa et al. 1987. It is shown that the shear strength predicted by Zsutty,1971 shows good agreement with the test results having a better correlation coefficient of 0.712, and a mean ratio of 1.941 in predicting the shear strength of the selected 56 test beams than EC2,2004, ACI 318 and Niwa et al.1987 with correlation coefficient of 0.569, 0.5035 and 0.661 respectively, which predict the shear strength conservatively.

The parametric study is carried out using the commercially available finite element package ABAQUS 6.14. The parametric study has been restricted to concrete compressive strength (25, 35, 40 and 60), longitudinal steel reinforcement ratio (0.679, 0.905 and 1.13) and shear span to depth ratio (1.5, 2 and 2.6). The result of finite element for analysis indicates that as concrete compressive strength increase, the shear capacity of reinforced beam without transverse reinforcement was increased. Also, by increasing the amount of longitudinal reinforcement to some limit, the shear capacity of RC beam without transverse reinforcement was increased, and in contrast, when the ratio of shear span to effective depth increase, the shear capacity of beam decreased.

TABLE OF CONTENTS

LIST OF TABLES

LIST OF FIGURES

ACRONYMS

AASHTO	American Association of State Highway and Transportation Officials'
ACI	American Concrete Institute
a/d	Shear span length to effective depth ratio
b_w	Width of beam
$C_iR_jS_k$	Concrete grade, Longitudinal reinforcement amount, Shear span to effective depth ratio for studied parameter
d	Effective Width of beam
d_c	Compression damage of concrete
d_t	Tensile damage of concrete
EBCS	Ethiopian Building Code Standard
EC	European code
e_{in}	Inelastic strain
F_c'	Compressive strength of concrete
Fyk	Characteristic yield strength of steel
FEM	Finite Element Method
KN	Kilo Newton
La	Anchorage length
Lc	Clear span Length
L_{eff}	Effective length
Ls or a_v	Shear span length
mm	Millimeter
MPa	Mega Pascal
RC	Reinforced Concrete

V	Shear loading
V_a	Shear resistant contribution by aggregate interlock
V_c	Total Shear resistance by concrete ($V_c=V_{cz}+V_a+V_d$)
V_{cr}	Critical shear loading
V_{cz}	Shear resistant contribution in compression zone
V_d	Shear resistant contribution by dowel action
V_s	Shear resistance by transversal reinforcement
V_u	Ultimate shear loading
ϕ	Diameter of the bar
ρ	Longitudinal reinforcement ratio
ε_t	Tensile strain of steel reinforcement

CHAPTER ONE

INTRODUCTION

1.1 Background of the Study

The shear strength in steel-reinforced concrete members has been the subject of many arguments and debates since the beginning of the 20th century. Shear failure is considered as the most critical structural failures modes for reinforced concrete beam, particularly for the members without shear reinforcement. The structural members failing in shear usually lead to loss of casualties and properties. Because, unlike other failure a mode like flexural failure, almost no warning occurs, signalizing that the structure is at the beginning of failing in shear. Therefore, it is become better to model effectively to identify the shear capacity of reinforced concrete beams under shear loading.

Shear reinforcement is usually used to prevent shear failures in structural elements of concrete. For some structural elements, such as slabs, footings, and joists and retaining walls, shear reinforcement is often omitted. Predicting, modeling and explaining the complex behavior of reinforced concrete members without shear reinforcement has been the objective for a large number of researchers.

Homogeneous materials like the concrete without reinforced steel occurs when the amount of shear stress value that produced from the applied loads exceeded the amount of shear resistance of this material shows failure in shear. The shear stress in the beams were caused by different percentage of any loads applied to the beam produce shearing forces, bending moments and in some cases torques.

In most current design procedures for shear analysis, the shear strength of reinforced concrete beam is taken as the sum of the concrete contribution (Vc) and the transverse reinforcement contribution (Vs). The concrete contribution is considered to be the shear of a beam without transverse reinforcement (Ahmad *et al*. 1986; Hamrat *et a*l. 2010).

Based on experimental results many standard codes and researcher allover world extended their study to estimate the shear resistance of beams. However, they have specified different formulae considering different parameters into consideration. The parameters considered are varying for different practical codes and researchers leading to disagreement between researchers, making it difficult to choose a suitable model or code for predicting shear resistance of reinforced concrete. This is due to doubts in the shear transfer mechanism, especially after cracks are initiated.

The most distinctive parameters considered for the case of shear failure of reinforced concrete beams without web reinforcement are shear span to effective depth ratio (a/d), longitudinal tension steel ratio(ρ), aggregate type, strength of concrete, type of loading, and support conditions (L,2011).

Although, some researcher has evaluated reinforced and post tensioned concrete beams by finite element method to validate the rational prediction of it behavior in shear observed in the experimental test program (Fanning, 2001). However, till yet studies to evaluating and generalizing the predicted shear capacity of reinforced concrete beam without transverse reinforcement are rare. But, one of the most effective numerical methods utilized for analyzing reinforced concrete members is the finite element method (Ammar *et al*. 2010). Using this method, many aspects including the tension - stiffening, non - linear multi - axial material properties, modeling of cracking and crushing, and many other properties related to the behavior of reinforced concrete members under stresses of the phenomenological behavior of reinforced concrete structures can be modeled rationally.

Therefore, this study concentrated on evaluation of few popular prediction like ACI 318-14, 2011, Eurocode 2, 2004, Zsutty, 1971, and Niwa *et al.* 1987 for shear strength of RC beam without transverse reinforcement compiled from different investigated test results. The results of parametric study carried out using finite element package ABAQUS 6.14 to investigate the influence of a/d, reinforcement ratio and compressive strength of concrete on the ultimate shear capacity of reinforced concrete without transverse reinforcement are also studied.

1.2 Statement of the Problem

The most common structural elements in the world are reinforced concrete elements. Therefore, it is the most needed task to determining the effect of load on those structure elements. From those structures concrete beam without transverse reinforcement which is exposed to shear need great attention. Because, unlike other failure a mode like flexural failure, almost no warning occurs, signalizing that the structure is at the beginning of failing in shear. Also, shear capacity of RC beam was affected by several parameters; among the most influencing parameters are concrete strength, shear span to effective depth ratio and longitudinal reinforcement ratio.

Even though, many building codes and researchers used these parameters to predict the shear capacity of RC beam without reinforced concrete beam. However, there is a controversial between them on the consideration of those parameters. Therefore, shear failure in concrete structures are very hazardous since they can rarely be predicted and often happen explosively.

Therefore, this study uses to evaluate some of predicted equation, also in order to gain an understanding of how different parameters such as concrete strength, shear span-to-depth ratio and amount of reinforcement affects the shear resistance of concrete beams without transverse reinforcement.

1.3 Research questions

This study will use to answer the following questions:

1. How were the existing predicted equations for shear capacity of RC beam without transverse reinforcement are appropriate?
2. What is the influence of concrete strength, shear span to effective depth ratio and amount of tension reinforcement on the shear capacity of reinforced concrete beam without transverse reinforcement when analyzed by Finite element method?

1.4 Objectives of the research

1.4.1 General objective

The main objective of this research is to evaluate shear capacity prediction of concrete beam without transverse reinforcement.

1.4.2 Specific Objectives

- To investigate the appropriate of the existing equations to predict the shear capacity of Reinforced concrete beam without transverse reinforcements.
- To investigate the influence of concrete strength, shear span to effective depth ratio and amount of tension reinforcement on the shear capacity of reinforced concrete beam without transverse reinforcement by using finite element software, ABAQUS package.

1.5 Significance of the study

Evaluation of shear capacity of reinforced concrete beam without transverse reinforcement will used to safe casualties and properties loosed by structure failing in shear. Therefore, the main importance of this study is to introduce the structural designer and practical design approach of our country that whether the existing equation of shear capacity of RC beam without transverse reinforcement is applicable. Also, it used to identify the most influencing parameters of shear capacity of RC beam without transverse reinforcement.

1.6 Scope and Limitation of the study

The evaluation has been restricted to rectangular reinforced concrete beam without transverse reinforcement because of the availability of such beams experimentally in literature. The considered equations predicted by researchers and code of practice limited to ACI 318-14, 2011, Eurocode 2, 2004, Zsutty, 1971, and Niwa *et al*. 1987 because they were used as basic for others codes and researchers. The parametric study is carried out using the commercially available finite element package ABAQUS 6.14. The beams were rectangular section which is subjected to four-point loading and the member response in terms of load-deflection and cracking characteristics was monitored. The loading and support steel plates are assumed to remain elastic, with young's modulus 200GPa and Poisson's ratio 0.3. The parametric study has been restricted as; concrete compressive strength (25, 35, 40 and 60MPa), longitudinal steel reinforcement ratio (0.679, 0.905 and 1.13) and shear span to depth ratio (1.5, 2 and 2.6).

CHAPTER 2

LITERATURE REVIEW

2.1 General

To estimate the shear resistance of beams, standard codes and researcher allover world have specified different formulae considering different parameters into consideration. The parameters considered are varying for different codes and researchers leading to disagreement between researchers, making it difficult to choose an appropriate model or code for predicting shear resistance of reinforced concrete. Therefore, an extensive research work on shear behavior of normal and high strength concrete is being carried out all over the world.

This chapter presents a comprehensive review of the existing knowledge of predicting and evaluating shear capacity of reinforced concrete beams without transverse reinforcement.

2.2. Shear transfer Mechanism of RC beam without transverse reinforcement

Reinforced concrete beams are designed to resist shear resulting from the combination of ultimate loads once the primary longitudinal reinforcement has been determined. Shear transfer actions and mechanisms in concrete beams are complex and difficult to clearly identify. Different researchers impose different levels of relative importance to the basic mechanisms of shear transfer. Considering the simple supported beam in Figure 2.1 as load is distributed across the span of the beam, principal compressive stresses take the form of an arch and tensile stresses assume the form of suspended cable.

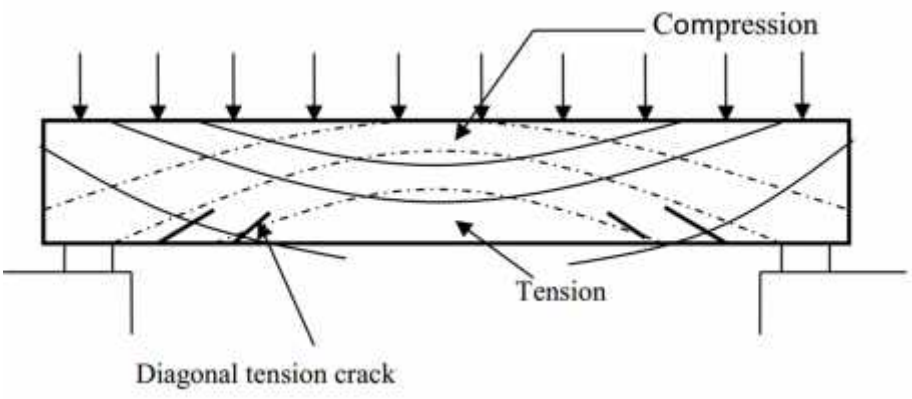

Figure 2.1 Principal stresses in a beam (Mosley et al, 1999)

At the supports the high shearing forces generate greater principal stresses which are inclined at an angle. This causes the tensile stress, which is dominant at the mid -span and almost parallel to the beam axis to develop diagonal cracks. When the diagonal tension exceeds the tensile strength of the concrete then shear reinforcement needs to be provided. It means that reinforced concrete beams which do not have transverse reinforcement possess some shear strength that can resist shear stresses before diagonal tension cracks develop.

(Yalavarthy, 2010) revealed that there are several mechanism by which shear is transmitted and he described the prominent among them as shear in an cracked concrete zone which contributes to shear resistance in a cracked concrete member (i.e. a beam or a slab) and its magnitude of shear resistance is limited by the depth of compression zone, interface shear transfer (aggregate interlock) which is a function of the crack width and aggregate size, dowel action which is a function of the amount of concrete cover beneath the longitudinal bars, and residual tensile stress.

(Yang, 2014) explained that, when flexural cracks have developed in a reinforced concrete member there are certain processes/mechanisms that can transfer shear in the concrete, and this includes shear stresses in the uncracked compressive zone, aggregate interlock along the cracks, dowel action in the bars, residual tensile stresses transmitted directly across cracks and arch action.

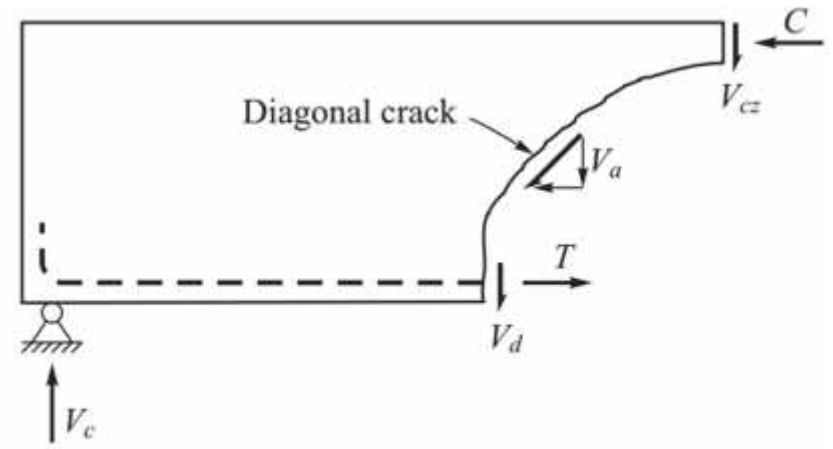

Figure 2.2. Mechanism behind shear failure (Yang, 2014)

(Cavagnis, 2017) stated that the shear – transfer actions are classified into beam shear- transfer actions and arching action and the shear resistance in a reinforced beam is almost always a

combination of these two mechanisms. These mechanism can be represented by strut and tie models (Reineck *et al*. 2017). Beam shear-transfer actions allow varying the force in the flexural reinforcement and carrying shear keeping constant the lever arm between the tension and compression chord. They are usually referred as cantilever action (or inclined compression chord, Figure 2.3a), aggregate interlock (Figure 2.3b), dowelling action (Figure 2.3c) and residual tensile strength of concrete (Figure 2.3d). On the contrary, the arching action (Figure 2.3e) allows carrying shear keeping constant the force in the flexural reinforcement.

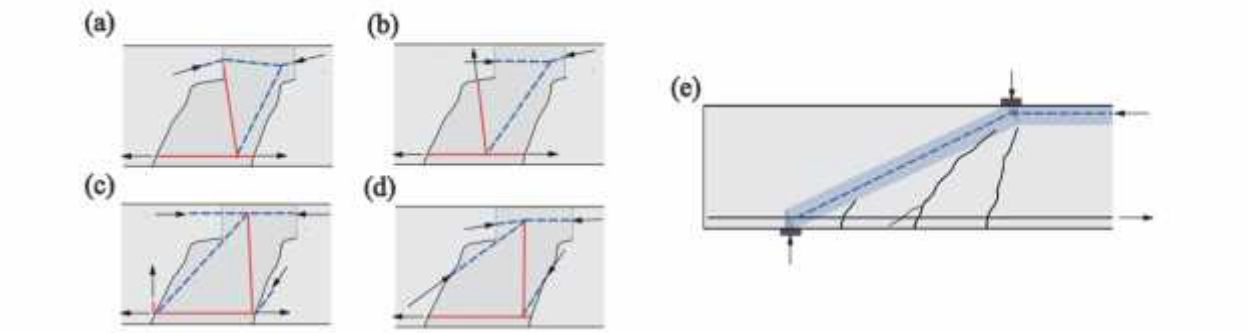

Figure 2.3: Shear-transfer actions (red: tensile forces, blue: compressive forces): a) cantilever action (or inclined compression chord); (b) aggregate interlock; (c) dowelling action; (d) residual tensile strength of concrete; (e) arching action (Cavagnis, 2017)

However, several researchers have decided that the shear capacity of the beam without transverse reinforcement is provided by; concrete in the compression zone, aggregate interlock across crack planes and dowel action of longitudinal reinforcement. But it is difficult to estimate and isolate the individual contributions of each component to shear. Therefore, the section of structural specimens resists the external shear after the flexural cracking and before the diagonal cracking. Load increase causes tensile stress build up in the reinforcement. As the applied shear increases, the dowel action is the first to reach capacity. When shear cracks occur, the concrete in between the cracks isolate and cuts the incremental tensile flow in the longitudinal reinforcement. Compressive stresses due to aggregates interlock intercept the cracks. As the load increases the aggregate interlock effect also decreases to allow transfer of large shear force to the concrete compressive zone. This results in a sudden, abrupt shear failure. The beams may fail depending on the type of beam and the shear span to effective depth ratio (Yalavarthy, 2010).

Many research works have shown that failure mode of RC beams without stirrups depend on shear span to effective depth ratio. Ahmed and Lue, 1987 observed that decrease in a/d increases shear capacity of reinforced concrete beams without web reinforcement. Fergusen,1956 explained that when the a/d is decreased, a direct load transfer to the supports causes local loading effect which increases the resistances to shear.

Taylor, 1974 reported that for RC beams without web reinforcement, shear strength can be derived from the contribution of compression shear zone, aggregate interlock ranging from 35% to 50% and the dowel action of longitudinal steel reinforcement ranging between 15%-25%. This shows how frictional forces that develop across the shear crack are a major component of shear capacity.

Increase in the amount of tension reinforcement is known to influence the shear strength of beams. Commenting on the ACI-318, Ahmed *et al.(*1986*)* concluded that the code provide conservative results for high strength concrete beams having low percentage of longitudinal steel reinforcement. Tempos and Frosch(2002) reported that to allow concrete resist shear, higher reinforcement ratio will reduce crack width to enhance 'aggregate interlock' and 'dowel action'. It was confirmed that reduction in tensile steel ratio in beams results in higher steel stresses and low strength. Many researchers have proposed models to calculate the shear crack load of reinforced concrete without web reinforcement at shear cracking levels. From Figure 2.4, the un-cracked section of concrete compressive zone provides resistance, V_{cz}, the force due to aggregates interlock, V_{ay}, and the force carried by the longitudinal bars crossed by the diagonal crack, V_d combines into the total shear resistance of the reinforced concrete without shear links. The total shear force V_c can then be expressed as:

$$V_c = V_{cz} + V_{ay} + V_d \qquad (2.14)$$

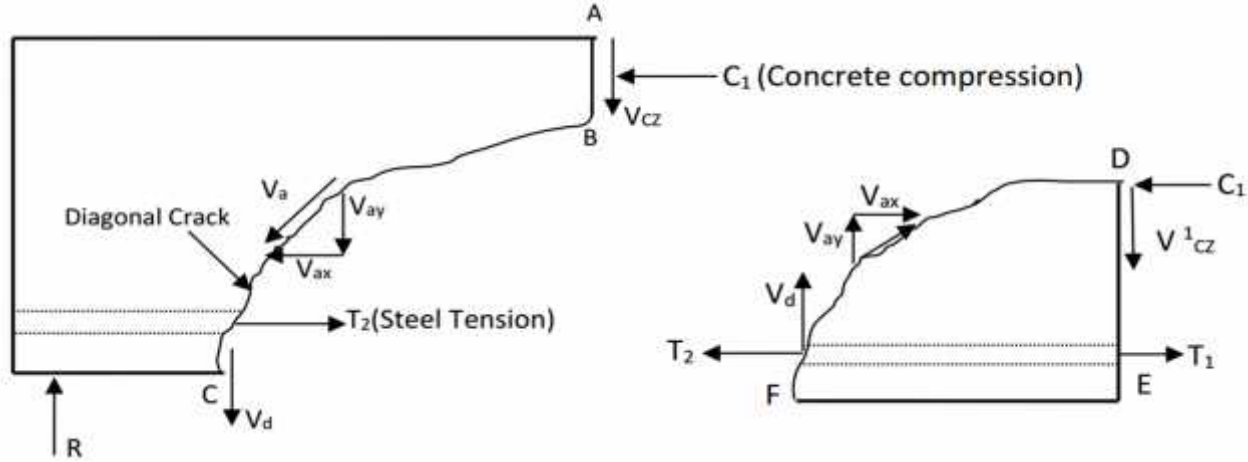

Figure 2.4 Internal forces in a cracked beam without stirrups (Ahmed *et al.(*1986*)*)

2.3 Shear failure of RC beam without transverse reinforcement (Modes of failure)

The shear failure process of reinforced concrete members without shear reinforcement is strongly related to the formation of a flexural shear crack in the shear span. Depending on whether or not the structure fails upon the formation of such a crack, two different failure modes can be distinguished, being flexural shear failure and shear compression failure. By definition, the second failure mode displays a higher shear capacity (Yang, Walraven, and Uijl, 2016).

As (Yang, Walraven and Uijl, 2017) discussed reinforced concrete beams without shear reinforcement when subjected to shear loading typically fail in two different manners; flexural shear crack which is usually denoted as a diagonal crack to indicate the overall direction of the crack, and shear compression failure which is often caused by crushing of the concrete in the compressive zone. By definition, when shear compression failure develops, the bearing capacity of the member is higher than that in case of the flexural shear failure mode.

In his study (Yang, 2014)explained, for the moment forces lead to the concrete cracking, usually on the tensile edge, where the cracks can be further propagated through shear stresses flexural shear type of failure is one of the more common shear failures, as cracking in the tensile edge is very common in concrete members.

In his study (Raju, 2014) explained when the principal tensile stress at any point reaches the tensile strength of concrete, a crack will occur and open normal to the direction of the principal tensile stress or parallel with the direction of the principal compressive stress.

Therefore, concrete members subjected to shear forces at ultimate load always have inclined cracks named diagonal cracks or shear cracks. Inclined cracks can be initiated in the web of beams where is proved to be the highest shear stress region and named web shear cracks. Inclined cracks developed from former flexural cracks are called flexure−shear cracks.

(Yalavarthy, 2010) identified that the presence of shear stress reduces the strength of concrete in compression as well as in tension. Shear failures are initiated by inclined cracks, and these cracks are typically divided into two types, i.e., web shear cracks and flexure shear cracks. In reinforced concrete beams of usual proportions, subjected to relatively high flexural stresses f_x and low shear τ, the maximum principal stress is invariably given by the flexural stress f_{xmax} in the outer fiber (bottom face of the beam) at the peak moment locations, the resulting cracks are termed flexural cracks. The maximum principal stress is generally located at the neutral axis level at an inclination of $\alpha=45^0$ and the resulting cracks are termed as web shear cracks of diagonal tension cracks.

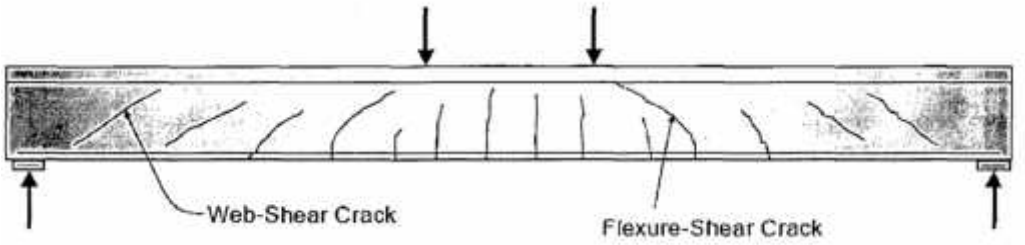

Figure 2.5 Different types of cracks in RC beam (Yalavarthy, 2010)

He concluded that the shear failures of members without transverse reinforcement are classified based on a/d ratios, and hence the failure modes of simply supported rectangular beams without transverse reinforcement were classified as:

a) In very slender beams (a/d>6), the members will likely fail in flexure even before the formation of inclined cracks.
b) In slender beams (2.5<a/d<6), some of the flexural cracks grow and may become flexure shear cracks. The diagonal cracks may continue to propagate towards the top and bottom of the beam and cause yield of the tension steel. The beam may split into two pieces at failure. This is called as diagonal tension failure.

c) In short beams (1<a/d<2.5), a diagonal crack may propagate along the tension steel causing splitting between the concrete and the longitudinal bars as shown in fig 2.6. This is called a shear tension failure. The diagonal crack may propagate toward the top of the beam resulting in crushing of the compression zone as shown in Fig 2.7. This is called a shear-compression failure.

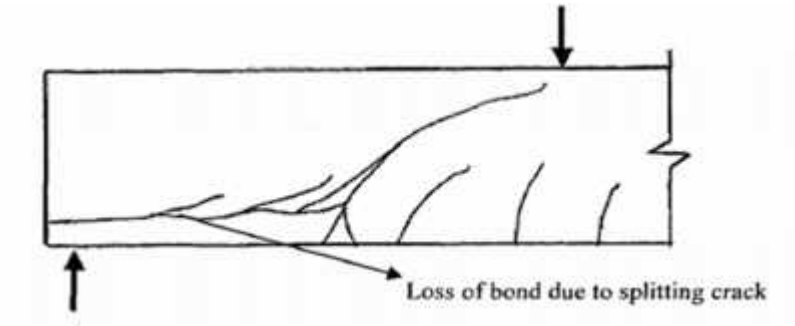

Figure 2.6 Shear tension failure in short beams (Yalavarthy, 2010)

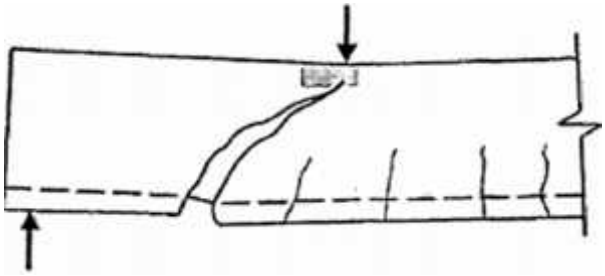

Figure 2.7 Shear compression failure in short beams (Yalavarthy, 2010)

2.4 Significant Parameters for Members without Transverse Reinforcement

a. Concrete Strength: As concrete strength increases, the shear strength also increases. Some researchers believe that concrete compressive strength has a large influence on the shear resistance while others believe that concrete tensile strength has a greater influence than compressive strength on shear strength. The concrete contribution to shear, in ACI 318-02, for example, is regarded as being that due to diagonal cracking shear, and therefore dependent on the tensile strength of the concrete. The concrete compressive strength f_c' is generally used to estimate the tensile strength because direct tension tests are difficult to conduct, require interpretation of the results, and usually show more scatter than compression test results. In most major design codes, the shear strength of a member is taken as directly proportional to $f_c^{0.2}$, $f_c^{0.3}$, $f_c^{0.5}$Those power values indicate that the concrete tensile strength is being used as the governing parameter.

b. Shear Span to Depth Ratio: The shear span is the distance, a, between a support and a point of concentrated load. As the shear span to depth ratio (a/d) decreases, the shear strength increases. Many empirical formulas for calculating shear strength include a/d ratio to account for the influence of this parameter. The increase in strength is significant in members with a/d ratios less than about 2.5 to 3.0, because a significant portion of the shear may be transmitted directly to the support by an inclined strut. This mechanism is frequently referred to as arch action and the magnitude of the direct load transfer increases with decreasing a/d-ratios. For deep members and the ends of beams, it is therefore more appropriate to use strut-and-tie models than sectional design approaches. The key characteristic of the a/d-ratio is obvious for simple beams subject to point loads. The term relates the maximum moment and the maximum shear force, since $M_{max}= V_{max}\times a$ and thus the moment to shear force ratio is $M_{max}/V_{max}d = a/d$. For distributed loading this term is also significant, as has already been pointed out by Kani (1964, 1967), and it gives $M_{max}/V_{max}d = l / 4d$, which means that "a" is the distance to the resultant of the loads in one half of the span. Therefore, the a/d-ratio characterizes the slenderness of a simple beam and the value influences the relationships between the different shear transfer actions. The value, a, also relates the flexural and shear capacities, i.e. the shear force at flexural failure can be calculated by dividing by "a" or the moment at mid-span corresponding to shear failure can be calculated by multiplying by "a".

c. Longitudinal Reinforcement Ratio: For the same magnitude of loading, as the longitudinal reinforcement ratio decreases, flexural stresses and strains increase. Thus, crack widths increase and the shear strength is lowered. Further, as the longitudinal reinforcement ratio decreases, dowel action decreases. It has also been reported that for members having longitudinal bars distributed over their height crack spacing are smaller and that improves shear strength significantly (Collins and Kuchma, 1999).

2.5 Building Codes and Other proposed Shear design provisions

2.5.1 European Codes EC2, 2004

In the current European Code, an empirical formula is given for calculation of the contribution from the concrete in resisting shear. The empirical formula for concrete contribution takes into account the longitudinal reinforcement ratio, the compressive stress capacity of the concrete and the presence of axial force.

2.5.2 (ACI 318-14)

The current ACI design procedure for shear defines the nominal shear strength as the sum of the shear strength provided by shear reinforcement, V_s, and the shear strength provided by concrete, V_c, which is assumed to be the same for beams with and without shear reinforcement and is taken as the shear causing significant inclined cracking. The value of Vc is defined for members subject to shear and flexure only and for members subject to axial compression separately. According to ACI 318-14 two alternatives are presented for calculation of V_c.

The first alternative has a simple formula. Unlike its European counterpart, the ACI provision for calculation of the concrete contribution doesn't contain the longitudinal reinforcement ratio as a factor. It only depends on the compressive strength of the concrete and the size of the member. The second alternative contains a more detailed calculation. In this case, many factors including ρ_w and $V_u d/M_u$ are shown to affect the concrete contribution.

2.5.3. Zsuty (1971)

The shear strength of concrete beam section without web reinforcement (V_c) can be calculated by Zsutty (1971). If the shear span to depth ratio, a/d, is greater than 2.5:

$V_c = 2.21(fc'\rho\frac{d}{a})^{1/3}$ bd

If the shear span to depth ratio, a/d, is smaller than 2.5:

$V_c = [2.21(fc'\rho\frac{d}{a})^{1/3}](2.5\frac{d}{a})$ bd

Where, V_c is the shear strength provided by concrete, ρ is ratio of longitudinal reinforcement equals $\frac{A}{b}$, As is the area of longitudinal reinforcement, b is the width of the web, d is the distance from the extreme compression fiber to the center of gravity of the steel, fc′ is the concrete compressive strength, a is the shear span and d/a is shear span to depth ratio.

2.5.4. Niwa *et al* (1987)

An important model on the diagonal strength of RC beams has been proposed by Niwa *et al.* (1987) as below;

$$V_c = 1.125\frac{\rho^{\frac{1}{3}}}{d^{\frac{1}{4}}}(f_c')^{\frac{1}{3}}(0.75+\frac{1.4}{\frac{a}{d}}), M$$

Where d= depth of beam, mm, ρ= percentage of beam longitudinal reinforcement, and f_c'= compressive strength of concrete, MPa.

2.6 FINITE ELEMENT METHOD

Now a day, in every scientific and engineering field computer has completely revolutionized research and practice and it becomes simple and favorable to every user. Consequently, analysis and design methods that provide computerized solutions to scientific and engineering problems have been developing rapidly for increasingly routine use (Hsu and Mo, 2018). Therefore, finite element method was the one which is significantly developed method.

A large number of constitutive models have been developed to date targeting at realistically predicting the nonlinear response of concrete structural forms under various types of loading, ranging from static and seismic to more extreme loading conditions such as those encountered in blast and high velocity impact problems. The inclusion of such models into various finite element analysis (FEA) schemes has led to the development of powerful tools (FEA packages) or the numerical investigation of reinforced concrete (RC) structures (Cotsovos, Zeris, Abbas, 2009).

The concept of the finite element method was originally introduced for structural analysis by Turner, Argyris and Kelsey in the mid-50. The name finite element was originally coined in a paper by Clough in 1960, in which the technique was presented for plane stress analysis. Since then general progress has been so rapid that the method is now one of the most powerful tools available in structural analysis. It has also been recognized as a general numerical method for approximately solving various systems of partial differential equations with known boundary conditions. Thus, its application covers a wider range of physical problems other than structural. For instance, problem arising in such fields as fluid mechanics, electro-dynamics, temperature fields, and from one dimensional problem to three dimensional problems can be solved (Akthem, 1983).

A FEA package is usually considered to be capable of yielding realistic predictions of the response of a concrete structural form when the deviation of the predicted from the experimentally measured values of particular structural characteristics does not exceed a value of the order of 20% of the corresponding measured quantity. Such structural characteristics usually include the load-carrying capacity, the relation between applied load and corresponding

displacements, reactions or first order deformation derivatives (e.g. rotations); furthermore, qualitative behavior pattern matches are also considered, such as the crack patterns at various load stages and the mode of structural failure. Moreover, a FEA package is considered to be characterized by objectivity and generality when it is capable of providing realistic predictions of structural behavior for any type of structural concrete configuration, without the need of recalibrating the constitutive model adopted or its parameters (Cotsovos, Zeris, Abbas, 2009).

Today, many popular finite element analysis packages used for reinforced concrete structures are available. Some of the popular packages include NASTRAN, LISA, ABACUS, ANSYS STAAD/PRO and ADINA. For this study Model by ABAQUS was used for analysis of parametric study.

ABAQUS

ABAQUS was first founded by Dr.David Hbbitt, Dr.Bengt Karlsson, and Dr. Paul Sorensen with original name of Hibbitt, Karlsson and Sorensen, Inc,. (HKS) in 1978. Later on, its name was changed to ABAQUS Inc in 2005 before achievement of Dassault Systèmes. ABAQUS is the influential finite element software that is capable to model 1D,2D and 3D elements with its broad selection of materials and elements. The system of this software consists of five core software products; Abaqus/Standard: a general-purpose finite element program, Abaqus/Explicit: an explicit dynamics finite element program, Abaqus/CFD: a general-purpose computational fluid dynamics program, Abaqus/CAE: an interactive environment used to create finite element models, submit Abaqus analyses, monitor and diagnose jobs, and evaluate results, and Abaqus/Viewer: a subset of Abaqus/CAE that contains only the postprocessing capabilities of the Visualization module(ABAQUS 6.14 Manual).

2.7 Concrete constitutive Model

The concrete resistance to tensile stresses is low. Concrete structures presenting a non-linear behavior for there is a reduction on the concrete structures stiffness and modify the internal stress distribution during they are subjected to even low levels of load. There are three crack models for reinforced concrete elements that ABAQUS software can modeling and simulating the damage. These are Smeared crack concrete model, Brittle crack concrete model, and Concrete damaged plasticity model.

For this study, the concrete damaged plasticity model which has the potential to represent complete inelastic behavior of concrete both in tension and compression including damage characteristics is considered for analysis. Even though, concrete damaged plasticity model can be used both in ABAQUS/Standard and ABAQUS/Explicit and thus enable the transfer of results between the two. The concrete damaged plasticity model assumes that the two main failure mechanisms in concrete are the tensile cracking and the compressive crushing. In this model, the uniaxial tensile and compressive behavior is characterized by damaged plasticity.

2.7.1 Concrete Damaged Plasticity Model

Considering damaged plasticity model in the cracking models for concrete beam uses the concepts of isotropic tensile and compressive plasticity to represent the inelastic behavior of concrete. These models reflected by the assumption of tensile cracking and compressive crushing of concrete composites failure mechanisms.

Uniaxial tensile and compressive stress- strain relationships under applied loads are characterized by hardening variables correspond to the extent of damage in concrete, and stiffness degradation parameter. The hardening variables are then used in cooperation with the yield surface to identify the failure mechanisms under tensile and compressive loading. In concrete modeling, a non - associated plastic flow potential is implemented using the Drunker Pager hyperbolic function to represent flow potential.

2.7.2 Concrete Compression Model

The compressive stress- strain response of the concrete under uniaxial compression is illustrated in Figure 2.8. It is observed that concrete behaves linearly within the elastic region until the initial yield, σ_{co}. After reaching the initial yield point, concrete starts behaving in a plastic fashion and exhibits some work- hardening up to the ultimate stress, σ_{cu}, followed by strain - softening.

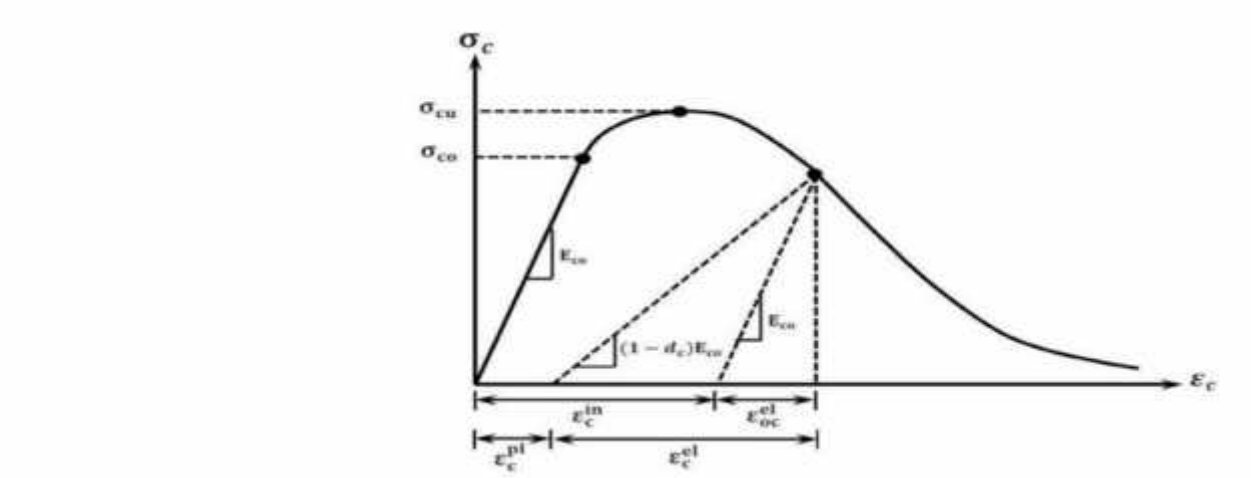

Figure 2.8 Compressive stress-strain response of concrete ABAQUS Manual (DSS, 2014)

The elastic compression behavior of concrete can be modeled by calculating the initial undamaged modulus of elasticity, E_{co}. For the inelastic response, compressive stresses are provided in a tabular form as a function of the inelastic strain, ε_c^{in} which can be calculated by the following equation:

$$\varepsilon_c^{in} = \varepsilon_c - \varepsilon_0^{el} = \varepsilon_c - \frac{\sigma}{E}$$

Where ε_c^{in} the inelastic strain, ε_c is the total compressive strain, ε_0^{el} is the elastic compressive strain corresponding to the undamaged material, σ_c is the compressive stress, and E_{co} is the initial undamaged modulus of elasticity. The inelastic strain data are inputted in the material definition section of ABAQUs model as positive values, starting at zero value corresponding to the initial yield point.

2.7.3 Concrete Tension Model

The tensile stress- strain response of a concrete member under uniaxial tensile loading is illustrated in Figure 2.9. It is concluded that the stress - strain response is linear elastic until the peak stress σ_{ot}. The onset of micro- cracks occurs when the tensile stress reaches the peak point, which leads to strain localization. The latter impacts the crack growth and may result in the unloading of regions beyond strain localization which in turn induces strain - softening post-peak response.

In a typical reinforced concrete beam, the concrete (a quasi - brittle material) is bonded to the reinforcement. When cracking initiates in the member, concrete continues to resist some tensile stresses between the cracks. This characteristic is referred to as "tension stiffening", and it helps improve the control of the deformation of an RC member and the growth of crack widths.

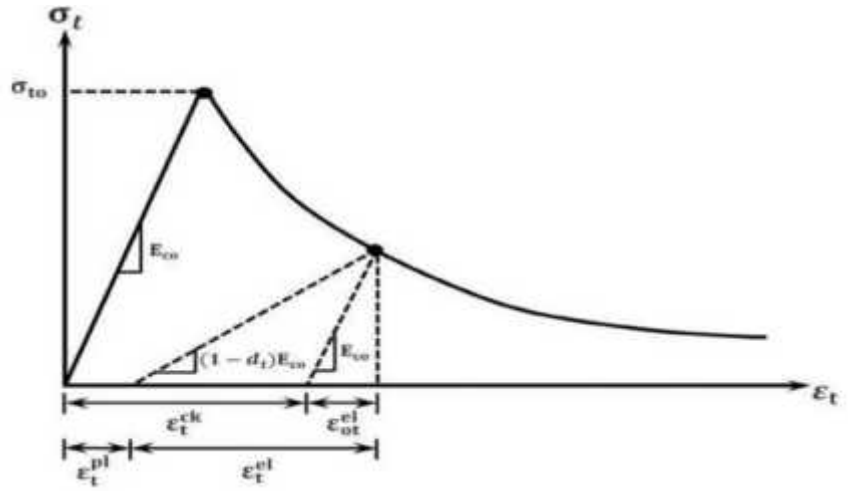

Figure 2.9 Tensile stress-strain response of concrete ABAQUS Manual (DSS, 2014)

In order to account for the interaction between the concrete and reinforcing bars in ABAQUS, the user is required to define the post- peak tensile response of concrete. The Concrete Damaged Plasticity Model in ABAQUS provides three different methods that can be used to characterize the post- peak response of concrete in tension:

- ✓ The tensile stress can be entered in a tabular form as a function of the crack opening displacement, w.
- ✓ The value of concrete fracture energy, Gf, can be simply inputted into the model.
- ✓ The tensile stress in concrete can be entered in a tabular form as a function of the corresponding cracking strain, ε_t^c

In the first method, the post- peak tensile behavior of concrete is defined in a way that the user has to input the tensile stress as a function of the crack - opening - displacement, w. Hillerborg *et al*.(1976) has proposed the concept of using fracture energy, Gf , in this method. This fracture energy of a brittle material corresponds to the energy required to open a crack of unit area. Therefore, the post- peak behavior of concrete in idealized by a stress-displacement response rather than a stress- strain response as in the first method. The user has

the liberty to modify the tension stiffening response of the concrete member by selecting one of the proposed examples of stress- displacement curves as shown in Figure 2.10.

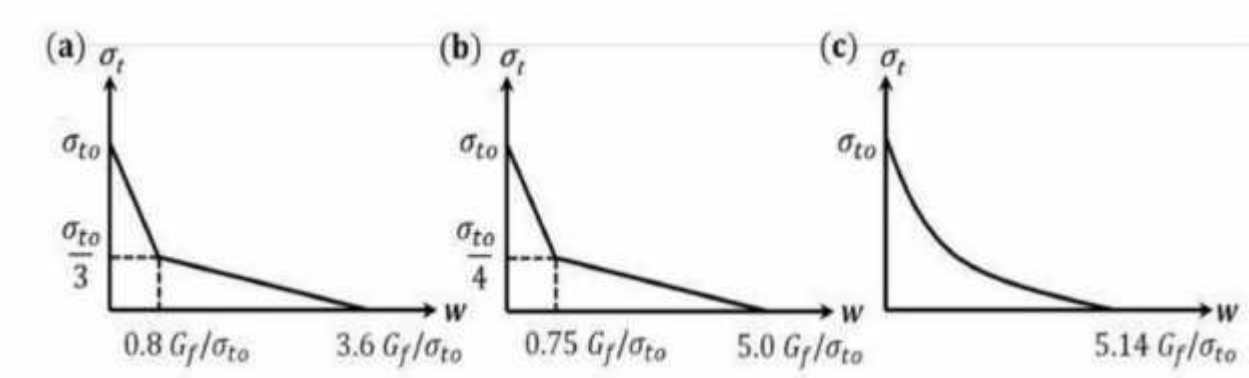

Figure 2.10 Various examples of stress-displacement curves (Stoner, 2015)

It is worth mentioning that the area under these curves represents the fracture energy of the material. Therefore, this method has the advantage of allowing the user to define the rate of strength loss after cracking and also the material's fracture energy (Stoner, 2015).

The second method allows the user to simply define the tensile peak stress, σ_{to}, and the value of the fracture energy, G . As it can be seen in Figure 2.11, this method assumes a linear stress-displacement post- failure response.

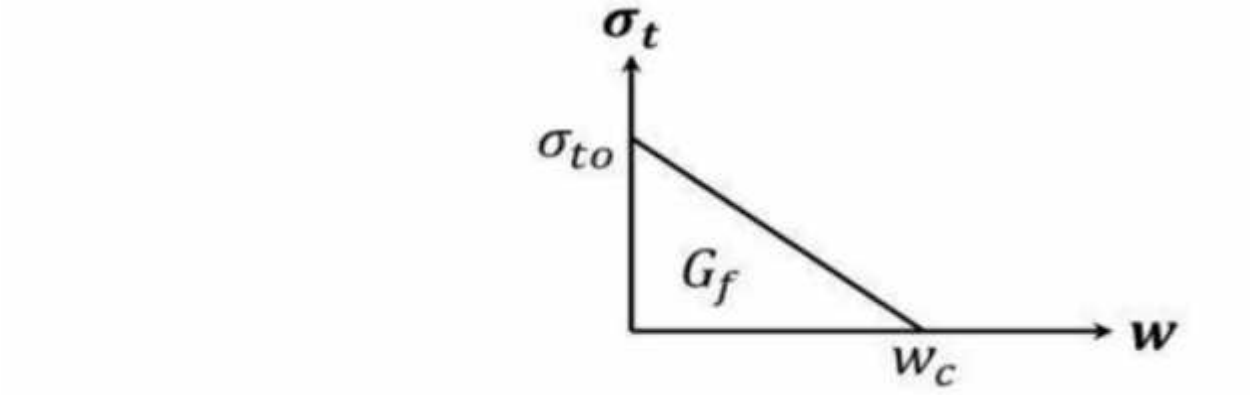

Figure 2.11 Linear stress-displacement curve (Stoner, 2015)

The user is expected to identify the value of the peak stress and the area under the linear curve (i.e. the calculated fracture energy). Then after, the maximum crack displacement corresponding to a complete loss of strength, w_c, is computed by the equation:

$W_c = \frac{2G}{\sigma t_0}$

In the third method, the user can plot a stress- strain curve similar to that illustrated in Figure 3.3. The post- peak response can be determined in a procedure similar to the one described in the concrete compression model. The cracking "inelastic" strain, ε_t^c , can be calculated using the following expression:

$$\varepsilon_t^c = \varepsilon_t - \varepsilon_0^e = \varepsilon_t - \frac{\sigma t}{E}$$

Where ε_t^c is the cracking strain, ε_t is the total tensile strain, ε_0^e is the elastic tensile strain corresponding to the undamaged material, σ_t is the tensile stress, and E_{co} is the initial undamaged modulus of elasticity. Similarly, the cracking strain data are entered in the concrete damaged plasticity model of ABAQUS model in a positively increasing manner. The first value is set as zero corresponding to the initial yield stress.

2.7.4 Damage Modeling

Sometimes, unloading of the concrete member can occur within the post-peak region of the compression and tension stress-strain curves. In such cases, the unloading response becomes weaker and degraded, and modulus of elasticity is utilized to account for this degradation as expressed in figure 2.8 and figure 2.9. This degradation during the unloading phases is identified by two damage variables, d_c and d_t for member subject to compression and tension, respectively. The damage parameters are functions of the plastic strains ε_c^p and ε_t^p , temperature θ, and other predefined file variables f_i, as can be seen in the next equations.

It is noted that the values of the damage parameters range from zero (corresponding to the undamaged material) to one (for the material with complete loss of strength).

$d_c = d_c (\varepsilon_c^p , \theta, f_i) 0 \leq d_c \leq 1.0$

$d_t = d_t (\varepsilon_t^p , \theta, f_i) 0 \leq d_t \leq 1.0$

As it has been mentioned previously, the damage parameters are functions of plastic strains, and hence, ABAQUS will automatically generate the plastic strains from the user-defined inelastic or

cracking strain. The plastic strain in compression is obtained by converting the inelastic strain ε_c^{in} , and damage parameters, d_c as expressed below:

$$\varepsilon_c^p = \varepsilon_c^{in} - \frac{d_c}{1-d_c}\frac{\sigma_c}{E_c}$$

Where E_{co} is the initial undamaged modulus of elasticity. However, the calculations of plastic strain in tension depends on the method used to define the tensile post-peak response of concrete. If the first method was used, damage parameters are provided as function of the cracking strains, ε_t^c , which are converted to plastic strain as shown below;

$$\varepsilon_t^p = \varepsilon_t^c - \frac{d_t}{1-d_t}\frac{\sigma_t}{E_c}$$

However, if method two or three was used to define the tensile post-peak curve of the concrete member, damage parameter values are considered as functions of the crack- opening displacement, u_t^c (also referred to as w). the plastic displacements are then obtained by the equation:

$$u_t^p = u_t^c - \frac{d_t}{1-d_t}\frac{\sigma_t l_0}{E_c}$$

And the term l_o corresponds to the specimen length which is assumed to be equal to 1.0. Furthermore, the value of the damage parameter ought to be conctrolled within the range of 0-0.99 to avoid severe damage, and thus possible convergence issues (Stoner, 2015). When the initial undamaged modulus of elasticity E_{co} is identified, the stress- strain response of the concrete under tension and compression will consideration of the degradation of the elastic stiffness can be represented by:

$\sigma_c = (1 - d_c)\, E_c \quad (\varepsilon_c - \varepsilon_c^p$

$\sigma_t = (1 - d_t)\, E_c \quad (\varepsilon_t - \varepsilon_t^p$

It should, however, be mentioned that a concrete structure subjected to uniaxial load will exhibit crack initiation and propagation. Therefore, a reduction in the expected load carrying area is expected which in turn increases the concrete effective stresses. ABAQUS accounts for that

phenomenon by calculating these effective compressive and tensile stresses, $\overline{\sigma_c}$ and $\overline{\sigma_t}$, respectively. These terms expressed in the following equation:

$$\overline{\sigma_c} = \frac{\sigma_c}{1 - d_c} E_{c0} \ (\varepsilon_c - \varepsilon_c^p)$$

$$\overline{\sigma_t} = \frac{\sigma_t}{1 - d_t} E_{c0} \ (\varepsilon_t - \varepsilon_t^p)$$

CHAPTER THREE

RESEARCH METHODOLOGY

3.1 Research Design

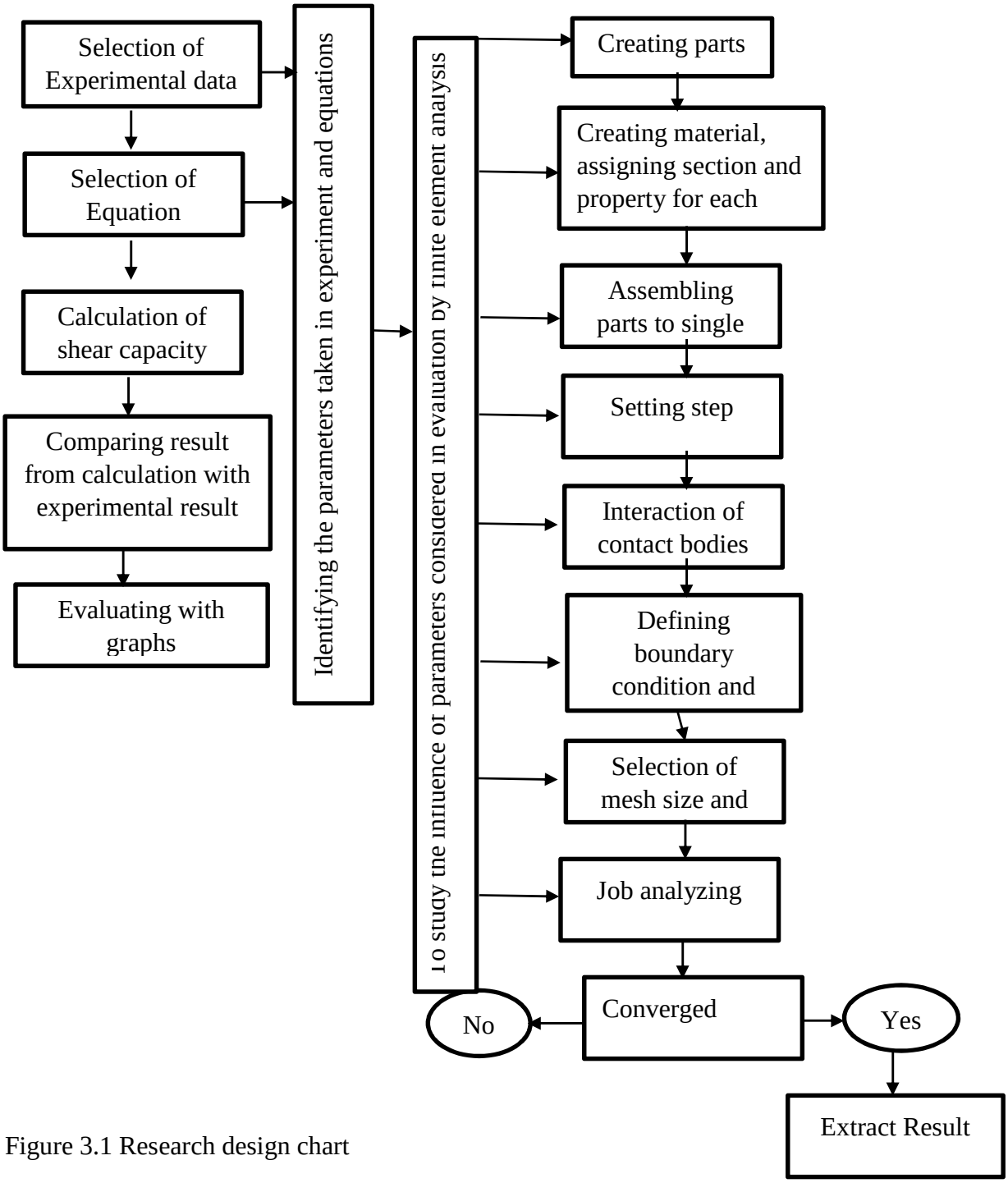

Figure 3.1 Research design chart

3.2 Statistical evaluation of RC beam without transverse reinforcement

3.2.1 Shear Capacity influencing parameters

Failing of a beam without transverse reinforcement in shear was arise because of the number of parameters influencing the beam strength including amount of steel, concrete strength, shape of cross-section, shear span to depth ratio, dimensions of the cross-section, type of loading, and type of beam. Therefore, for present study the following parameters were considered for they are the most influencing parameters of shear capacity shear span to depth ratio (a/d), amount of steel reinforcement (ρ) and concrete strength (f_{ck}).

3.2.2 Selected Experimental Model

Fifty-six beams are used for evaluation of shear capacity of RC beam without transverse reinforcement which is taken from different investigated experimental result. The experimental investigations are carried out by different investigators (Adom-asamoah, 2016, Althin, 2018), Arezoumandi *et al*. (2014), Birgisson, 2011, Hamrat, 2012, Thamrin *et al.*(2011), Thamrin *et al.* (2016), Hu and Wu, 2018) by consideration of influencing parameters like amount of longitudinal reinforcement, compressive strength of concrete and shear span to depth ratio (a_v/d). The experiment result was taken to evaluate the prediction of some building code and existing researchers' investigation as ACI 318-14, 2011,Eurocode 2, 2004, Zsutty, 1971, and Niwa *et al*. 1987 by using Regression Analysis method. The detail of the experimental beam is given below.

Table 3.1 Selected experimental models

Researchers	**Name of Beam**	**b(m)**	**d(m)**	**a/d**	**Steel ratio%**	**Fc'(Mpa)**	**Experimental shear load**
Adom-asamoah, 2016	PS1	140	280	2.45	1	23.5	73.78
	PS2	140	280	2.45	2	23.5	84.6
	PS3	140	235	2.45	1	23.5	72.716
	PS4	140	235	2.45	2	23.5	87.927
	PS5	110	195	2.48	1	23	55.935
	PS6	110	195	2.48	2	23	55.935
	PS7	110	154	2.46	1	23	45.945
	PS8	110	154	2.46	2	23	52.826
	PS9	90	120	2.35	1	23	33.345
	PS10	90	120	2.35	2	23	47.655
	GS1	140	280	2.45	1	27.1	80.29
	GS2	140	280	2.45	2	27.1	93.31

	GS3	140	235	2.45	1	27.1	72.716
	GS4	140	235	2.45	2	27.1	107.59
	GS5	110	195	2.48	1	26.4	58.163
	GS6	110	195	2.48	2	26.4	58.163
	GS7	110	154	2.46	1	26.4	52.826
	GS8	110	154	2.46	2	26.4	62.137
	GS9	90	120	2.35	1	26.4	49.95
	GS10	90	120	2.35	2	26.4	57.105
Althin, 2018	A1	160	166	2.5	1.51	38	63.7
	B1	160	216	2.5	1.16	38	64.6
	C1	160	266	2.44	0.94	38	56.7
	D1	100	125	2.52	1.26	38	27
Hu and Wu, 2018	N1.9	180	300	1.9	3.27	36.8	220.7
	N2.5	180	300	2.5	3.27	43	161.3
	N3.1	180	300	3.1	3.27	44.6	96.5
Birgisson, 2011	BS-105	200	81	4.81	1.55	31.43	25.9
	BS-131	200	106	3.68	1.48	31.43	35.1
	BS-164	200	139	2.81	1.41	31.43	47
	BS-189	200	163	2.39	1.39	31.43	48.5
	BS-236	200	210	1.86	1.35	31.43	64.6
	BS-335	200	307	1.14	1.31	31.43	168.6
Arezoumandi et al. (2014)	NS-4	300	400	3	1.27	37.3	121.2
	NS-4	300	400	3	1.27	34.2	129.9
	NS-6	300	400	3	2.03	37.3	143.2
	NS6	300	400	3	2.03	34.2	167
	NS-8	300	400	3	2.71	37.3	173.5
	NS-8	300	400	3	2.71	34.2	170.8
Hamrat, 2012	A44-1.5N	100	135	1.5	1.2	44	129.4
	B44-1.5N	100	133	1.5	2.4	44	143.6
	A44-2N	100	135	2	1.2	44	85.1
	B44-2N	100	133	2	2.4	44	100.5
	A44-3N	100	135	3	1.2	44	47.3
	B44-3N	100	133	2	2.4	44	55
(Thamrin *et al*.(2016)	R-01E	125	219	3.7	1	32	32.6
	R-02E	125	219	3.7	1.5	32	37
	R-03E	125	212	3.8	2.5	32	37.6
Thamrin *et al*.(2011)	BSL-02	130	200	2.3	0.60	13	42.5
	BSL-03	130	200	2.3	0.91	13	44.9
	BSN-05	130	200	2.3	0.60	33.5	48.9
	BSN-06	130	200	2.3	0.91	33.5	53.9
	BSL-08	130	200	3	0.60	13	27.4
	BSL-09	130	200	3	0.91	13	29.2
	BSN-11	130	200	3	0.60	33.5	35.7
	BSN-12	130	200	3	0.91	33.5	43.9

3.2.3 Building code and existing equations

Many design Code/Standard provisions for shear strength evaluation are applied around the world. The main component of some of these Codes/Standards for shear strength evaluation is based on empirical formulas. Some of code and present equations for this study include ACI 318-14, 2011,Eurocode 2, 2004, Zsutty, 1971, and Niwa *et al*. 1987.

1. Eurocode 2(2004)

The design value for the shear resistance $V_{Rd,c}$ is given by:

$V_c = [0.12k(100\rho fc)^{1/3}]bd$

Where $\rho = As/bd \leq 0.02$ and $k = 1 + \frac{(2\quad)^{1/2}}{(d)\hat{}1/2}$

2. American Concrete Institute, ACI 318-14 (2011)

ACI code presents the following basic equations for normal-weight Reinforced concrete beam without transverse reinforcement;

$V_c = (1.9\sqrt{(f\ '}) + 2500\rho\frac{V}{M} * d)b \quad < 3.5(\sqrt{f\ '})b$

Simplified version: $V_c = 2\sqrt{(f\ '}bd$

3. Zsuty (1971)

The shear strength of concrete beam section without web reinforcement (V_c) can be calculated by Zsutty (1971). If the shear span to depth ratio, a/d, is greater than 2.5:

$V_c = 2.21(fc'\rho\frac{d}{a})^{1/3}\ bd$

If the shear span to depth ratio, a/d, is smaller than 2.5:

$V_c = [2.21(fc'\rho\frac{d}{a})^{1/3}](2.5\frac{d}{a})\ bd$

Where, V_c is the shear strength provided by concrete, ρ is ratio of longitudinal reinforcement equals $\frac{A}{b}$, As is the area of longitudinal reinforcement, b is the width of the web, d is the distance from the extreme compression fiber to the center of gravity of the steel, fc′ is the concrete compressive strength, a is the shear span and d/a is shear span to depth ratio.

4. Niwa *et al* (1987)

An important model on the diagonal strength of RC beams has been proposed by Niwa *et al.* (1987) as below;

$$V_c = 1.125 \frac{\rho^{\frac{1}{3}}}{d^{\frac{1}{4}}} (f_c')^{\frac{1}{3}} (0.75 + \frac{1.4}{\frac{a}{d}}), M$$

Where d= depth of beam, mm, ρ= percentage of beam longitudinal reinforcement, and f_c'= compressive strength of concrete, MPa.

3.3 Finite element model for RC beam without transverse reinforcement

Finite element method is a powerful numerical tool mostly used to simulate the nonlinear problems of elasticity and solids structures. Therefore, this part describes the development of a finite element model that can simulate the RC beam without transverse reinforcement to investigate its shear capacity under two-point loading. A 3D nonlinear FEM was developed to investigate the shear capacity behavior of reinforced concrete beam without transverse reinforcement using the commercial package ABAQUS 6.14 software which can used to solve linear and nonlinear problems. The results generated from the models were compared with the previous experimental results for verification through the shear force–midspan deflection, ultimate load, and cracking patterns in RC beams. Experimental model of (Thamrin *et al*.,2016) is adopted as a reference test specimen for finite element modeling with the help of general-purpose nonlinear finite element program ABAQUS 6.14, then the results from this analytical model were compared with the results of the same experimental specimen.

3.4 Properties of Materials

3.4.1 Concrete

A. Compressive behavior of concrete damage plasticity

A typical set of compressive strength of concrete curve are obtained at normal, moderate testing speed on concrete of 28 days old. The performance of materials of structure under load be represented by stress-strain diagram. The development of the yield criterion in FE analysis was defined by uniaxial compression behavior of concrete models, hence, the stress-strain curves of concrete and definition of material parameters becomes imperative task. The formula suggested

by Eurocode 2, has been implemented mathematical model from concrete stress-strain curve of figure 3.2 below.

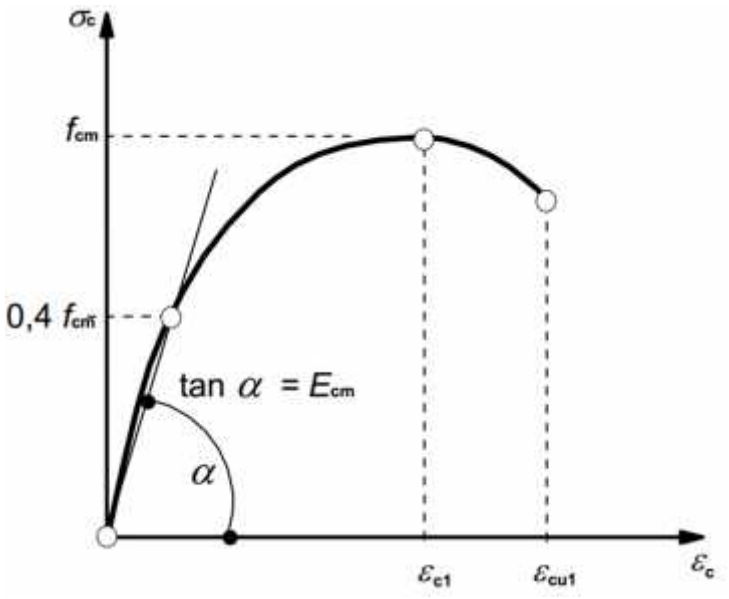

Figure 3.2: Schematic representation of the stress-strain relation for structural (Eurocode 2, 2004) analysis

The relation between σ_c and ε_c from figure above was used to express the concrete compression damage plasticity (CDP) under uniaxial loading as;

$$\frac{\sigma c}{fc} = \frac{k\eta - \eta^2}{1 + (k-2)\eta}$$

Where $\eta = \frac{\varepsilon c}{\varepsilon C}$

$\varepsilon_{c1} = 0.7(f_{cm})^{0.31}$ <28: (strain at peak stress); (Eurocode 2, 2004 table 3.1)

$\varepsilon_{cu} = 0.0035$ (ultimate strain or Maximum compressive strain)

$k= 1.05E_{cm} (\frac{\varepsilon C}{fc})$

$f_{cm}= f_{ck}+8(MPa)$ (Eurocode 2, 2004 table 3.1)

$Ecm = 22[\frac{fc}{1}]^{0.3}$ (Eurocode 2, 2004 table 3.1)

The uniaxial behavior of concrete in compression in damaged plasticity model in ABAQUS must be determined as the stress-inelastic strain for compressive behavior. The compressive response of concrete can be characterized by concrete damaged plasticity as σ_c-ε_c as shown in figure 3.3 below.

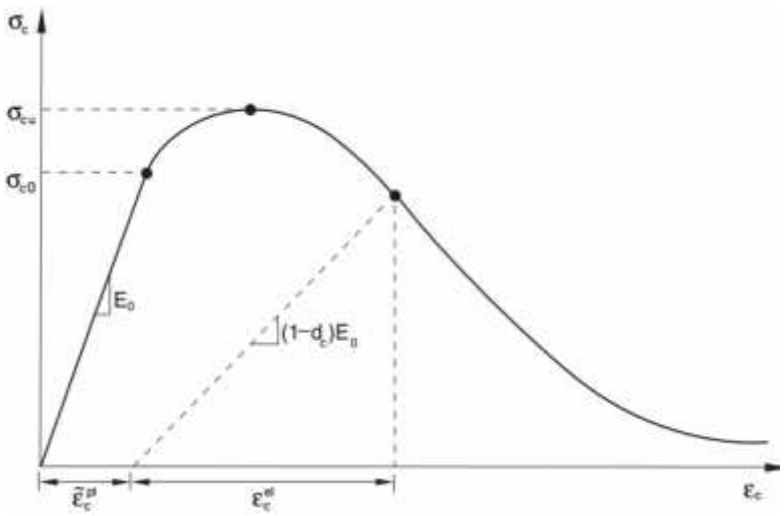

Figure 3.3: Response of concrete to uniaxial loading in compression (ABAQUS user manual, 2008)

From above figure, the compressive inelastic strain is defined as the difference of total strain and the elastic strain corresponding to the undamaged material as;

$$\tilde{\varepsilon}_c^{in} = \varepsilon_c - \varepsilon_0^{el}$$

Where $\varepsilon_0^{el} = \frac{\sigma_c}{E_0}$

Also, ABAQUS user's manual presented the way to converts the inelastic strain values to plastic strain values using relationship of compressive damage curve and compressive inelastic strain as;

$$\tilde{\varepsilon}_c^{pl} = \tilde{\varepsilon}_c^{in} - \frac{d_c}{1-d_c}\frac{\sigma_c}{E_0}$$

B. Tensile Behavior of Concrete Damage

The behavior of concrete in tension without cracks is assumed linear elastic and can be defined only by initial elastic modulus and peak tensile stress. To obtain a formula based on the compressive strength of concrete, Eurocode 2, 2004 states the following two equations;

$f_{ctm} = 0.3(fck)^{2/3}$

To model the tensile behavior of concrete in ABAQUS as damaged plasticity model, the post failure stress-strain relationship for concrete in and the damage parameter values were required. Also, the concrete uniaxial behavior in tension must be defined as the stress-cracking strain to account the phenomenon called tension stiffening. The tensile response of concrete can be characterized by concrete damage plasticity as shown in figure 3.4.

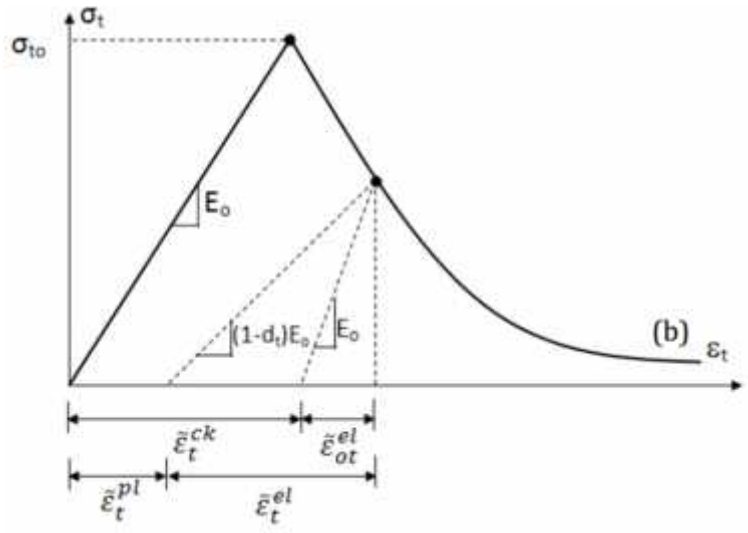

Figure 3.4: Behavior of concrete under uniaxial tensile strength (Abaqus User Manual, 2008)

Cracking strain $\tilde{\varepsilon}_t^{ck}$ in tension behavior of concrete is defined as the difference between the total strain and the elastic strain for the undamaged material for concrete damage plasticity model numerical analysis as:

$$\varepsilon_t^{\sim c} = \varepsilon_t - \varepsilon_0^e$$

Where $\varepsilon_0^e = \frac{\sigma_t}{E_0}$

Also, ABAQUS user's manual presented the way to converts the inelastic strain values to plastic strain values using relationship of tensile damage curve and cracking strain as;

$$\tilde{\varepsilon}_t^{p} = \tilde{\varepsilon}_t^{c} - \frac{d_t}{1 - d_t}\frac{\sigma_t}{E_o}$$

Even if some design standards discounted the tensile strength of concrete beyond the cracking, but concrete is capable of carrying some tensile stresses between cracks when there is sufficient bond between the concrete and the internal reinforcement. Therefore, Wang and Hsu, 2001 proposed the equation of tensile strength of concrete from $\sigma_t - \varepsilon_t$ as;

$\sigma_t = E_c\, \varepsilon_t$ if $\varepsilon_t \leq \varepsilon_c$

$\sigma_t = f_{ct}\ (\varepsilon_c / \varepsilon_t)0.4$ if $\varepsilon_t \geq \varepsilon_c$

3.4.2 Other Concrete damaged plasticity parameter for material definition of concrete

In Abaqus the following mandatory parameters for a full definition of CDP model should be inputted, and ABAQUS default for each parameter is also used in Table 3.2:

- Dilation angle ψ in the p-q plane,
- The ratio f_{b0}/f_{c0} of biaxial compressive yield stress to uniaxial compressive yield stress,
- Flow potential eccentricity(γ),
  - The ratio K of the second stress invariant on the tensile meridian to that on the compressive meridian for the yield function,
  - The viscosity parameter (relaxation time),

Table 3.2 Parameters used in modeling of concrete damage

Parameters	Value
Dilation angle (ψ)	36
Eccentricity (γ)	0.1
σ_b / σ_{cc}	1.16
K	0.667
Viscosity parameter	0

3.4.3 Steel reinforcement

Mechanical properties steel and reinforcement bars used in finite element analysis was based on linear elastic response up to yielding (elastic) and a constant stress from the point of yielding to the ultimate strain(plastic). Therefore, it is supposed that steel for modeling with ABAQUS has been assumed to be elasto-plastic material. Hence, the elastic properties like young's modulus and poisons ratio used for steel was accepted, and for plastic properties; yield stress and yield strain should be converted to true stress and true strain. For conversion of yield stress and strain into true stress and true plastic strain, (Phama and Hancockb, 2010) suggested the following equation as;

$\sigma_{ti} = \sigma\ (1 + \varepsilon)$

$\varepsilon_{ti} = ln\ (1 + \varepsilon) - \sigma_{ti} / E$

3.4.4 Geometry and Element types

Eight beams are considered for analysis of shear capacity of RC beam without transverse reinforcement which are varied with amount of longitudinal reinforcement (0.679%, 0.905%, and 1.13%), concrete compressive strength (25MPa, 35MPa, 40MPa and 60MPa) and shear span to depth ratio (1.5, 2, and 2.6). The yield strength of steel (of reinforcement bar and plates) used in all beam is constant and f_y = 420Mpa. The span length of beam for all is 3000mm. The end anchorage length beyond the support (La) is constant with value of 100mm and shear span length (Ls or a_v) of 562.5mm, 750mm and 1050mm. Clear cover of 25mm were used. To control crushing of concrete edge under concentrated load support plate of 300x100x20mm was taken. The dimension and the designation of the models for the study were presented as table 3.3 below.

Table 3.3 Value of parameter of the study

Name of beam	b_w(mm)	d(mm)	Fc'(Mpa)	P	a/d
C1R1S1	300	375	25	0.679	1.5
C1R1S2	300	375	25	0.679	2
C1R1S3	300	375	25	0.679	2.6
C2R1S1	300	375	35	0.679	1.5
C3R1S1	300	375	40	0.679	1.5
C4R1S1	300	375	60	0.679	1.5
C1R2S1	300	375	35	0.905	1.5
C1R3S1	300	375	35	1.13	1.5

Geometric description of sample of RC beam without transverse reinforcement and longitudinal tensile reinforcement profile was shown in figure 3.5 below.

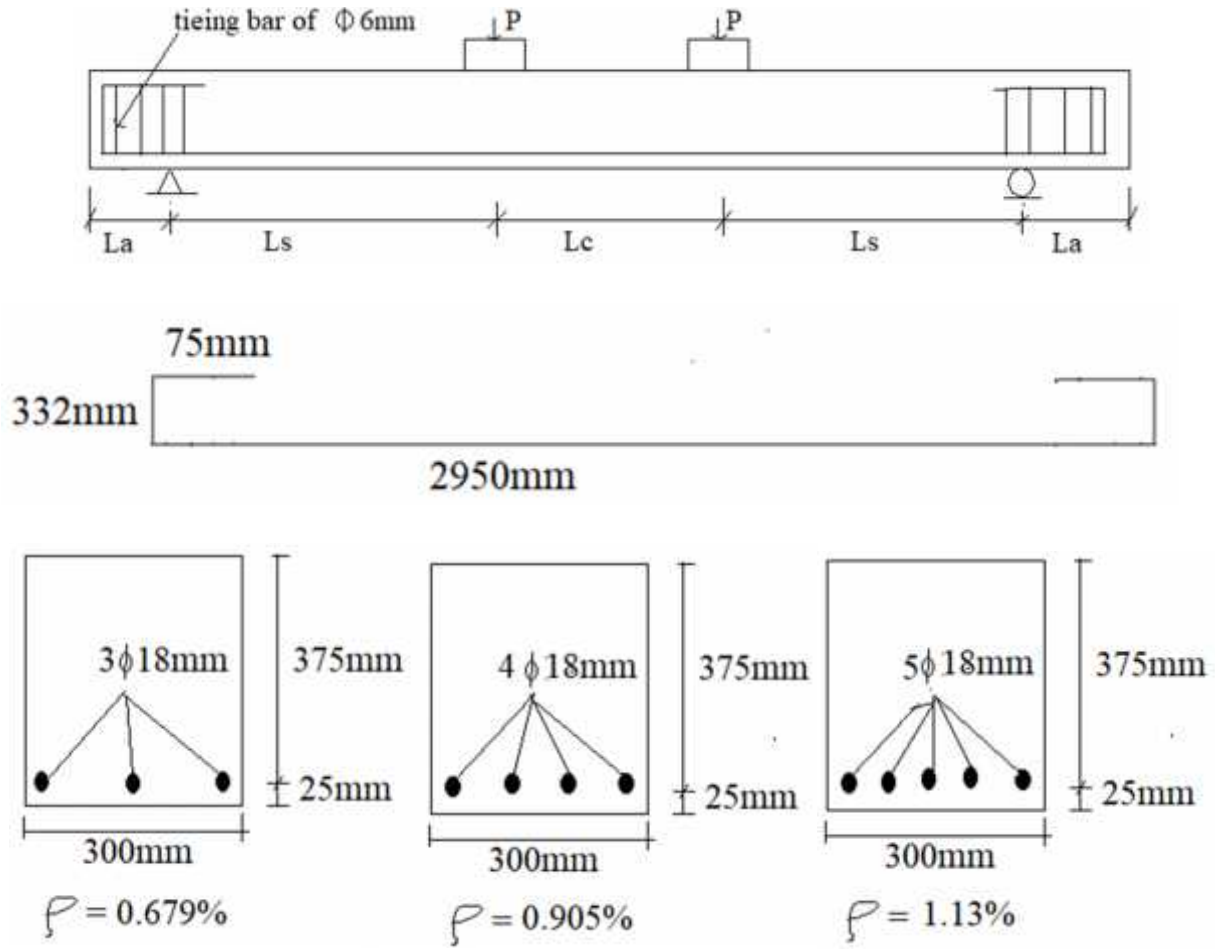

Figure 3.5: Sample of RC beam profile and longitudinal rebar scheme

To analyze the overall sets of element response under loading was proceeded after assembling of those sets of elements under global assembling set. However, to model the reinforced concrete beam without transverse reinforcement selecting the element type is needed task to get appropriate numerical result. So, for bending element using eight-nodded linear 3D brick solid element with reduced integration (C3D8R) type is recommended. Also, the supporting plates (steel plates) which are used to avoid concrete crushing and stress concentration the same element type (C3D8R) were adopted. This element type can be used for both linear and complex non-linear analysis involving contact, plasticity, and large deformations and it provides reliable solution to most applications. As the longitudinal reinforcement carries only axial loads(forces) induced from the lateral loading applied to the RC beams, the longitudinal reinforcement was

modeled by using two-nodded linear 3D truss elements (T3D2). The type of element type was shown in figure 3.6 and 3.7 below

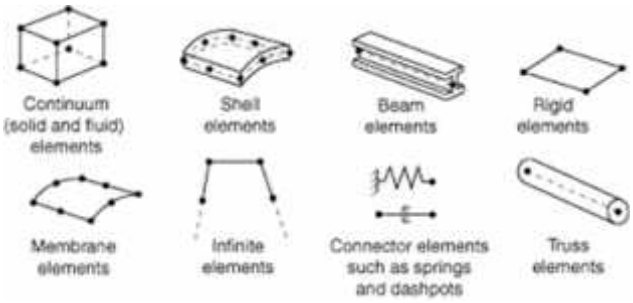

Figure 3.6: Various elements types ABAQUS Manual (DSS, 2014)

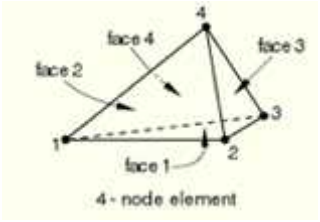

Tetraherdal element(C3D4)

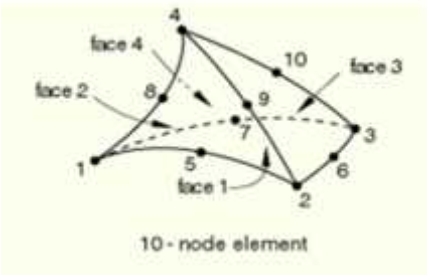

Modified second order element (10-Node tetrahedron C3D10M)

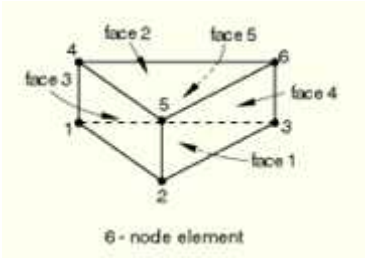

Tetrahedral element(C3D6)

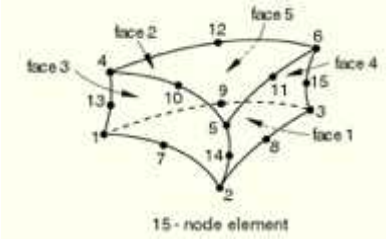

Triangular Prism element (C3D15M)

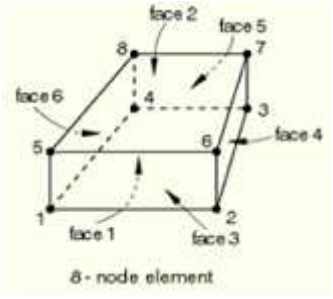

Linear element (8-node brick, C3D8)

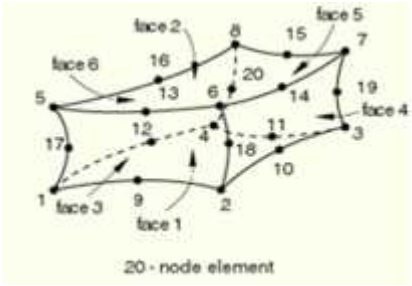

Quadratic element (20-node brick, C3D20)

Figure 3.7: Major 3D types of Element used in ABAQUS Manual (DSS 2014)

3.4.5 Interaction and Meshing of parts of model

To model the beam specimen for study many numbers of constraints were created. A certain number of constraints were created to model the reinforced concrete beam specimens. However, the embedded region constraints were applied for the interaction between embedded steel reinforcement and plain concrete beam to form perfect concrete- steel bond. Also, the interact between support steel plates and RC beam without transverse reinforcement were simulated by tie constraint.

In finite element analysis the first analysis was dividing the model into a number of small elements by using meshing. Therefore, to ensure that two contacting parts share common nodes and obtain good meshing topology all the elements in model were meshed with the same element size. Therefore, for present study, the mesh size of 25mm was used for modeling the concrete and steel plates at supports and loading points (using eight-noded linear brick elements). Also, to ensure that two contacting parts (concrete element and steel reinforcements) share common nodes, a mesh size of 25 mm was used for longitudinal reinforcement (using two -noded linear truss elements). Figure 3.8 below shows the meshing and interaction profiles of the model.

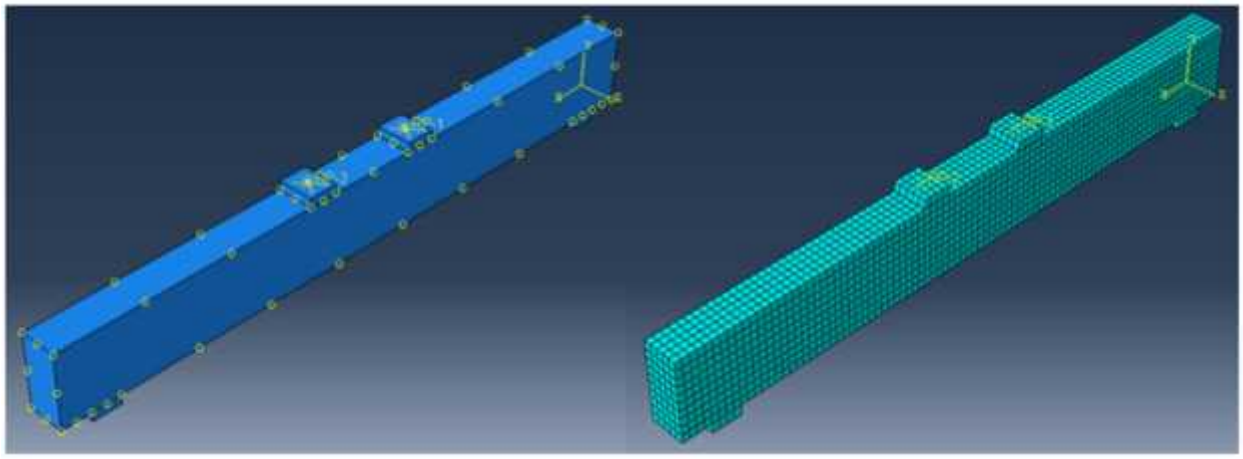

a b

Figure 3.8: a) Interaction of parts b) Meshing of beam model

3.4.6 Loading and Boundary condition

For the purpose of getting a unique solution displacement boundary conditions were applied to constrain the beam in one side considered as roller (ux=uy=0) and other side as pin support (ux=uy=uz=0) as shown in figure below.

The load was applied at two loading points at distance (Ls-100mm where Ls= 750mm, 900mm, 1050mm) from interior support face. To determine the numerical instability difficulties occurred when large amount of load had been applied, the load was applied in small increments. For the nonlinear analysis, automatic time stepping in the Abaqus program predicts and controls load step size. Based on the previous solution history and the physics of the models, if the convergence behavior is smooth, automatic time stepping will increase the load increment up to a selected maximum load step size. If the convergence behavior is abrupt, then the automatic time stepping will bisect the load increment until it is equal to a selected minimum load step size. The maximum and the minimum load step sizes are required for the automatic time stepping. In this particular study the time period, the maximum number of increments, the initial increment, minimum increment size and maximum increment size were set to 1, 10000, 0.001, 1E - 020 and 1 respectively. The boundary conditions and loading of the beam profile is shown in figure.

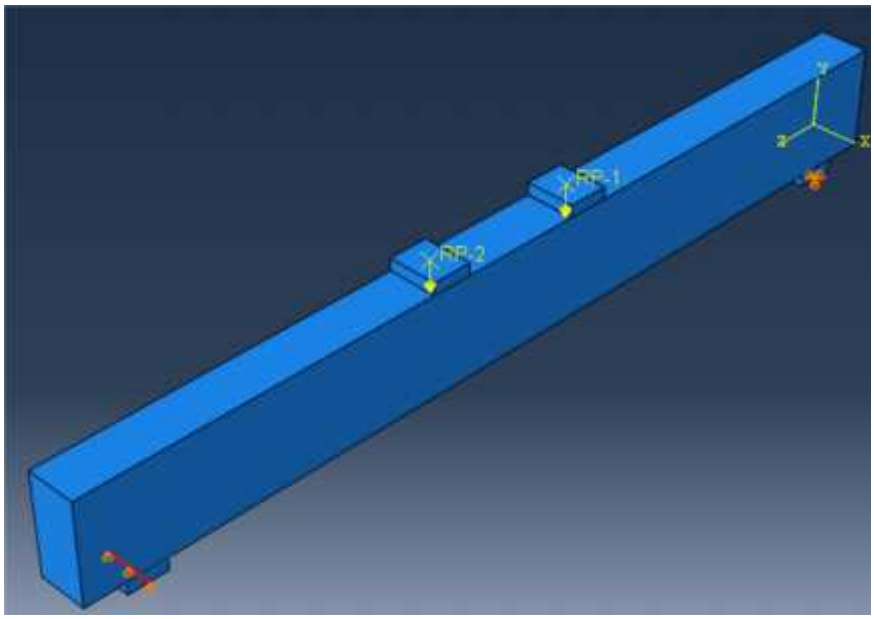

Figure 3.9: Loading and boundary condition

3.4.7 Validation

Verifying that the proposed numerical model result was related with experimental result by extensive comparison is appropriate. Therefore, the analytical result of RC beam without transverse reinforcement under two-point load is compared with experimental result.

General description of the experiment data taken from Thamrin *et al*.(2011)

This part presents the test data of experimental study presented by (Thamrin *et al*.(2011)) on shear strength of reinforced concrete beam without stirrups. The clear span of the beam was 2000 mm, the shear span length (Ls) was 800 mm and the end anchorage length beyond the support (La) was 150 mm. The beam section had dimensions of 125 mm width and 250 mm height. The shear span to effective depth ratio of the beam was 3.7.

Deformed steel bars with 13 mm diameter, 550 MPa yield strength, and 204 GPa modulus of elasticity were used as longitudinal reinforcement. 1.5% amount of longitudinal reinforcement was used as shown in Fig.3.10. The bottom and side concrete covers were 30 mm and 20 mm, respectively. The longitudinal reinforcements were suspended using 6mm diameter of steel wire at the middle position of the beam. The average concrete cylinder strength obtained from compression tests was 32 MPa at age 28 days. Loading position and dimension of the beam are shown in Fig. 3.10.

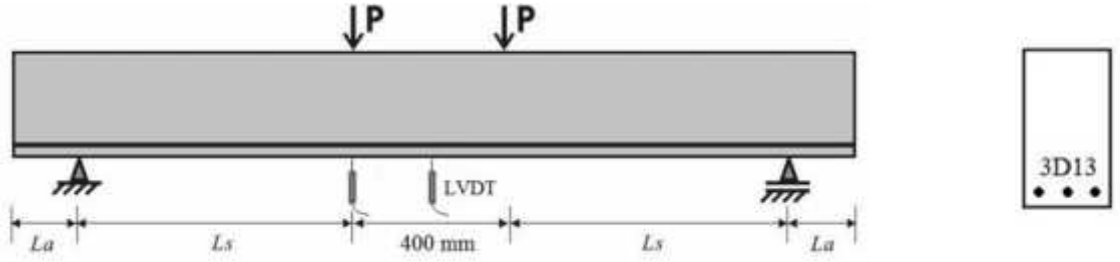

Figure 3.10: Test setup and beam dimensions (Thamrin *et al*.(2011))

a. Properties of Concrete

The modulus elasticity and poison's ratio of concrete was taken as 24000MPa and 0.2 respectively. The constitutive damage plasticity of concrete for validation were presented in table 3.4-3.5 below with its stress- strain curve as shown in figure 3.11-3.12 below.

Compressive Behavior		Compressive damage	
σ_c	ε_{in}	d_c	εin
16	0	0	0
22.43208	8.77E-05	1.42E-05	8.46E-07
27.90699	0.000174	0.00052	3.06E-05
32.39829	0.000289	0.001512	8.77E-05
35.87857	0.000435	0.003061	0.000174
38.31935	0.000611	0.005249	0.000289
39.69111	0.00082	0.008179	0.000435
40	0.000997	0.011978	0.000611
39.96318	0.001062	0.016791	0.00082
39.10372	0.001338	0.021125	0.000997
37.07963	0.001648	0.022777	0.001062
33.85653	0.001995	0.030108	0.001338
29.39865	0.002379	0.038959	0.001648
23.93454	0.002782	0.049507	0.001995
		0.061919	0.002379
		0.075706	0.002782

Table 3.4 Concrete compressive damage

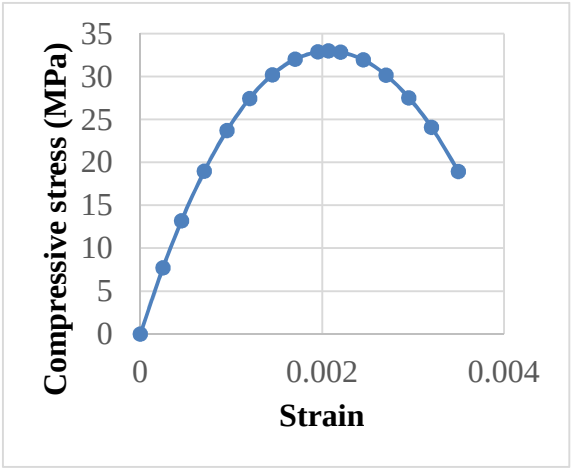

Figure 3.11: Compressive Stress Vs elastic strain curve of concrete

Compressive Behavior		Compressive damage	
σ_t	ε_{cr}	d_t	ε_{cr}
3.039938	0	0	0
2.277873	0.000433	0.005841	1.09E-05
1.725145	0.001249	0.225144	0.000433
1.33444	0.002461	0.55687	0.001249
1.062733	0.004069	0.822403	0.002461
0.874637	0.006074	0.950062	0.004069
0.74293	0.008478	0.989986	0.006074
0.737441	0.010898		
0.647745	0.011281		
0.575249	0.014483		
0.516264	0.018085		
0.465019	0.022086		
0.418128	0.026488		
0.373797	0.031289		
0.331237	0.03649		
0.290244	0.042091		
0.250924	0.048092		
0.213508	0.054494		
0.178241	0.061295		
0.145326	0.068496		

Table 3.5 Concrete tensile damage

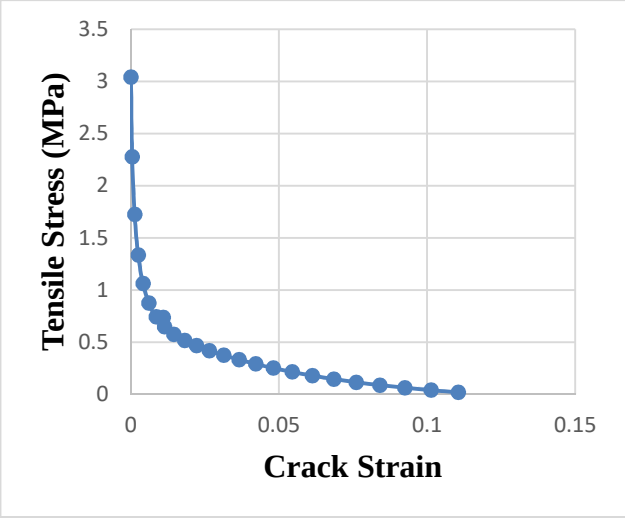

Figure 3.12 Tensile Stress Vs Crack strain curve of concrete

b. Properties of Reinforcement steel

Steel reinforcement of 13mm and 6mm diameters with yielding strength of 550MPa and density of 7850KN/m3 were used in the experimental model. The Young's modulus (modulus of elasticity) and Poison's ratio of the reinforcement bar was 204GPa and 0.3 respectively. The summary of plastic properties of steel reinforcement used in ABAQUS was tabulated in table 3.6 below.

Φ13mm		Φ6mm	
F_y	ε_t	F_y	εt
550	0	550	0
579.45	0.003246	571.07	0.0332
617.30	0.008	610.9	0.0382
667.35	0.133	661.87	0.167

Table 3.6 Plastic properties of steel reinforcement

3.4.8 Comparison of the Results

The results obtained from finite element were compared with experimental result obtained from laboratory test. Therefore, the finite element model was progressed by consideration of parameters from laboratory test and properties of materials. To compare the agreement between finite element analysis by ABAQUS software and experimental result the load deflection curve of both results has been presented in figure 3.13. Hence, the result shows that there is respectable agreement between experimental and finite element result. The difference of result of experiment and FEM is $(\frac{Fi \quad -E}{Fi} = \frac{4 \quad -3}{4} \; x100 = 7.5\%)$ that is acceptable.

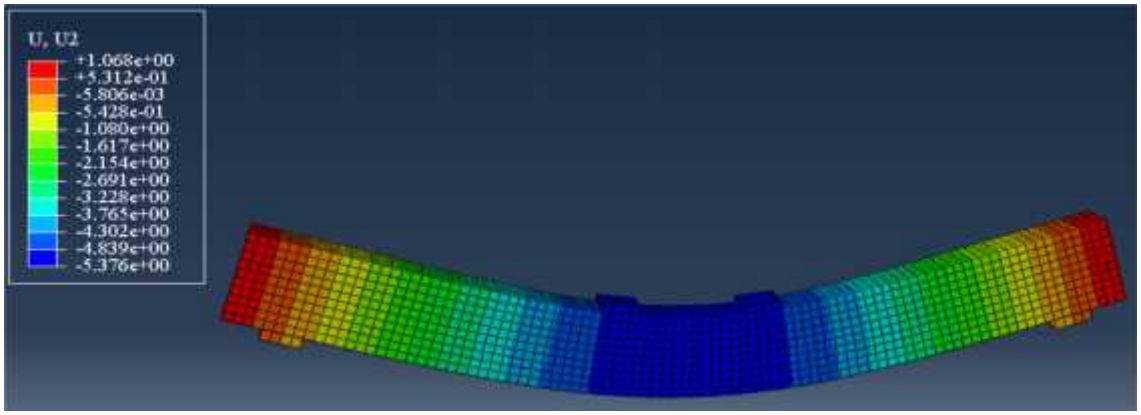

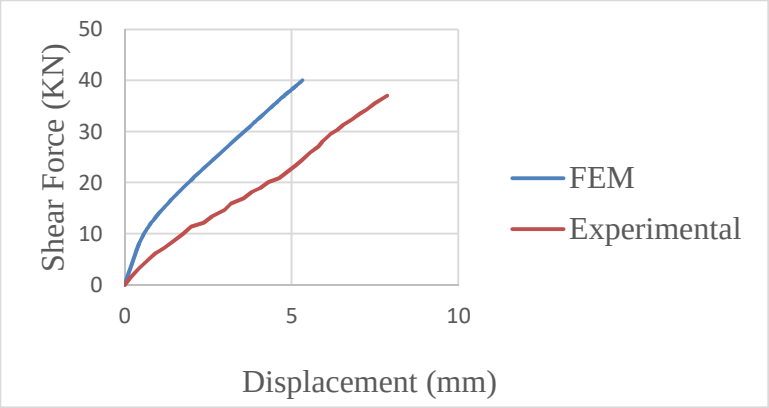

Figure 3.13 Deformed shape of deflection and force vs displacement

Crack Pattern Comparison

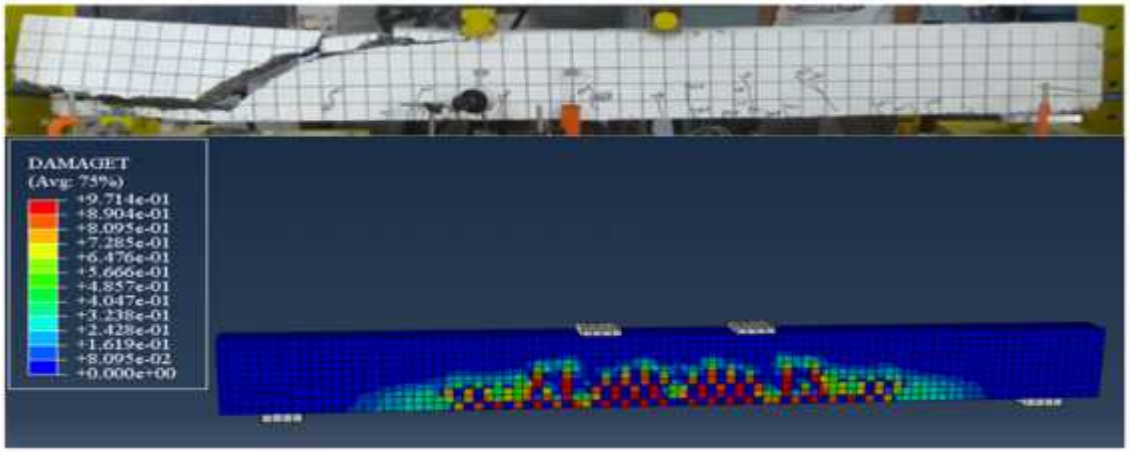

Figure 3.14 Crack pattern of experimental model FEM model

CHAPTER 4

RESULT AND DISCUSSION

4.1 The result of evaluation of building codes and existed equations

The shear strength of all beam specimens total 56 beams without web reinforcement from experimental research conducted by previous researchers (Adom-asamoah, 2016, Althin, 2018), Arezoumandi *et al*. (2014), Birgisson, 2011, Hamrat, 2012, Thamrin *et al.*(2011), Thamrin *et al.* (2016), Hu and Wu, 2018) described in previous section) are calculated based on Codes and existing equations. The performance of Codes/existing equations is studied in terms of the ratio of experimental (Ve) to predicted (Vp) value (Ve/Vp) of shear strength of beams. Various Codes ACI 318-14, 2011, Eurocode 2, 2004, and other existing equations like Zsutty, 1971 and Niwa *et al*. 1987 as described in Chapter 2 are used for performance evaluation. The predicted shear strength values for beams without stirrups based on Codes/formulas are presented tables 4.1 below.

Table 4.1 The predicted shear strength and Ratio of experiment-to-predicted shear strength value.

Name of beams	V_{exp}(KN)	$V_{predicted}$(KN)				V_{exp}/V_{pred}			
		EC 2, 2004	ACI 318	Zsutty, 1971	Niwa *et al*	EC2, 2004	ACI 318	Zsutty, 1971	Niwa *et al*
PS1	73.78	24.861	31.545	40.466	40.805	2.968	2.339	1.823	1.808
PS2	84.6	31.323	31.545	50.983	51.411	2.701	2.682	1.659	1.646
PS3	72.716	21.741	26.475	33.962	35.781	3.345	2.747	2.141	2.032
PS4	87.927	27.392	26.475	42.790	45.081	3.210	3.321	2.055	1.950
PS5	55.935	14.733	17.077	21.631	24.141	3.796	3.276	2.586	2.317
PS6	55.935	18.563	17.077	27.253	30.415	3.013	3.276	2.052	1.839
PS7	45.945	12.369	13.486	17.268	20.294	3.715	3.407	2.661	2.264
PS8	52.826	15.584	13.486	21.756	25.569	3.390	3.917	2.428	2.066
PS9	33.345	8.444	8.598	11.701	14.049	3.949	3.878	2.850	2.373
PS10	47.655	10.639	8.598	14.743	17.701	4.479	5.543	3.232	2.692
GS1	80.29	26.071	33.875	42.435	42.791	3.080	2.370	1.892	1.876
GS2	93.31	32.847	33.875	53.464	53.913	2.841	2.755	1.745	1.731
GS3	72.716	22.799	28.431	35.615	37.522	3.190	2.558	2.042	1.938
GS4	107.59	28.724	28.431	44.872	47.274	3.746	3.784	2.398	2.276
GS5	58.163	15.426	18.295	22.648	25.276	3.770	3.179	2.568	2.301
GS6	58.163	19.436	18.295	28.534	31.846	2.993	3.179	2.038	1.826
GS7	52.826	12.951	14.449	18.080	21.249	4.079	3.656	2.922	2.486
GS8	62.137	16.317	14.449	22.779	26.772	3.808	4.301	2.728	2.321
GS9	49.95	8.841	9.212	12.252	14.710	5.650	5.423	4.077	3.396

GS10	57.105	11.139	9.212	15.436	18.533	5.127	6.199	3.699	3.081
A1	63.7	25.787	27.179	35.939	42.061	2.470	2.344	1.772	1.514
B1	64.6	28.747	35.365	42.829	46.932	2.247	1.827	1.508	1.376
C1	56.7	31.404	43.551	50.791	51.687	1.805	1.302	1.116	1.097
D1	27	12.337	12.791	15.881	19.938	2.189	2.111	1.700	1.354
N1.9	220.7	58.113	54.378	134.851	107.151	3.798	4.059	1.637	2.060
N2.5	161.3	61.209	58.781	98.509	99.436	2.635	2.744	1.637	1.622
N3.1	96.5	61.959	59.864	92.817	92.326	1.557	1.612	1.040	1.045
BS105	25.9	18.256	15.076	16.689	23.098	1.419	1.718	1.552	1.121
BS131	35.1	21.717	19.730	23.513	30.219	1.616	1.779	1.493	1.162
BS164	47	25.966	25.872	33.194	40.234	1.810	1.817	1.416	1.168
BS189	48.5	29.040	30.339	42.770	48.288	1.670	1.599	1.134	1.004
BS236	64.6	34.734	39.087	76.230	65.054	1.860	1.653	0.847	0.993
BS335	168.6	45.977	57.141	211.917	112.715	3.667	2.951	0.796	1.496
NS-4	121.2	88.946	121.659	143.341	132.891	1.363	0.996	0.846	0.912
NS-4	129.9	86.410	116.494	139.255	129.102	1.503	1.115	0.933	1.006
NS-6	143.2	103.998	121.659	167.598	155.379	1.377	1.177	0.854	0.922
NS6	167	101.033	116.494	162.820	150.949	1.653	1.434	1.026	1.106
NS-8	173.5	114.512	121.659	184.541	171.087	1.515	1.426	0.940	1.014
NS-8	170.8	111.247	116.494	179.280	166.209	1.535	1.466	0.953	1.028
A441.5N	129.4	13.475	14.865	35.109	28.137	9.603	8.705	3.686	4.599
B441.5N	143.6	16.794	14.645	43.580	35.056	8.550	9.805	3.295	4.096
A44-2N	85.1	13.475	14.865	23.924	24.237	6.315	5.725	3.557	3.511
B44-2N	100.5	16.794	14.645	29.696	30.197	5.984	6.862	3.384	3.328
A44-3N	47.3	13.475	14.865	16.720	20.337	3.510	3.182	2.829	2.326
B44-3N	55	16.794	14.645	29.696	30.197	3.275	3.756	1.852	1.821
R-01E	32.6	20.396	25.706	26.754	28.679	1.598	1.268	1.218	1.137
R-02E	37	23.347	25.706	30.626	32.829	1.585	1.439	1.208	1.127
R-03E	37.6	27.011	24.885	34.840	37.652	1.392	1.511	1.079	0.999
BSL-02	42.5	12.375	15.562	20.216	20.958	3.434	2.731	2.102	2.028
BSL-03	44.9	14.218	15.562	23.227	24.080	3.158	2.885	1.933	1.865
BSN-05	48.9	16.966	24.981	27.716	28.734	2.882	1.958	1.764	1.702
BSN-06	53.9	19.493	24.981	31.844	33.013	2.765	2.158	1.693	1.633
BSL-08	27.4	12.375	15.562	17.023	18.767	2.214	1.761	1.610	1.460
BSL-09	29.2	14.218	15.562	19.558	21.563	2.054	1.876	1.493	1.354
BSN-11	35.7	16.966	24.981	23.338	25.730	2.104	1.429	1.530	1.387
BSN-12	43.9	19.493	24.981	26.814	29.562	2.252	1.757	1.637	1.485
					Mean	3.093	2.960	1.941	1.841
					Standard deviation	3.482	3.452	2.096	1.994
					Covariation	0.7541	0.7095	0.8438	0.8170

From the above table 4.1 the average (AVG), the standard deviation (STD), and the coefficient of variation (COV) of the ratio of experimental value to predicted value are shown. For the limited data obtained from these selected experimental works, the standard deviation in using the

various codes for Reinforced concrete beam without transverse reinforcement were computed as EC 2,2004 (std=3.482), ACI 318 (std=3.452), Zsutt,1971 (std=2.096) and Niwa et al (std=1.994). However, the least standard deviation was recorded by Niwa et al., as (std 1.994) and relatively standard deviation recorded by Zsutty, 1971 was (2.096). This suggests significant improvement in the prediction uniformity of Niwa et al., and Zsutty, 1971 equation for providing a shear strength expression.

By the statistical regression method, the recorded coefficient of correlation of experimental result and codes was recorded for each. Therefore, the coefficient of correlation for EC2, 2004, ACI 318, Zsutty, 1971 and Newa et al was 0.569, 0.5035, 0.712 and 0.661 respectively. Statistically, when two variables are being investigated, the location of the co-ordinates on a rectangular co-ordinate system is shown by a scatter diagram as shown below in figure 4.1.

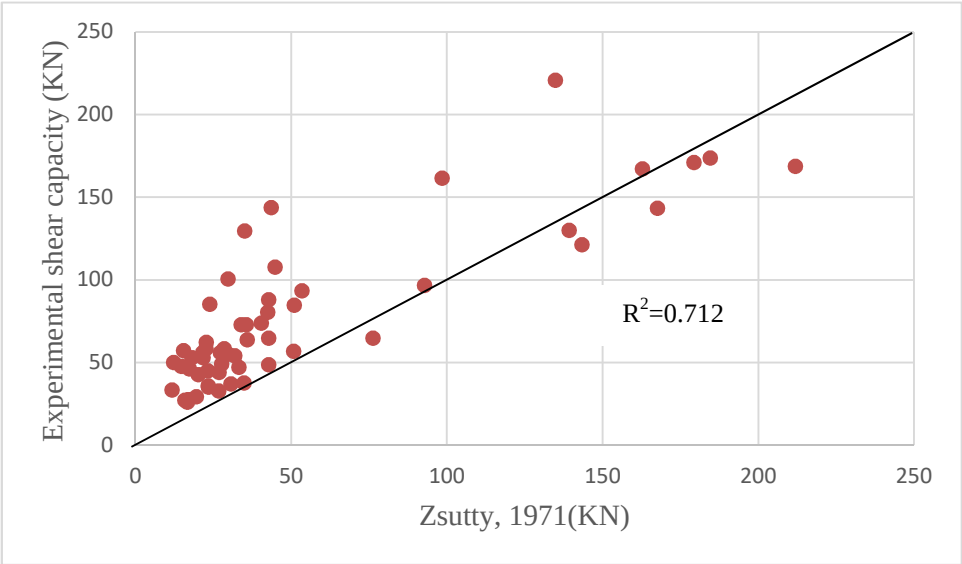

a)

b)

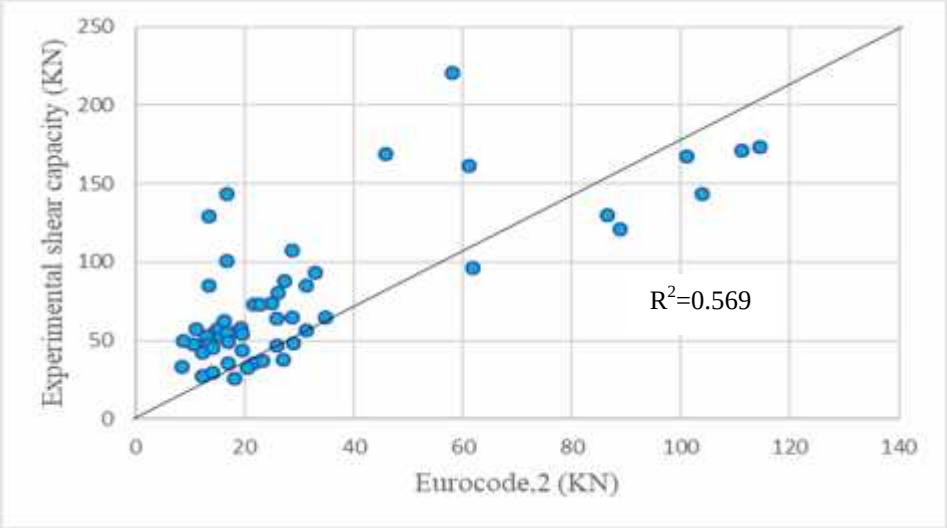
Experimental shear capacity (KN)
250
200
150
100
50
0
0
20
40
60
80
100
120
140
Eurocode.2 (KN)
R2=0.569

c)

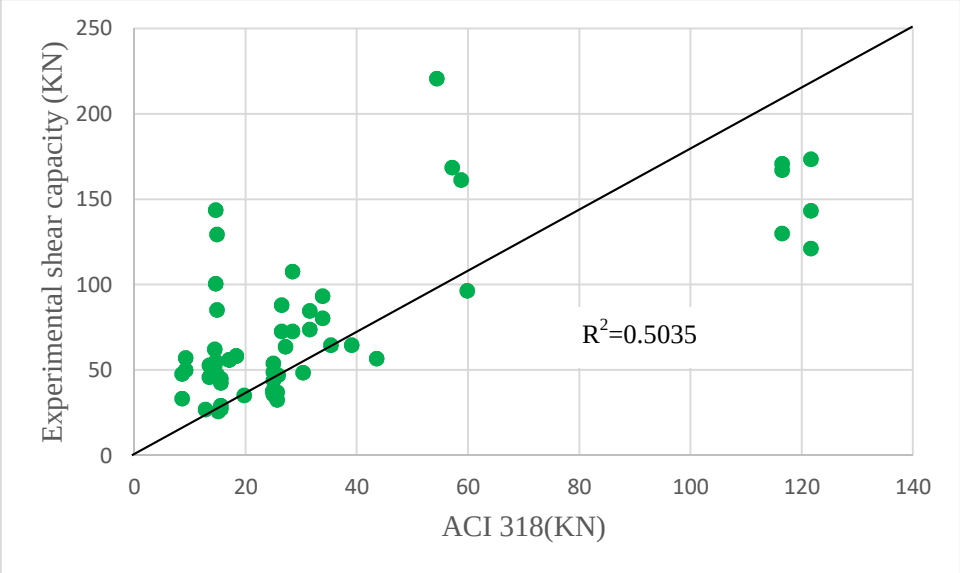
Experimental shear capacity (KN)
250
200
150
100
50
0
0
20
40
60
80
100
120
140
ACI 318(KN)
R2=0.5035

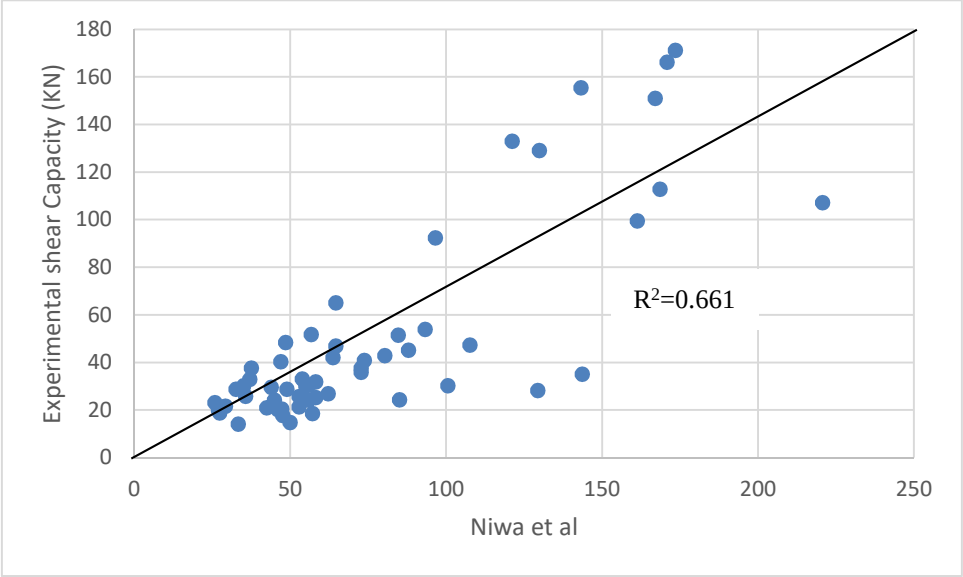

d)

Fig 4.1 Correlation of Experimental result and predicted equations

Fig 4.1 above shows, the comparisons between predicted values of shear capacity and experimental value. The coefficient of correlation for each building and proposed equations to compare with experimental were shown in scatter line in Fig 4.1.

But, the results of coefficient of correlation determination give values lying between -1 and 1, where 1 indicates perfect direct correlation, -1 indicates perfect inverse correlation and 0 indicates that no correlation exists. However, in between these values, the smaller the value of coefficient of correlation, the less is the amount of correlation which exists. Generally, values of coefficient of correlation in the ranges 0.7 to 1 and - 0.7 to -1 show that there is a fair amount of correlation exists.

Therefore, from Fig. 4.1 and Table 4.1, it is inferred that the shear strength predicted by the Zsutty,1971 shear strength equation shows good agreement with the test results having a better correlation coefficient of 0.712, and a mean ratio of 1.941 in predicting the shear strength of the selected 56 test beams than EC2,2004, ACI 318 and Niwa *et al* with correlation coefficient of 0.569, 0.5035 and 0.661 respectively, which predict the shear strength conservatively.

4.2 The Results of Finite Element Analysis for Parametric Study

The concentrated load was assigned at shear span length from both supports of simply supported RC beam without transverse reinforcement to study influence of concrete strength, longitudinal reinforcement ratio and shear span to depth ratio on its shear capacity. All beams were modeled and analyzed in ABAQUS software package in order to determine the ultimate shear load to be resisted. The load deflection curve and failure crack patterns recorded from ABAQUS are studied.

The following subtopics shows the ultimate shear load that resisted by each beam under influence of shear span to depth ratio, longitudinal reinforcement ratio and concrete compressive strength obtained from analysis by finite element Package.

Table 4.2 The response of RC beam without transverse reinforcement under different influences in terms of its shear capacity;

Name of beam	b_w(mm)	d(mm)	Fc'(Mpa)	ρ	a/d	Vu (KN)
C1R1S1	300	350	25	0.679	1.5	41.5
C1R1S2	300	350	25	0.679	2	33
C1R1S3	300	350	25	0.679	2.6	22.3
C2R1S1	300	350	35	0.679	1.5	51
C3R1S1	300	350	40	0.679	1.5	55
C4R1S1	300	375	60	0.679	1.5	71
C1R2S1	300	350	25	0.905	1.5	43
C1R3S1	300	350	25	1.13	1.5	46

4.2.1 Effect of Shear span to depth ratio

In figure 4.2 the effect of shear span to depth ratio on load deflection curve of reinforced concrete beams without transverse reinforcement had been studied, and it shows the numerical results of the FEA of load deflection of RC beams without transverse reinforcement. The figure was to show the shear load versus deflection curve result of RC beam without transverse reinforcement with the same amount of reinforcement and concrete grade with different shear span to depth ratio.

It can be understood from the figure that, as the ratio of shear span to effective depth of the beams increases, the capacity of beam to resist the load decreases. The load carrying capacity of RC beam without transverse reinforcement for C1R1S1, C1R1S2 and C1R1S3 was 41.5KN, 33KN and 22.3KN respectively. This shows that the load carrying capacity of beam without transverse reinforcement is decreasing as the shear span to depth ratio increases.

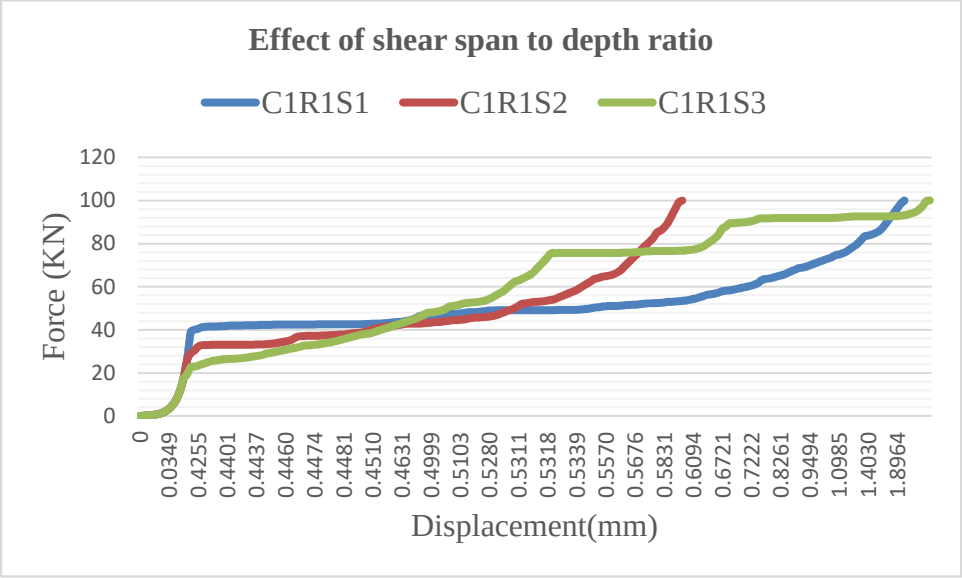

Figure 4.2 Load vs Displacement curve (Effect of shear span to effective depth ratio)

Figure 4.3 shows the cracks on the specimens due to the effect of shear span to effective depth ratio. All specimens developed flexural cracks on the mid-bottom of the member with the largest bending moment, and flexural cracks spread toward the upper area and the supporting point with an increasing load. The flexural cracks that developed toward the supporting point are in the form of flexural-shear cracks and shear cracks. Shear failure is reached when the diagonal cracks and shear bond failure spread toward the supporting point. As shown in Figure 4.3, diagonal length toward the support increases in proportion to the shear-span to effective depth ratio.

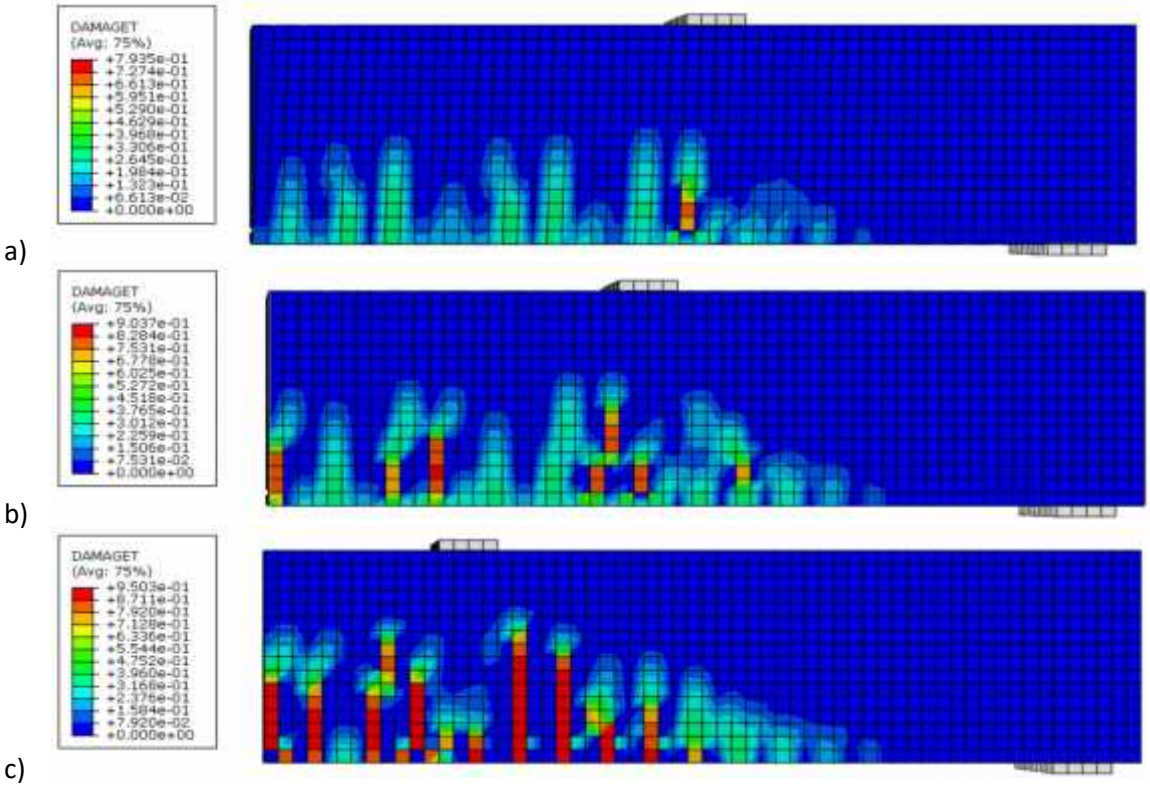

Figure 4.3 Crack Pattern of effect of shear span to effective depth ratio

a) CR1S1 b) C1R1S2 c) C1R1S3

4.2.2 Effect of Concrete

In figure 4.4 the effect of concrete grade on load deflection curve of reinforced concrete beams without transverse reinforcement had been studied, and it shows the numerical results of the FEA of load deflection of RC beams without transverse reinforcement. The figure was to show the load versus deflection curve result of RC beam without transverse reinforcement with the same length, depth, width and steel reinforcements with different concrete compressive strength.

It can be understood from the figure that, as concrete strength increases, the capacity of beam to resist the load also increases. The load carrying capacity of RC beam without transverse reinforcement for C1R1S1, C2R1S1, C3R1S1 and C4R1S1 was 41.5KN, 51KN, 55KN and 71KN respectively. Hence, due to increasing the compressive strength of concrete, the load carrying capacity of a beam also increases.

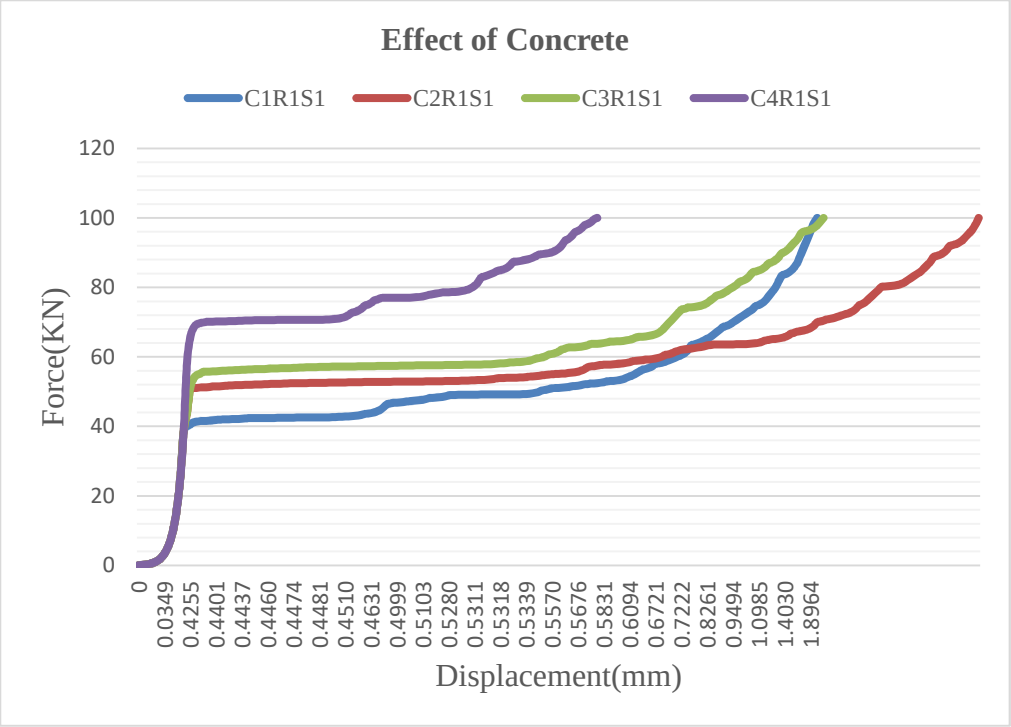

Figure 4.4 Load vs Displacement curve (Effect of concrete compressive strength)

The crack patterns observed at different concrete grade are shown in Figure 4.5 for C1R1S1, C2R1S1, C3R1S1 and C4R1S1 beams. All the beams failed in flexural shear in a brittle manner symmetrically on both side of the shear spans due to the effect of concrete compressive strength. In figure 4.5 it shown that the flexural crack length toward the bottom edge of beam was decreased as the concrete grade. Therefore, it is observed from the figure that, as the concrete compressive strength increased, the crack failure of reinforced concrete beam without transverse reinforcement was reduced.

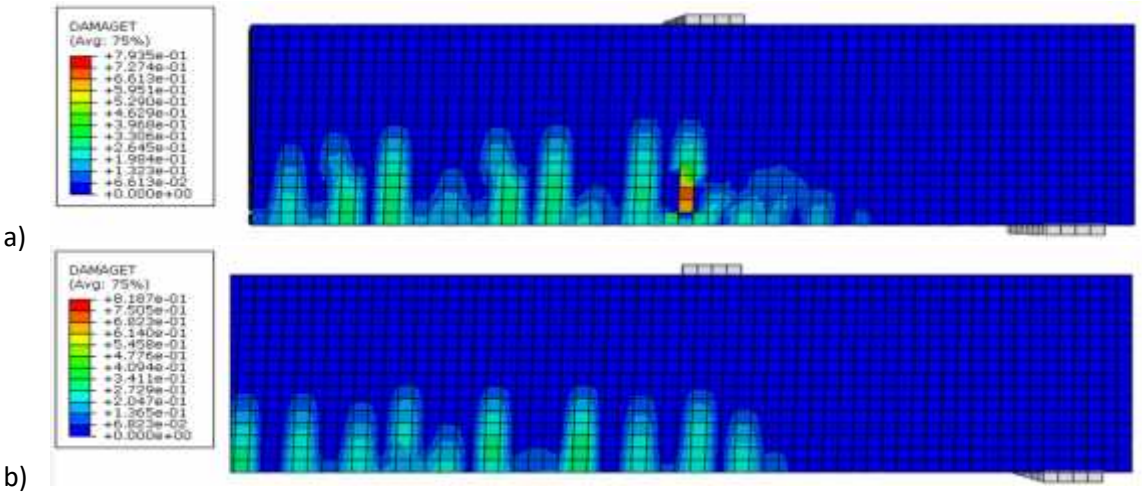

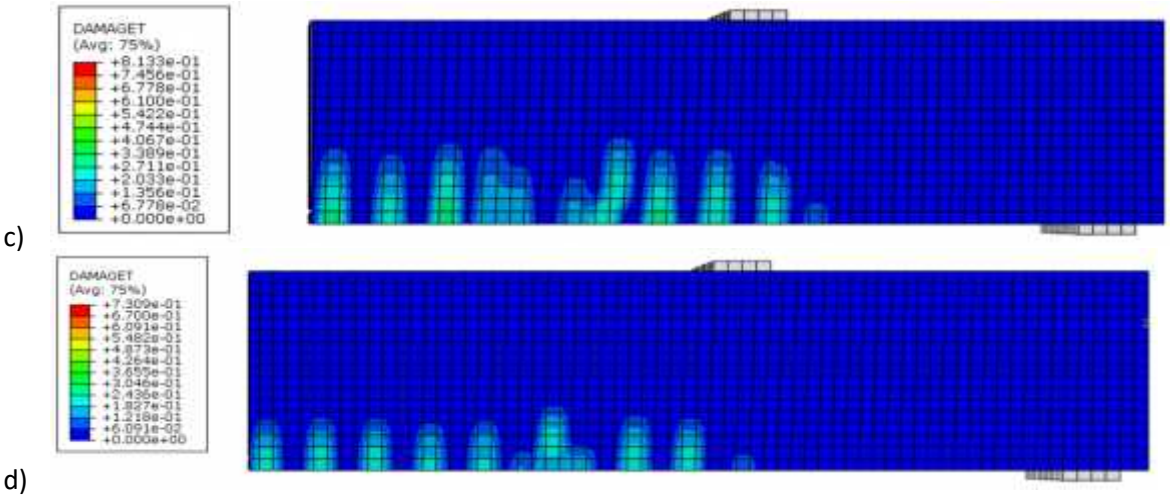

Figure 4.5 Crack pattern of RC beam (effect of concrete compressive strength)

a) C1R1S1 b) C2R1S1 c) C3R1S1 d) C4R1S1

4.2.3 Effect of Reinforcement ratio

The effect of reinforcement ratio on load deflection curve of Reinforced concrete beam without transversal reinforcement had been also studied. Figure 4.6 shows the numerical results of the finite element analyses of load deflection curve of Reinforced concrete beam without transversal reinforcement by considering different amount of longitudinal reinforcement with the same concrete grade and shear span to depth ratio. The ultimate load resisted by the reinforced concrete beam without transverse reinforcement is increased, as the amount of longitudinal reinforcement increased. However, the effect of amount of longitudinal reinforcement is less than the effect of concrete grade on the load deflection of the reinforced concrete beam without transverse reinforcement.

From the finite element result it is revealed that the load carrying capacity of RC beam without transverse reinforcement increase with increasing in longitudinal reinforcement, with value for C1R1S1, C1R2S1 and C1R3S1is 41.5KN, 43KN and 46KN respectively. This shows in addition to contributes to enhanced dowel action, increasing tension reinforcement in the flexural zone serves to control the propagation of flexural cracks and contributes to increasing the depth of neutral axis and thereby the depth of the un-cracked concrete in compression. Therefore, this enhances the contributions of aggregate interlock and shear resistance of un-cracked portion of concrete. Thus, increasing the percentage of longitudinal tension reinforcement upto standardized limit, increase the shear resistance in the concrete.

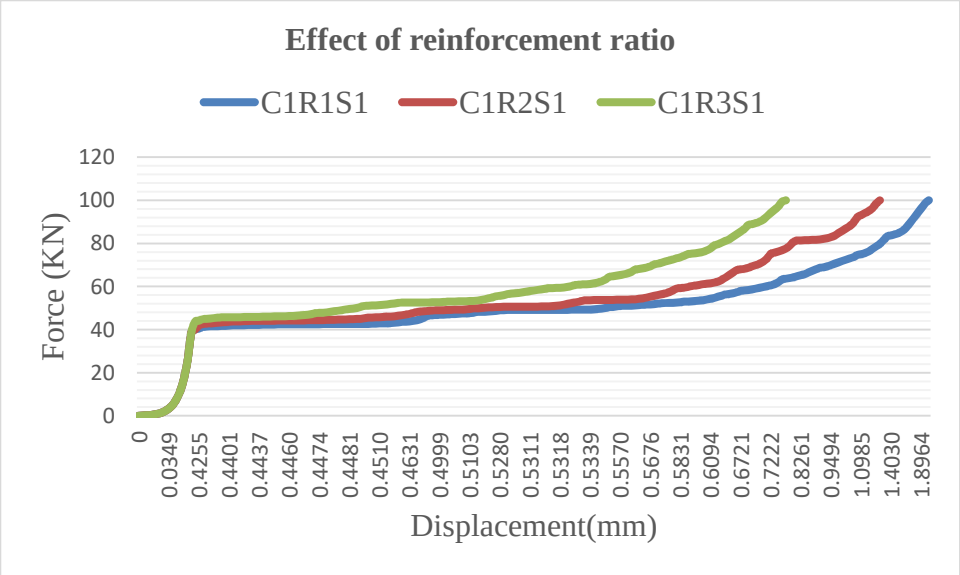

Figure 4.6 Load vs Displacement curve (Effect of amount of longitudinal reinforcement bar)

The propagated crack by finite element method for the specimens of different amount of longitudinal reinforcement was shown in figure 4.7. From the figure it is revealed that, the crack type is flexural crack which developed from the bottom edge face of beam to compression zone face. In figure 4.7 it shown that the flexural crack length toward the bottom edge of beam was decreased insignificantly as the amount of reinforcement increased. Therefore, it is observed from the figure that, as the amount of longitudinal reinforcement increased, the crack failure of reinforced concrete beam without transverse reinforcement was reduced.

Crack Patterns

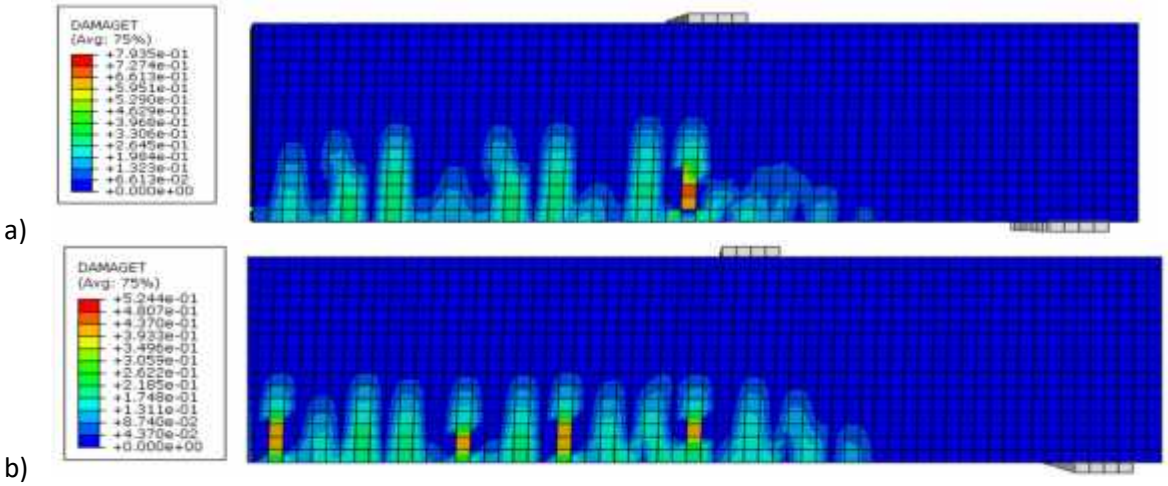

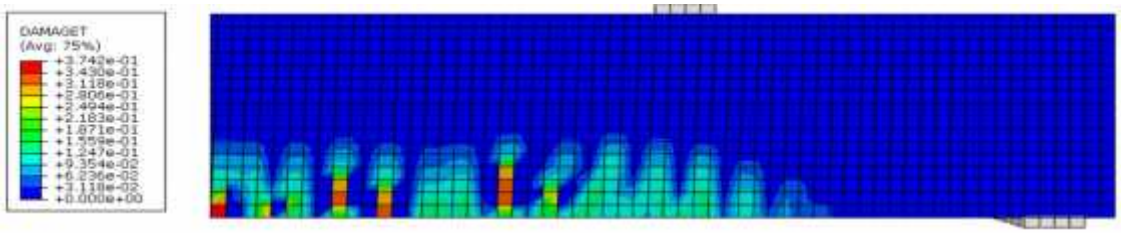

c)

Figure 4.7 Crack pattern of RC beam (effect of amount of longitudinal reinforcement bar)

a) C1R1S1 b) C1R2S1 c) C1R3S1

4.3 Comparisons of FEM result with practical codes and equations

Table 4.3 shows the result of FE package to analyze the shear load capacity of reinforced concrete without transverse reinforcement with different influencing parameters considered in this study was compared with the predicted practical equations of considered codes and existing equations.

Name of beam	b_w(mm)	d(mm)	Fc' (MPa)	ρ	a/d	FEA (KN)	EC 2, 2004	ACI-318	Zsuty, 1971	Niwa et al
C1R1S1	300	350	25	0.679	1.5	41.5	56.86	87.15	187.07	118.15
C1R1S2	300	350	25	0.679	2	33	56.86	87.15	127.47	101.77
C1R1S3	300	350	25	0.679	2.6	22.3	56.86	87.15	93.44	90.43
C2R1S1	300	350	35	0.679	1.5	51	63.61	103.12	209.27	132.17
C3R1S1	300	350	40	0.679	1.5	55	66.51	110.24	218.80	138.19
C4R1S1	300	375	60	0.679	1.5	71	80.38	135.01	250.46	158.19
C1R2S1	300	350	25	0.905	1.5	43	62.58	87.15	205.87	130.02
C1R3S1	300	350	25	1.13	1.5	46	67.38	87.15	221.69	140.01

Table 4.3 Result of beams considered for parametric study by practical codes and existing equations

Statically, the uniformity of considered practical codes equation and existing equation were compared with the result from FEA for reinforced concrete beam without transverse reinforcement as in table 4.4 below.

Name of beams	FEA/EC,2004	FEA/ACI	FEA/Zsuty	FEA/Niwa et al
C1R1S1	0.729863	0.47619	0.221842	0.351248
C1R1S2	0.580373	0.378657	0.258884	0.324261
C1R1S3	0.392191	0.255881	0.238656	0.2466
C2R1S1	0.801761	0.494569	0.243704	0.385867
C3R1S1	0.826943	0.498911	0.251371	0.398003
C4R1S1	0.883304	0.525887	0.283478	0.448827
C1R2S1	0.68712	0.493402	0.20887	0.330718
C1R3S1	0.682695	0.527826	0.207497	0.328548
Mean	0.698031	0.456416	0.239288	0.351759
Std	0.664901	0.433209	0.22746	0.33392

Table 4.4 comparison of FEA result and practical codes and existing equations

From table 4.4 the mean average (mean) and the standard deviation (Std) of the ratio of Finite Element Analysis value to predicted value of practical and existed equations are shown. For the considered different parameters, the standard deviation in using the various codes and existing equations for Reinforced concrete beam without transverse reinforcement were computed as EC 2,2004 (std=0.6649), ACI 318 (std=0.4332), Zsutty,1971 (std=0.22746) and Niwa et al (std=0.33392). However, the least standard deviation was recorded by Zsutty, 1971 as (std 0.22746). This suggests significant improvement in the prediction uniformity of FEA and Zsutty, 1971 equation for providing a shear strength expression when compared other equations. Therefore, prediction of shear capacity of reinforced concrete beam without transverse reinforcement by FEM is related to Zsutty, 1971 equation which is improved as applicable equation in this paper.

CHAPTER 5

CONCLUSION AND RECOMMENDATION

5.1 Conclusion

The study presents the prediction of shear strength of the selected 56 RC test beams without shear reinforcement by the four shear evaluation methods namely EC2,2004, ACI 318-14, Zsutty, 1971 and Niwa et al , and parametric studies are carried out to study the influence of the parameters concrete strength, reinforcement ratio and shear span to depth ratio by finite element method.

The following conclusions are drawn.

1. Comparisons between the shear strength calculations of the current codes of practice and existing equations EC2, 2004, ACI 318-14, Zsuty, 1971 and Niwa et al statistically indicated that the shear strength predicted by the Zsutty, 1971 equation shows good agreement with the test results, whereas EC2,2004, ACI 318-14 and Niwa *et al* predict the shear strength conservatively.

2. The result obtained from finite element analysis carried out by ABAQUS 6.14 on influence parameters (concrete grade, shear span to effective depth ratio and amount of reinforcement) on load carrying capacity of RC beam without transverse reinforcement shear capacity indicate the following conclusion;

- ✓ As concrete compressive strength increase, the shear capacity of Reinforced beam without transverse reinforcement was increased.
- ✓ Also, by increasing the amount of longitudinal reinforcement to some limit, the shear capacity of RC beam without transverse reinforcement was increased. However, the amount of longitudinal reinforcement has minimum effect, whereas the shear strength of reinforced concrete without transverse reinforcement are more sensitive to shear span to effective depth ratio and concrete compressive strength.
- ✓ In contrast, when the ratio of shear span to effective depth increase, the shear capacity of beam decreased. As soon as shear span to depth ratio is increased, the beams more prominent to flexural failure rather than shear failure.

3. The comparisons of the result obtained from FEA package ABAQUS and practical codes and existing equations to determine shear capacity prediction of RC without transverse reinforcement were carried out statically, and it is indicated that predicting by FEM had uniformity with Zsutty, 1971 equation shows good agreement with the test results.

5.2 Recommendations

1. The performance of Codes and other existing methods should be investigated with more experimental data having wide range of influencing parameters.
2. In order to gain more knowledge on contribution of concrete on shear capacity of reinforced beam, more tests with varying the influencing parameters could be made.

REFERENCES

ACI Committee 318,(2011). Building Code Requirements for Structural Concrete (ACI318M.11) and Commentary. American Concrete Institute, Farmington Hills, Michigan, USA.

ADINA R&D. (2015).ADINA. Watertown, MA, USA.

Adom-asamoah, M. (2016) 'Shear Strength Characteristics Of Reinforced Concrete (Rc) Beams Made From Phyllite Aggregates', Kwame Nkrumah University of Science and Technology, Kumasi, Ghana.

Ahmad, S.H., Khaloo, A.R. and Poveda, A. (1986). "Shear capacity of reinforced high-strength concrete beams", ACI Structural Journal, Vol. 83, No. 2, pp. 297–305

Ahmed S.H, Lue D.M, (1987): "Flexural-shear interaction of reinforced highstrength concrete beams". ACI Structural Journal 330-341

Akthem, A.A. (1983) 'A Nonlinear Finite Element Study of Reinforced Concrete Beams', Ph.D. thesis, University of Glasgow.

Althin, A. (2018) 'Size effects in shear force design of concrete beams', Faculty of Engineering, LTH. Thesis, Lunds University.

Ammar, Y. A., etal (2015) 'Experimental Investigation and Nonlinear Analysis of Hybrid Reinforced Concrete Deep Beams', Al-Qadisiyah Journal for Engineering Sciences. 8(2):Page 99- 119

Angelakos, D. (1999) 'Reinforced concrete'.

ANSYS.(2015). ANSYS. Pittsburgh, PA, USA.

Arezoumandi, M., Smith, A., Volz, J. and Khayat, K. (2014) 'An Experimental Study on Shear Strength of Reinforced Concrete Beams with 100% Recycled Concrete Aggregate', Construction and Building Material 53, 612-620.

Argyris, J. H., Kelsey, G. (1960).Energy theorems and structural analysis.Butterworth.

Birgisson, S.R.(2011)'HSear resistance of reinforced concrete beams without stirrups', Thesis

in civil engineering, school of science and engineering.

Cavagnis, F. (2017) 'Shear in reinforced concrete without transverse reinforcement : from refined experimental measurements to mechanical models PAR', 8216.

Clough, R. W. (1960).The finite element method in plane stress analysis.Proc.2nd Conf.on Electronic Computation, ASCE, New York.

Cotsovos, D. M., Zeris, C. and Abbas, A. A. (2009) 'Finite element modelling of structural concrete'.

Eurocode 2 (2004). Design of concrete structures - Part 1- 1: General rules and rules for buildings.

Ex-, T. F. (1980) 'Proposed Design Equation For Shear Strength Of Reinforced Concrete Beams By Hajime Oka M Ura * And T Akeshi Hi Ga I **', (300).

Fanning, P.(2001) 'Non-linear models forreinforced and post-tensioned concretebeams', Electronic Journal of Structural Engineering. Vol. 2:pp. 111-119.

Ferguson P.M, (1956): "Some implication of recent diagonal tension test". Journal of ACI 28(2)(1956): 157-172.

Hamrat, M. *et al*. (2012) 'Effects of the Transverse Reinforcement on the Shear Behaviour of High Strength Concrete Beams', 15(8), pp. 1291–1306.

Hillerborg, A., Modeer, M., Petersson, P. (1976) 'Analysis of crack formation and crack growth in concrete by means of fracture mechanics and finite elements', Cement and Concrete Research. 6(6): Page 773- 782

Hsu, T.C., and Mo, Y.L.(2018) 'Unified Theory of Concrete Structures', University of Houston, USA, A John Willey and Sons Limited Publishers.

Hu, B. and Wu, Y. F. (2018) 'Effect of shear span-to-depth ratio on shear strength components of RC beams', *Engineering Structures*. Elsevier, 168(April), pp. 770–783. doi: 10.1016/j.engstruct.2018.05.017.

Journal, I., Civil, O. F. and Engineering, S. (2010) 'Shear Resistance of High Strength Concrete Beams Without Shear Reinforcement', 1(1), pp. 101–113. doi:

10.6088/ijcser.00202010009.

L, S. R. (2011) ‘Evaluation Of Shear Resistance Of High Strength Concrete Beams Without Web Reinforcement’, 6(2), pp. 1–7.

Niwa J., Yamada K., Yokozawa K., Okamura H. (1987) 'Revaluation of the equation for shear strength of reinforced concrete beams without web reinforcement',Concrete Library of JSCE, 9: 65–84

Phama, C., Hancockb, G. (2010). Numerical simulation of high strength cold - formed purlins in combined bending and shear, Journal of Constructional Steel Research. 66:1205 - 1217.

Raju, O. (2014) ‘Review on Shear Behaviour of Reinforced Concrete Beam without Transverse Reinforcement’, 4(4), pp. 116–121.

Reineck K, Bentz E, Fitik B, Kuchma DA, Bayrak O.(2014) 'ACI-DAfStb Databases for Shear Tests on Slender Reinforced Concrete Beams with Stirrups', ACI Structural Journal, 11 (5): 1147-1156.

Stoner, J. G. (2015).Finite element modelling of GFRP reinforced concrete beams.Master's Thesis, University of Waterloo, Canada.

Taylor, R. (1960) 'SomeShearTests onReinforced ConcreteBeams withoutShear Reinforcement'. Magazine of Concrete Research. 12(36):145-154.

Taylor H.P, (1974): “The fundamental behaviour of reinforced concrete beams in bending and shear”. Proceedings ACI –ASCE Shear symposium, Ottawa (ACI SP-42), Detroit: 43-77.

Tempos E.J, Frosch R.J, (2002): “Influence of beams size, longitudinal reinforcement and stirrup effectiveness on concrete shear strength”. ACI Journal 99(5): 559-67.

Thamrin, R. *et al.* (2011) ‘Experimental Study On Diagonal Shear Cracks Of Concrete Beams Without Stirrups’, pp. 1–8.

Thamrin, R. *et al.* (2016) ‘Shear Strength Of Reinforced Concrete T-Beams Without Stirrups’, 11(4), pp. 548–562.

Vegera, P. *et al.* (2016) 'The Shear Strength Of Reinforced Concrete Beams Without Shear Concrete Beams Without Shear', (January). doi: 10.7862/rb.2015.209.

Wang T., Hsu T. C. (2001). Nonlinear finite element analysis of concrete structures using new constitutive models, Computers and Structures. 79(32): Page 2781 –2791.

Yalavarthy, S. H. (2010) 'Shear Strength Predictions Of Longitudinally Reinforced Concrete Beams', 667.

Yang, Y. (2014) '*Shear Behaviour of Reinforced Concrete Members without Shear Reinforcement', A New Look at an Old Problem*. PhD thesis, TU Delft.

Yang, Y., Walraven, J., Uijl, J. (2016)'The Critical Shear Displacement theory: on the way to extending the scope of shear design and assessment for members without shear reinforcement', pp. 1–25. doi: 10.1002/suco.201500135.Submitted.

Yang, Y., Walraven, J. and Uijl, J. Den (2017) 'Shear Behavior of Reinforced Concrete Beams without Transverse Reinforcement Based on Critical Shear Displacement', 143(1), pp. 1–13. doi: 10.1061/(ASCE)ST.1943-541X.0001608.

Zsutty, T.C. (1971) 'Shear strength prediction for separate categories of simple beam tests', ACI Journal Proceedings, 68(2), pp. 138–143.

Appendix A: Compiled experimental set of RC beam without transverse reinforcement

Researchers	Name of Beam	b(m)	d(m)	a/d	Steel ratio%	Fc'(Mpa)	Experimental shear load (KN)
Adom-Asamoah, 2016	PS1	140	280	2.45	1	23.5	73.78
	PS2	140	280	2.45	2	23.5	84.6
	PS3	140	235	2.45	1	23.5	72.716
	PS4	140	235	2.45	2	23.5	87.927
	PS5	110	195	2.48	1	23	55.935
	PS6	110	195	2.48	2	23	55.935
	PS7	110	154	2.46	1	23	45.945
	PS8	110	154	2.46	2	23	52.826
	PS9	90	120	2.35	1	23	33.345
	PS10	90	120	2.35	2	23	47.655
	GS1	140	280	2.45	1	27.1	80.29
	GS2	140	280	2.45	2	27.1	93.31
	GS3	140	235	2.45	1	27.1	72.716
	GS4	140	235	2.45	2	27.1	107.59
	GS5	110	195	2.48	1	26.4	58.163
	GS6	110	195	2.48	2	26.4	58.163
	GS7	110	154	2.46	1	26.4	52.826
	GS8	110	154	2.46	2	26.4	62.137
	GS9	90	120	2.35	1	26.4	49.95
	GS10	90	120	2.35	2	26.4	57.105
Althin, 2018	A1	160	166	2.5	1.51	38	63.7
	B1	160	216	2.5	1.16	38	64.6
	C1	160	266	2.44	0.94	38	56.7
	D1	100	125	2.52	1.26	38	27
Hu, 2018	N1.9	180	300	1.9	3.27	36.8	220.7
	N2.5	180	300	2.5	3.27	43	161.3
	N3.1	180	300	3.1	3.27	44.6	96.5
Birgison	BS-105	200	81	4.81	1.55	31.43	25.9
	BS-131	200	106	3.68	1.48	31.43	35.1
	BS-164	200	139	2.81	1.41	31.43	47
	BS-189	200	163	2.39	1.39	31.43	48.5
	BS-236	200	210	1.86	1.35	31.43	64.6
	BS-335	200	307	1.14	1.31	31.43	168.6
Arezoumandi *et al*. (2014)	NS-4	300	400	3	1.27	37.3	121.2
	NS-4	300	400	3	1.27	34.2	129.9
	NS-6	300	400	3	2.03	37.3	143.2
	NS6	300	400	3	2.03	34.2	167
	NS-8	300	400	3	2.71	37.3	173.5

	NS-8	300	400	3	2.71	34.2	170.8
M Hamrat, 2012	A44-1.5N	100	135	1.5	1.2	44	129.4
	B44-1.5N	100	133	1.5	2.4	44	143.6
	A44-2N	100	135	2	1.2	44	85.1
	B44-2N	100	133	2	2.4	44	100.5
	A44-3N	100	135	3	1.2	44	47.3
	B44-3N	100	133	2	2.4	44	55
R Thamrin et al	R-01E	125	219	3.7	1	32	32.6
	R-02E	125	219	3.7	1.5	32	37
	R-03E	125	212	3.8	2.5	32	37.6
Thamrin et al. (2011)	BSL-02	130	200	2.3	0.60	13	42.5
	BSL-03	130	200	2.3	0.91	13	44.9
	BSN-05	130	200	2.3	0.60	33.5	48.9
	BSN-06	130	200	2.3	0.91	33.5	53.9
	BSL-08	130	200	3	0.60	13	27.4
	BSL-09	130	200	3	0.91	13	29.2
	BSN-11	130	200	3	0.60	33.5	35.7
	BSN-12	130	200	3	0.91	33.5	43.9

Appendix B: Regression analysis

Table B.1 Statistical analysis of Eurocode 2, 2004 result with experimental result

SUMMARY OUTPUT								
Regression Statistics								
Multiple R	0.753989							
R Square	0.5685							
Adjusted R	0.560509							
Standard E	30.44476							
Observatic	56							
ANOVA								
	df	*SS*	*MS*	*F*	*ignificance F*			
Regressior	1	65942.86	65942.86	71.14472	1.97E-11			
Residual	54	50051.7	926.8833					
Total	55	115994.6						
	Coefficients	*andard Erı*	*t Stat*	*P-value*	*Lower 95%*	*Upper 95%*	*ower 95.0%*	*pper 95.0%*
Intercept	37.40686	6.165813	6.066817	1.33E-07	25.04515	49.76858	25.04515	49.76858
EC, 2004	1.26553	0.150038	8.434733	1.97E-11	0.964722	1.566338	0.964722	1.566338

Table B.2 Statistical analysis of ACI 318-14 result with experimental result

SUMMARY OUTPUT								
Regression Statistics								
Multiple R	0.709572							
R Square	0.503493							
Adjusted R	0.494299							
Standard E	32.65762							
Observatic	56							
ANOVA								
	df	*SS*	*MS*	*F*	*ignificance F*			
Regressior	1	58402.46	58402.46	54.75981	9.23E-10			
Residual	54	57592.1	1066.52					
Total	55	115994.6						
	Coefficients	*andard Erı*	*t Stat*	*P-value*	*Lower 95%*	*Upper 95%*	*ower 95.0%*	*pper 95.0%*
Intercept	41.55169	6.428957	6.463208	3.06E-08	28.66241	54.44097	28.66241	54.44097
ACI	1.017067	0.137442	7.399987	9.23E-10	0.741513	1.292622	0.741513	1.292622

Table B.3 Statistical analysis of Zsutty, 1971 result with experimental result

SUMMARY OUTPUT								
Regression Statistics								
Multiple R	0.843636							
R Square	0.711721							
Adjusted R	0.706382							
Standard E	24.88448							
Observatic	56							
ANOVA								
	df	*SS*	*MS*	*F*	*ignificance F*			
Regressior	1	82555.75	82555.75	133.3185	3.31E-16			
Residual	54	33438.81	619.2372					
Total	55	115994.6						
	Coefficients	*andard Erı*	*t Stat*	*P-value*	*Lower 95%*	*Upper 95%*	*ower 95.0%*	*pper 95.0%*
Intercept	37.06005	4.766249	7.775518	2.27E-10	27.5043	46.6158	27.5043	46.6158
Zsuty	0.763405	0.066116	11.54636	3.31E-16	0.630849	0.89596	0.630849	0.89596

Table B.4 Statistical analysis of Niwa *et al*.1987 result with experimental result

SUMMARY OUTPUT								
Regression Statistics								
Multiple R	0.816842							
R Square	0.667231							
Adjusted R	0.661068							
Standard E	26.73583							
Observatic	56							
ANOVA								
	df	*SS*	*MS*	*F*	*ignificance F*			
Regressior	1	77395.11	77395.11	108.2745	1.64E-14			
Residual	54	38599.45	714.8046					
Total	55	115994.6						
	Coefficients	*andard Erı*	*t Stat*	*P-value*	*Lower 95%*	*Upper 95%*	*ower 95.0%*	*pper 95.0%*
Intercept	31.77101	5.588439	5.685131	5.43E-07	20.56686	42.97515	20.56686	42.97515
Niwa et al	0.900857	0.086575	10.4055	1.64E-14	0.727284	1.07443	0.727284	1.07443

Appendix C: Properties of materials

Table C.1 Parameters use in modelling of concrete damage for all type of concrete is the same and given as;

Parameters	Value
Dilation angle (ψ)	36
Eccentricity (γ)	0.1
σ_{b0}/σ_{c0}	1.16
K	0.667
Viscosity parameter	0

Table C.2 Compression and tension behavior of concrete damage plasticity of C25

Fck= 25Mpa, Fcm= 33MPa, Ecm= 31.47581Gpa			
Compression behavior		Compression damage	
σ_c	ε_{in}	d_c	ε_{in}
13.2	0	0	0
18.9744955	0.000100927	7.26968E-05	4.94744E-06
23.7190025	0.000200192	0.000508943	3.43856E-05
27.45948181	0.000331356	0.001518107	0.000100927
30.22102907	0.00049362	0.003082095	0.000200192
32.02791046	0.000686215	0.005253648	0.000331356
32.90359672	0.000908394	0.00810033	0.00049362
33	0.001020942	0.011700128	0.000686215
32.87079545	0.001159436	0.016137014	0.000908394
31.95148191	0.001438643	0.018495697	0.001020942
30.16692825	0.001745339	0.021496623	0.001159436
27.53773149	0.00207887	0.02786221	0.001438643
24.08384002	0.002438601	0.035310983	0.001745339
18.94994436	0.002897952	0.043910921	0.00207887
		0.053718133	0.002438601
		0.066959359	0.002897952
Tension behavior		Tension damage	
σ_t	ε_c	d_t	ε_c
2.578643728	0	0	0
2.000683435	0.000429504	0.005412079	1.14848E-05
1.563456851	0.001243135	0.197420124	0.000429504
1.239596346	0.002453232	0.503752441	0.001243135

1.003256263	0.0040606	0.774985224	0.002453232
0.832111308	0.006065936	0.925497852	0.0040606
0.707981947	0.008469806	0.981750506	0.006065936
0.702739695	0.010889969		
0.616715925	0.011272651		
0.547711009	0.014474802		
0.493305939	0.018076498		
0.448166112	0.022077906		
0.408728116	0.026479135		
0.372729832	0.031280258		
0.338831359	0.036481314		
0.306320665	0.042082328		
0.274892645	0.048083308		
0.244488679	0.054484256		
0.215184138	0.061285169		
0.187112695	0.068486045		
0.160418006	0.076086877		
0.13522516	0.084087662		
0.11162592	0.092488398		
0.08967321	0.101289082		
0.069381479	0.110489715		

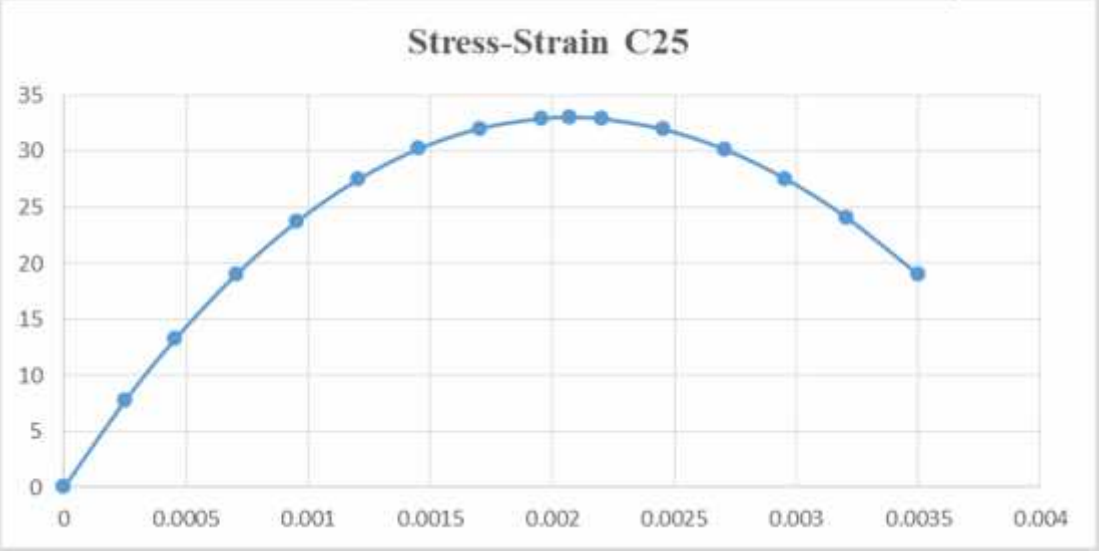

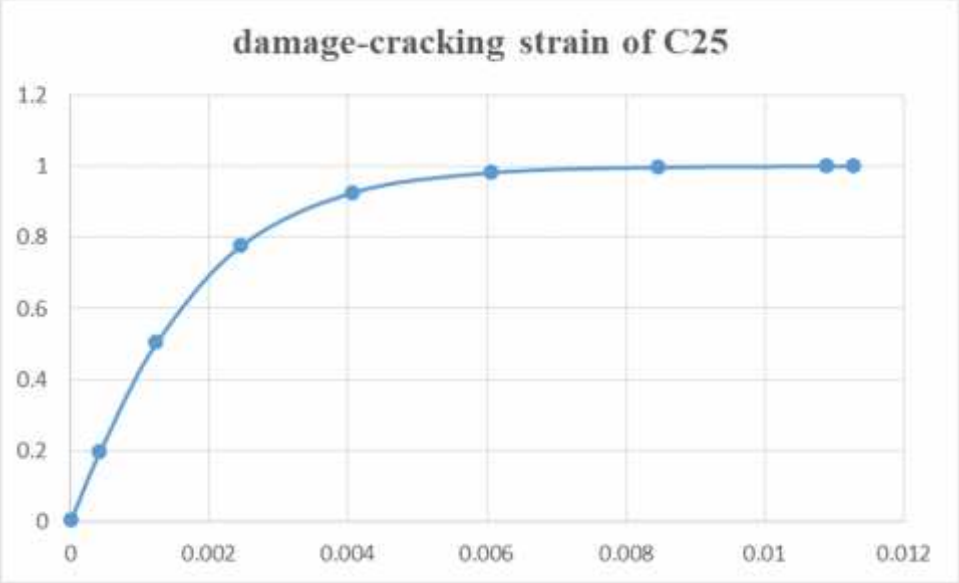
damage-cracking strain of C25
1.2
1
0.8
0.6
0.4
0.2
0
0
0.002
0.004
0.006
0.008
0.01
0.012

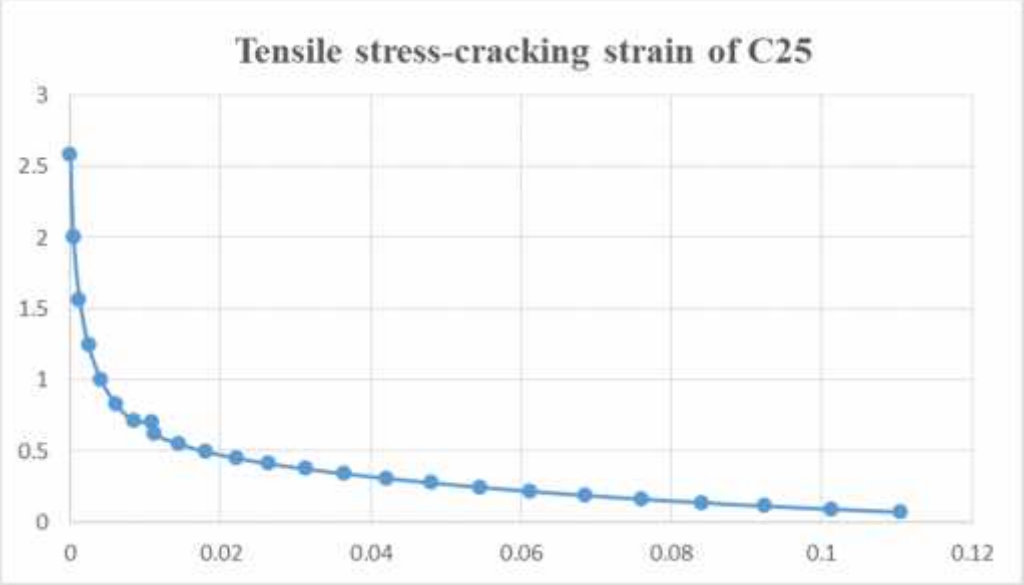
Tensile stress-cracking strain of C25
3
2.5
2
1.5
1
0.5
0
0
0.02
0.04
0.06
0.08
0.1
0.12

Table C.3 Compression and tension behavior of concrete damage plasticity of C35

Fck= 35MPa, Fcm= 43Mpa, Ecm= 34.07715GPa			
Compression behavior		Compression damage	
σ_c	e_{in}	d_c	e_{in}
17.2	0	0	0
23.8950244	8.2368E-05	8.70452E-06	4.93104E-07
29.66402906	0.000163076	0.000513311	2.88347E-05
34.46330926	0.00027224	0.00148936	8.2368E-05
38.24636606	0.000411225	0.003016634	0.000163076
40.96367932	0.000581485	0.005186629	0.00027224
42.56245835	0.000784569	0.008117375	0.000411225
43	0.000984486	0.011953676	0.000581485
42.98636733	0.001022129	0.016866291	0.000784569
42.17522263	0.001295932	0.022039934	0.000984486
40.06465863	0.001607867	0.023049914	0.001022129
36.585758	0.001959956	0.030719809	0.001295932
31.66464218	0.002354367	0.040107023	0.001607867
26.17863653	0.002731783	0.051452122	0.001959956
		0.064997487	0.002354367
		0.078682576	0.002731783
Tension behavior		Tension damage	
σ_t	ε_c	d_t	ε_c
2.385378785	0.000434519	0.005900695	1.04939E-05
1.78500417	0.001251656	0.235949376	0.000434519
1.368413625	0.002463547	0.576437678	0.001251656
1.084091857	0.004071663	0.838305095	0.002463547
0.890508787	0.006077188	0.957350446	0.004071663
0.756452289	0.008481015	0.989967	0.006077188
0.750880318	0.010901174		
0.65974213	0.011283775		
0.585408332	0.014485897		
0.523877868	0.018087653		
0.469408203	0.022089208		
0.418841369	0.026490652		
0.370669913	0.031292026		
0.324370437	0.036493348		
0.279950013	0.042094616		
0.237652933	0.048095823		
0.197782839	0.054496961		
0.160604348	0.061298023		
0.126296994	0.068499002		
0.09494173	0.076099897		

0.066526197	0.084100708		
0.040959507	0.092501438		
0.018090646	0.10130209		

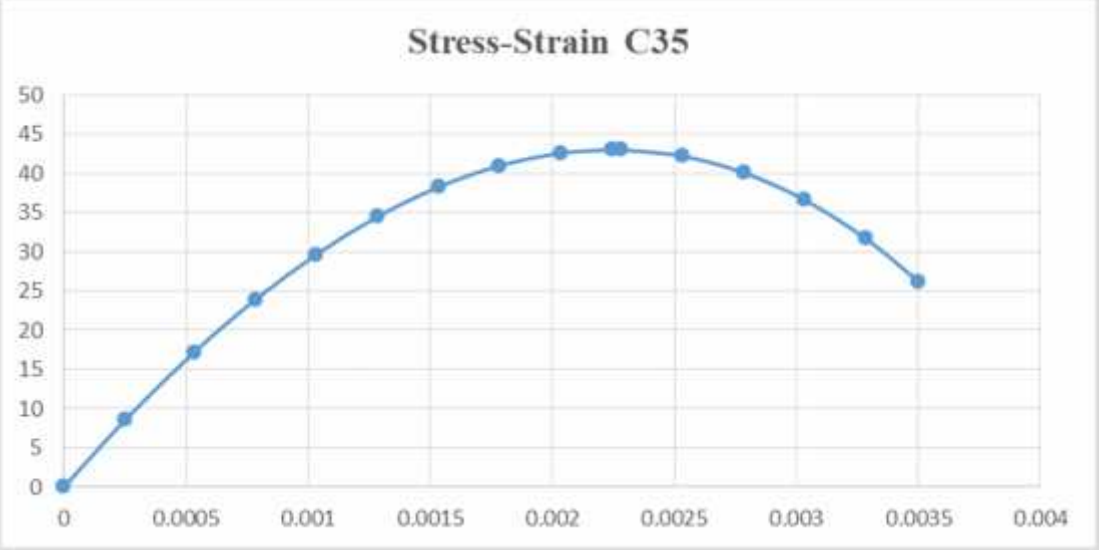

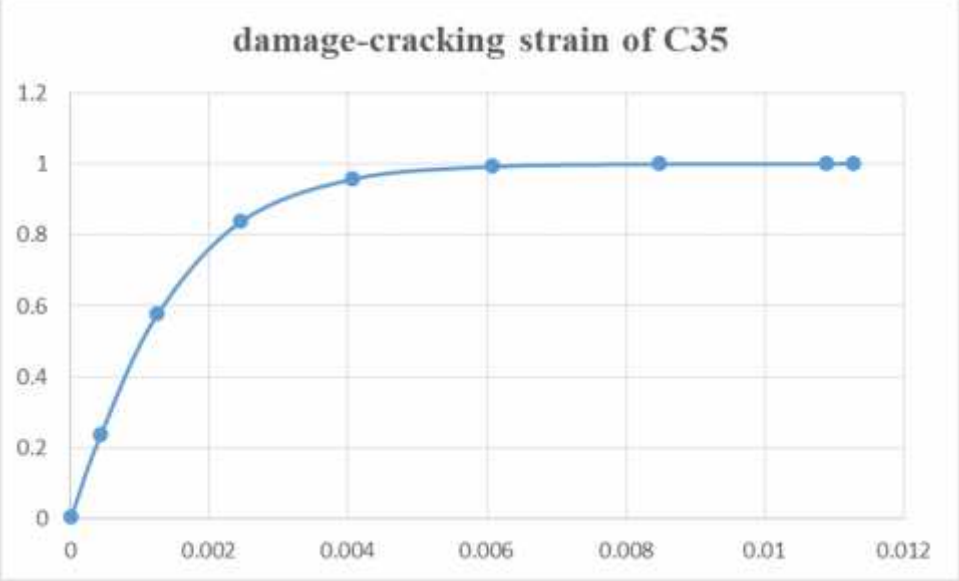

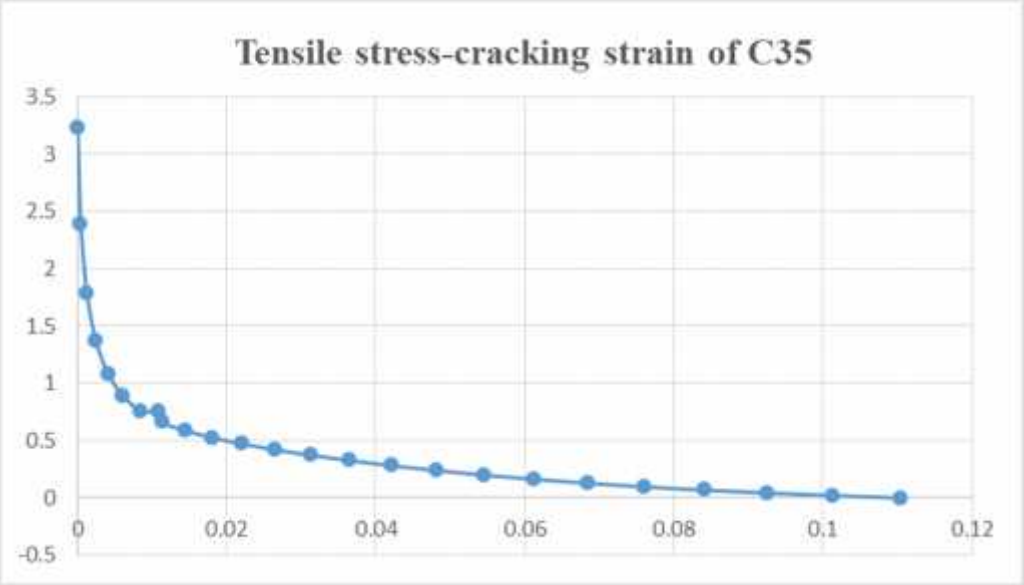

Table C.4 Compression and tension behavior of concrete damage plasticity of C40

Fck= 40MPa, Fcm = 48MPa, Ecm=35.22046GPa			
Compression behavior		Compression damage	
σ_c	e_{in}	d_c	e_{in}
19.2	0	0	0
26.31213769	7.36988E-05	3.24447E-05	2.45086E-06
32.54946324	0.000146605	0.000341064	2.56308E-05
37.84492262	0.000246253	0.000991141	7.36988E-05
42.12442923	0.000374747	0.002002867	0.000146605
45.30591713	0.000534416	0.003435071	0.000246253
47.29823703	0.000727849	0.005364226	0.000374747
48	0.000957928	0.007887106	0.000534416
47.99986385	0.000961406	0.011123521	0.000727849
47.29737703	0.001227874	0.015219021	0.000957928
45.06366581	0.001541294	0.015282909	0.000961406
41.15579934	0.001902249	0.020347453	0.001227874
35.41248652	0.002315316	0.0267132	0.001541294
30.064436	0.002646393	0.034552875	0.001902249
		0.044136186	0.002315316
		0.052247193	0.002646393
Tension behavior		Tension damage	
σ_t	ε_c	d_t	ε_c
3.527534999	0	0	0
2.552410205	0.000436538	0.005849075	9.70639E-06
1.875005329	0.001255177	0.25280156	0.000436538
1.418518719	0.002467738	0.605725295	0.001255177

1.115917256	0.004076065	0.860570738	0.002467738
0.91487749	0.006081596	0.966728966	0.004076065
0.777530331	0.008485376	0.989999454	0.006081596
0.771828683	0.010905533		
0.67811416	0.011288111		
0.600115672	0.014490257		
0.533625842	0.018092087		
0.473182675	0.02209375		
0.416144115	0.02649532		
0.361532658	0.031296822		
0.309258398	0.036498261		
0.259625557	0.042099626		
0.21304016	0.048100908		
0.169853472	0.054502097		
0.130292382	0.061303185		
0.094442047	0.068504172		
0.062257202	0.076105057		
0.033586878	0.084105846		
0.008203187	0.092506545		

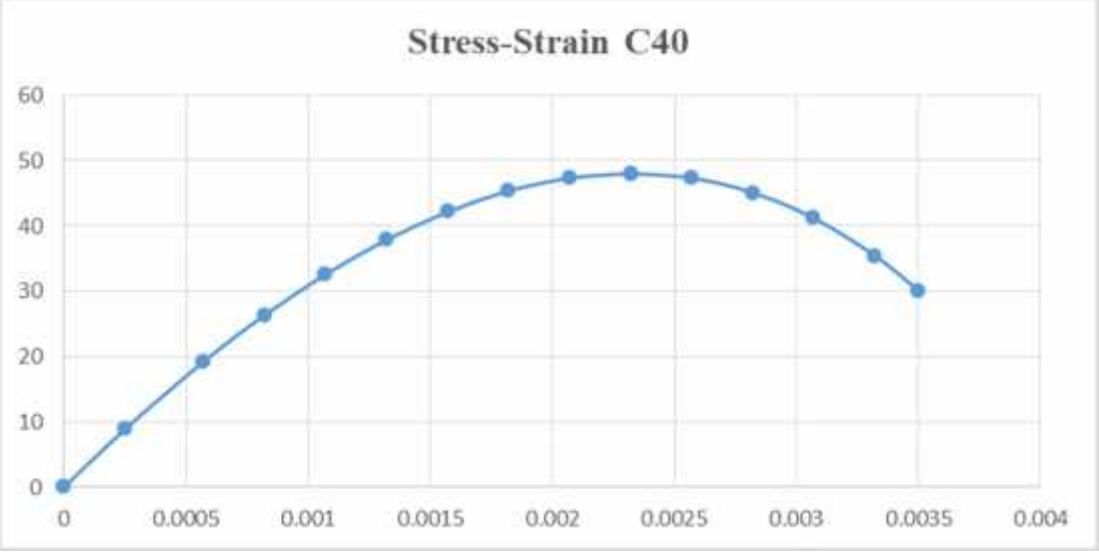

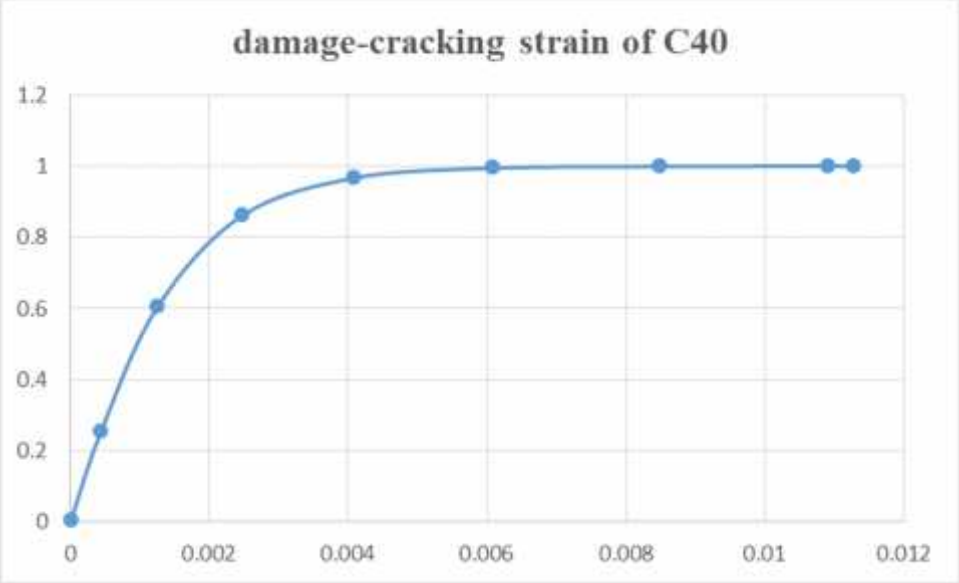

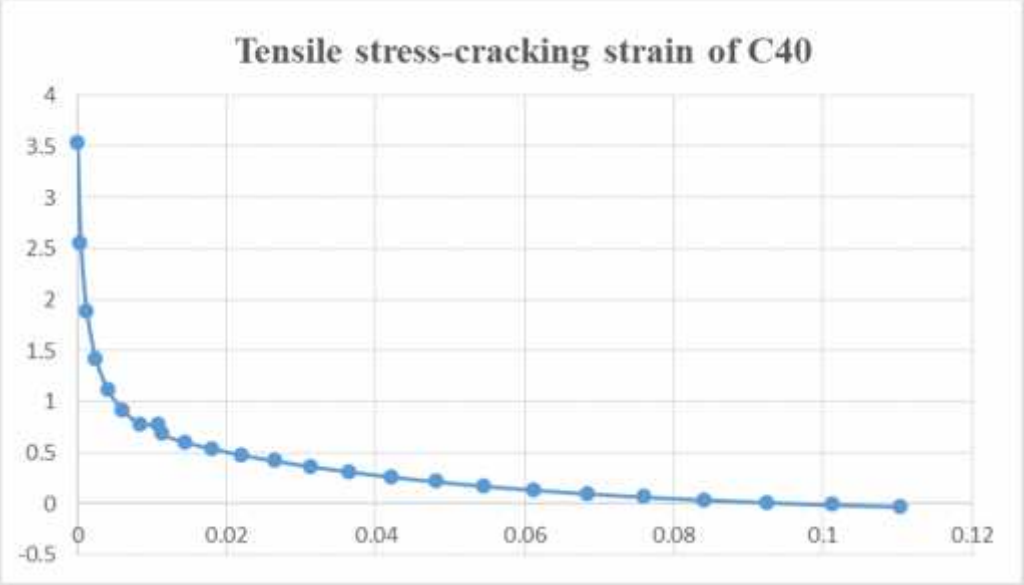

Table C5: Compression and tension behavior of concrete damage plasticity of C60

Fck= 60MPa, Fcm = 68MPa, Ecm=39.09987GPa			
Compression behavior		Compression damage	
27.2	0	0	0
48.02725	0.000129	0.00011	6.55E-06
54.57521	0.000211	0.000192	1.14E-05
60.08118	0.00032	0.002243	0.000129
64.34064	0.000461	0.003763	0.000211
67.09187	0.000641	0.005867	0.00032
67.99429	0.00085	0.008741	0.000461

68	0.000868	0.012643	0.000641
66.5965	0.001154	0.017508	0.00085
62.28708	0.001514	0.017941	0.000868
54.21685	0.00197	0.025158	0.001154
47.46291	0.002286	0.035054	0.001514
41.1709	0.002554	0.048732	0.00197
21.34783	0.003311	0.058854	0.002286
		0.067821	0.002554
		0.094755	0.003311
Tension behavior		Tension damage	
4.622378	0	0	0
3.108915	0.000442	0.004	5.39E-06
2.150677	0.001266	0.309542	0.000442
1.567338	0.00248	0.693876	0.001266
1.215631	0.004089	0.916885	0.00248
0.996261	0.006094	0.985931	0.004089
0.846835	0.008498	0.998485	0.006094
0.84047	0.010918		
0.731548	0.011301		
0.631903	0.014503		
0.539712	0.018105		
0.452347	0.022108		
0.369781	0.02651		
0.29289	0.031311		
0.222592	0.036513		
0.159479	0.042115		
0.103721	0.048116		
0.055114	0.054517		
0.013179	0.061318		

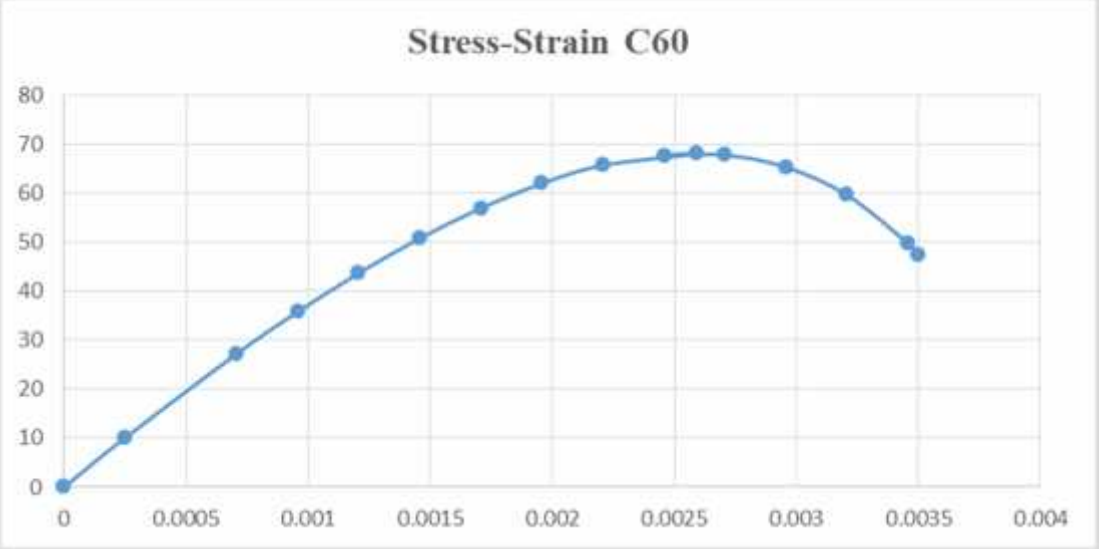
Stress-Strain C60
80
70
60
50
40
30
20
10
0
0
0.0005
0.001
0.0015
0.002
0.0025
0.003
0.0035
0.004

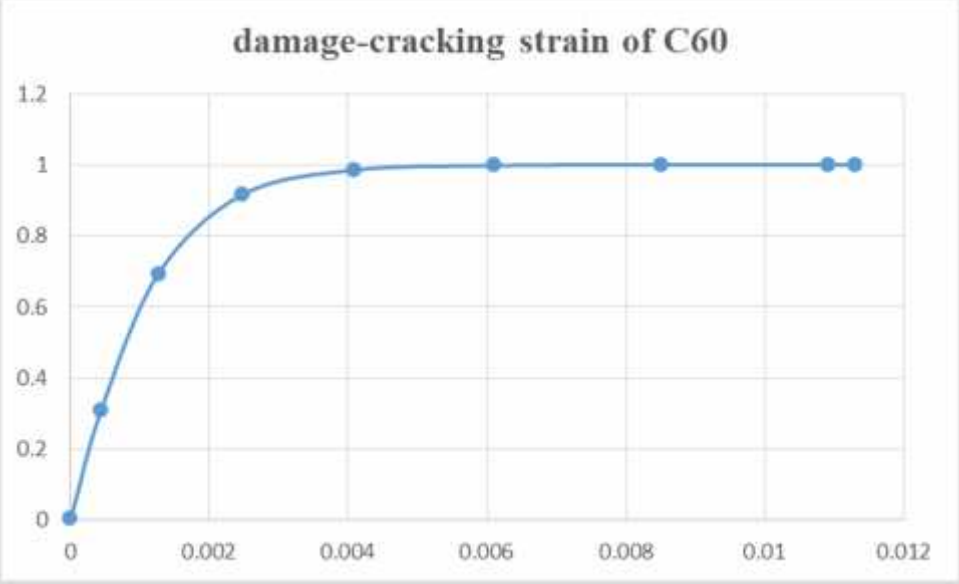
damage-cracking strain of C60
1.2
1
0.8
0.6
0.4
0.2
0
0
0.002
0.004
0.006
0.008
0.01
0.012

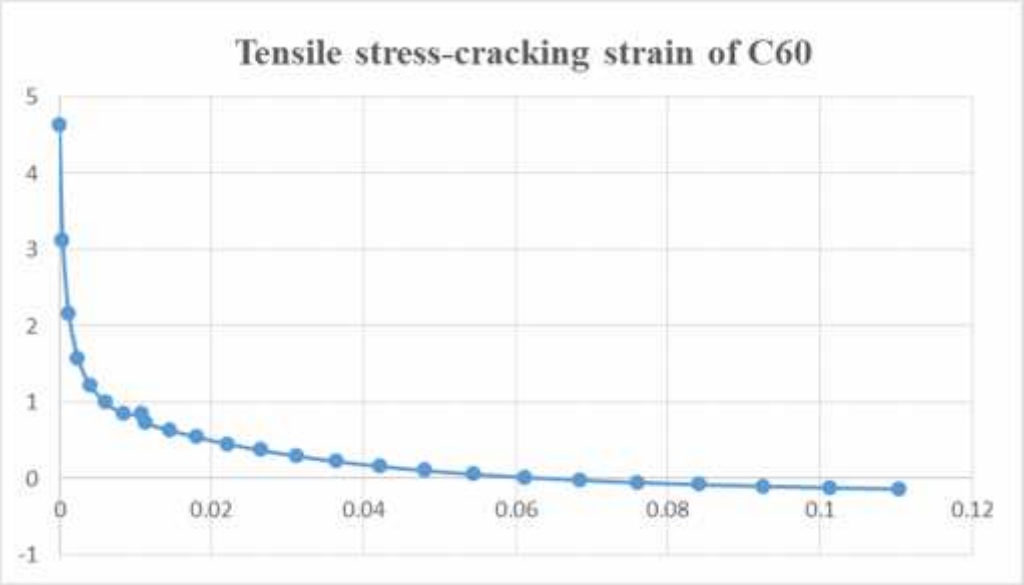
Tensile stress-cracking strain of C60
5
4
3
2
1
0
-1
0
0.02
0.04
0.06
0.08
0.1
0.12

Appendix D: Load vs displacement response

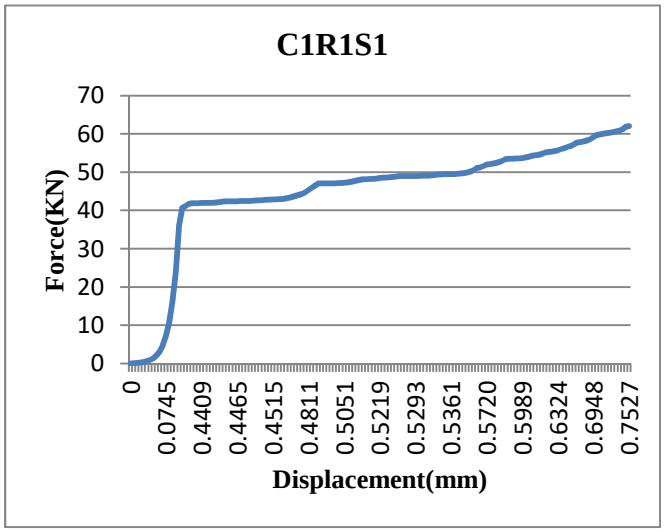

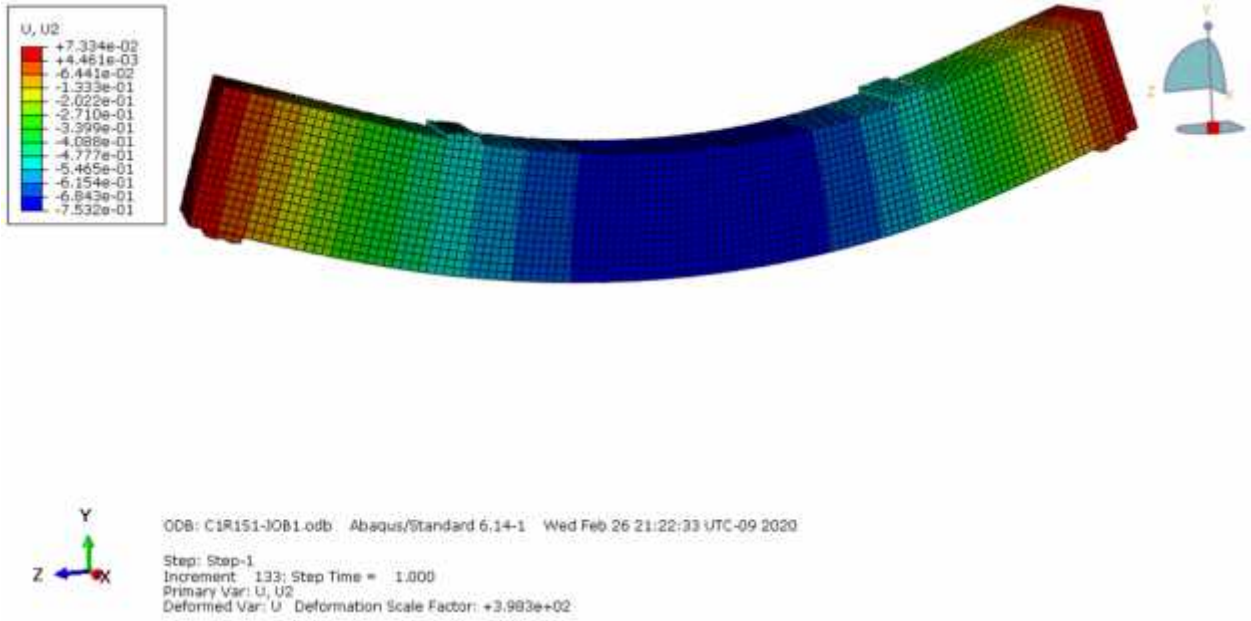

Figure D.1 Load vs displacement and deflection of C1R1S1

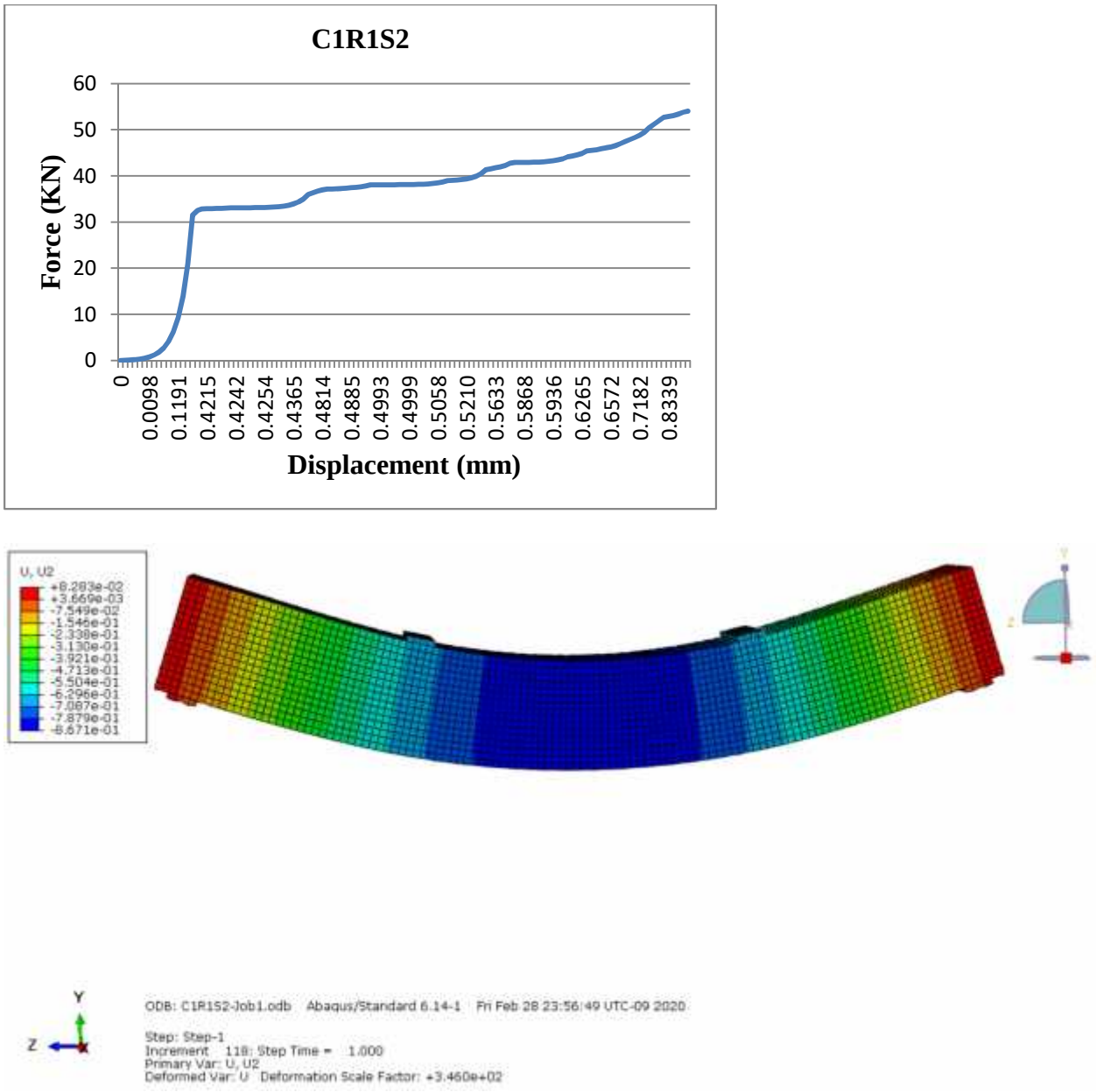

Figure D.2 Load vs displacement curve and deflection of C1R1S2

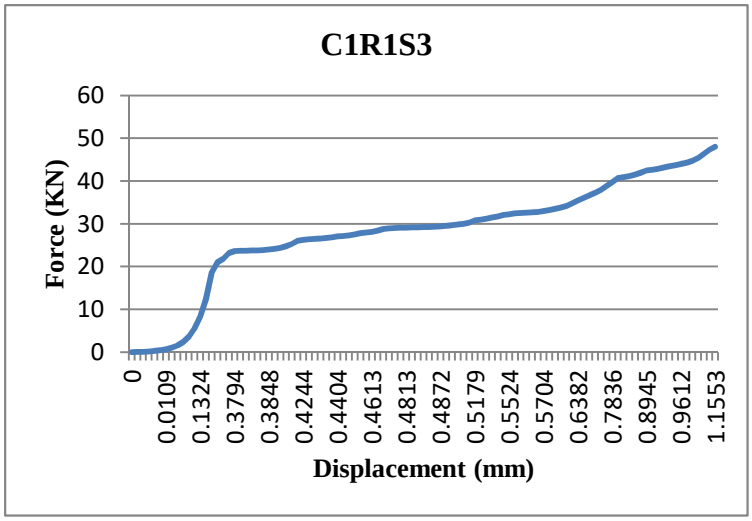

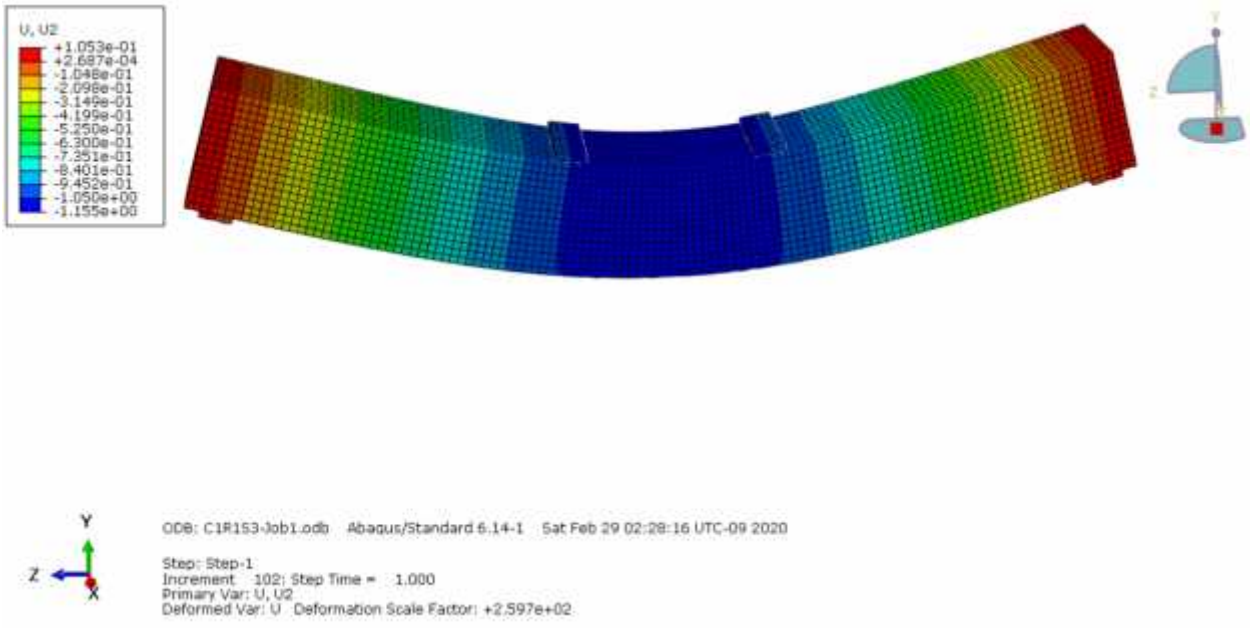

Figure D.3 Load vs displacement and deflection of C1R1S3

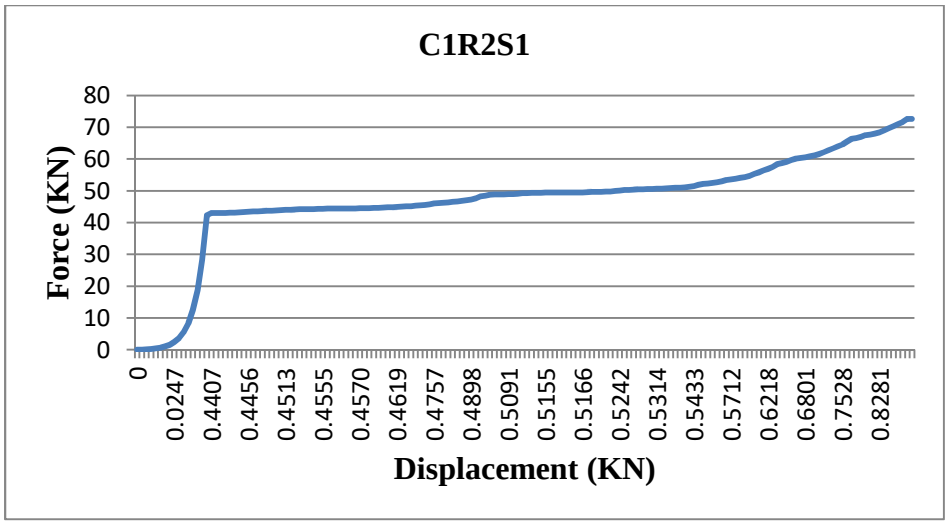

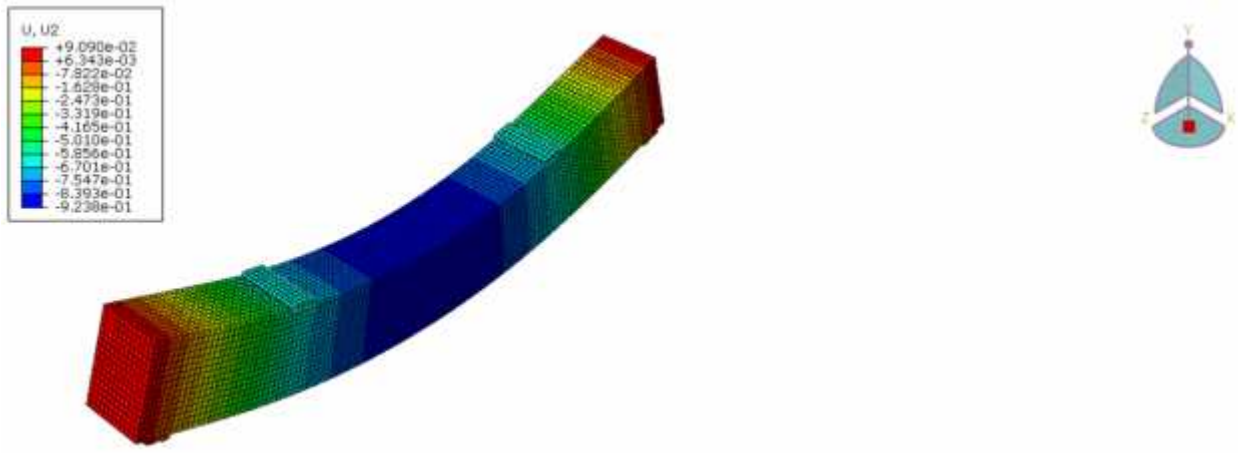

Figure D.4 Load vs displacement and deflection of C1R2S1

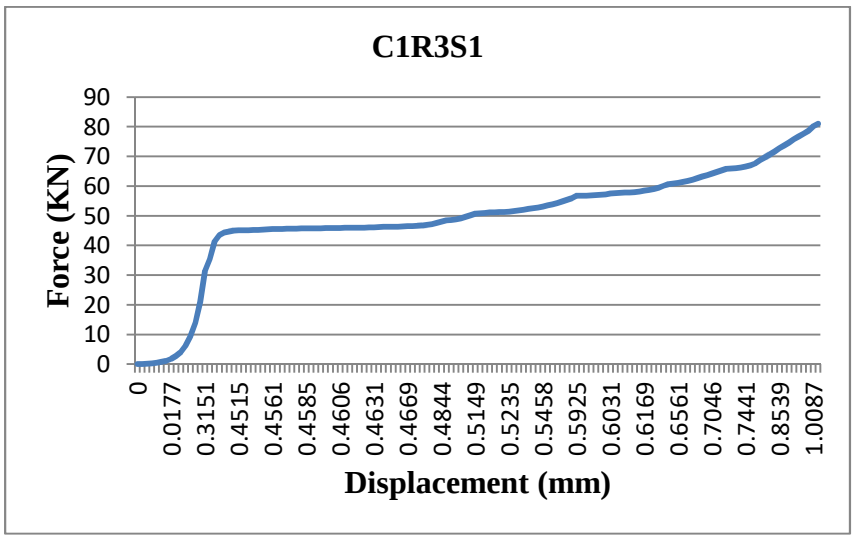

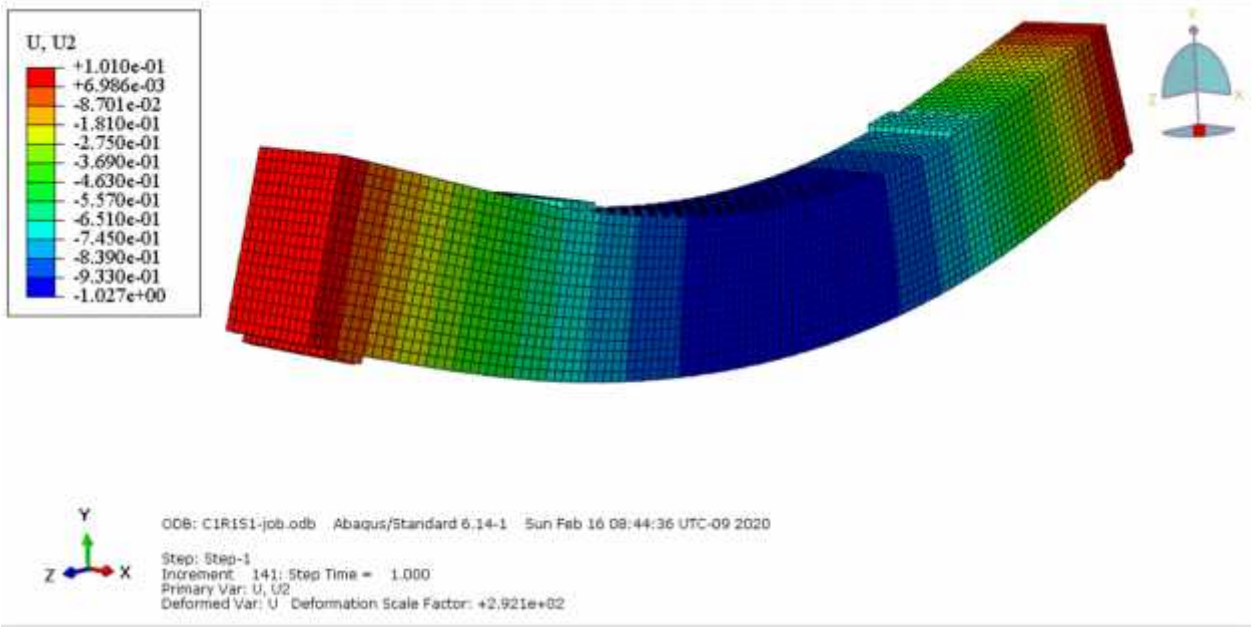

Figure D.5 Load vs displacement and deflection of C1R3S1

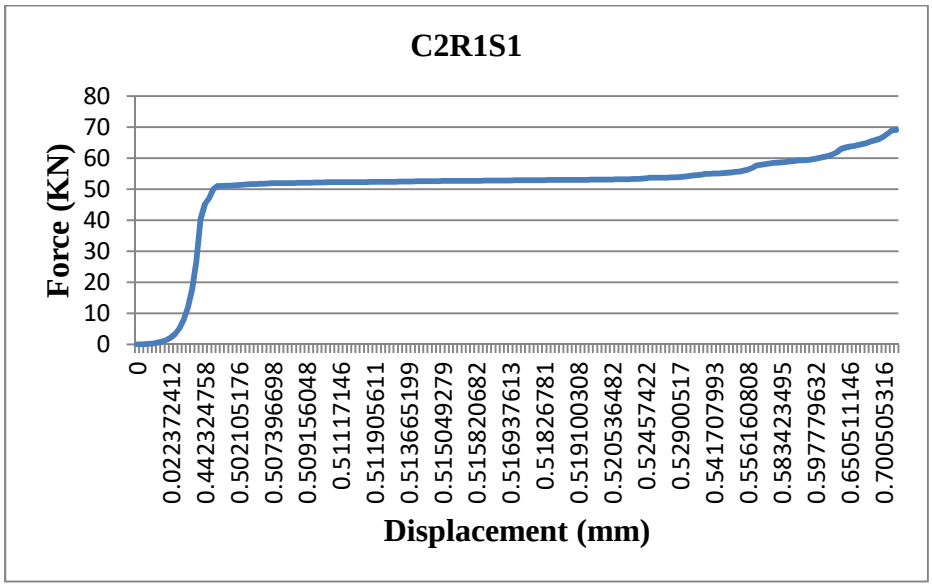

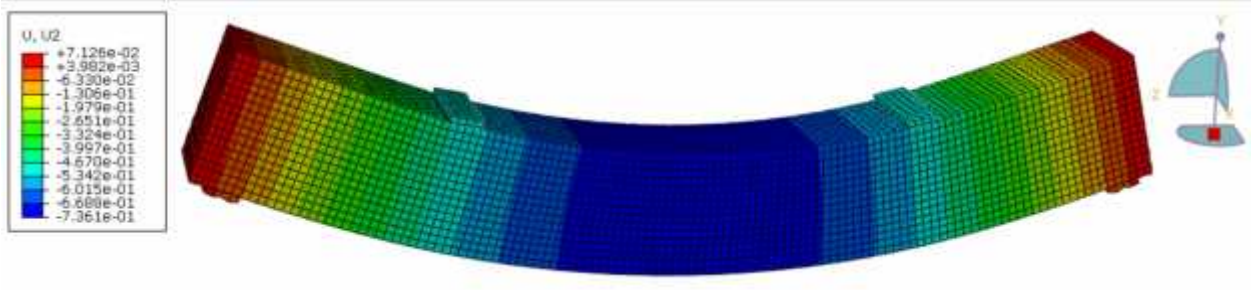

Figure D.6 Load vs displacement and deflection of C2R1S1

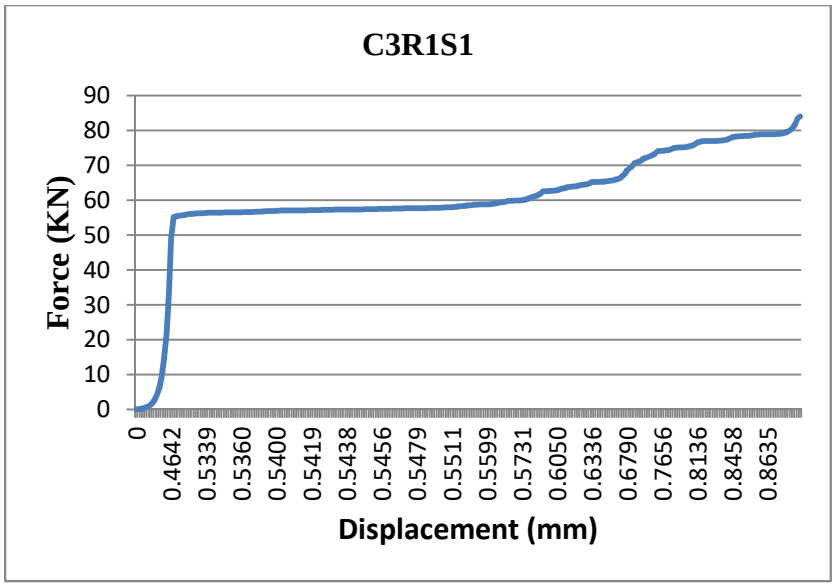

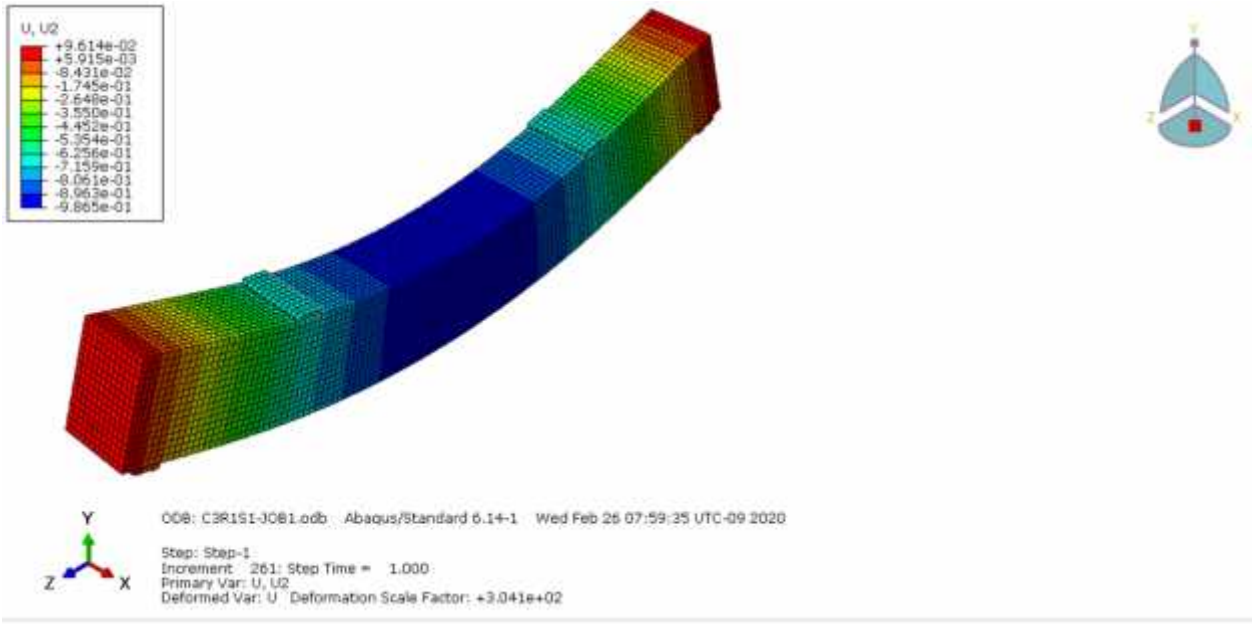

Figure D.7 Load vs displacement curve and deflection of C3R1S1

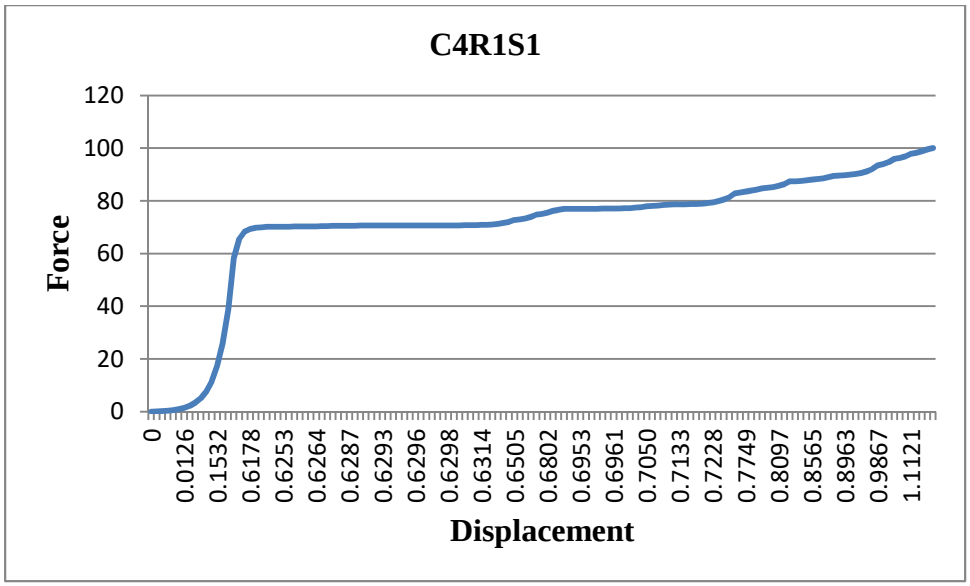

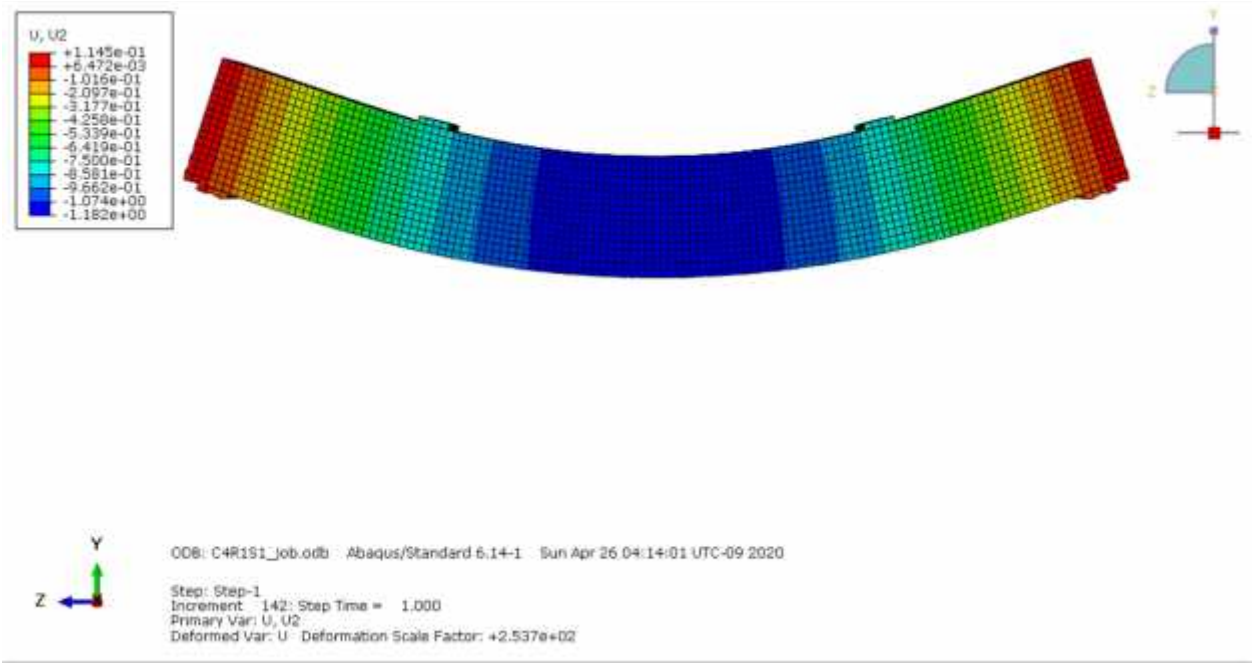

Figure D.8 Load vs displacement curve and deflection of C4R1S1

Appendix E: Crack Pattern

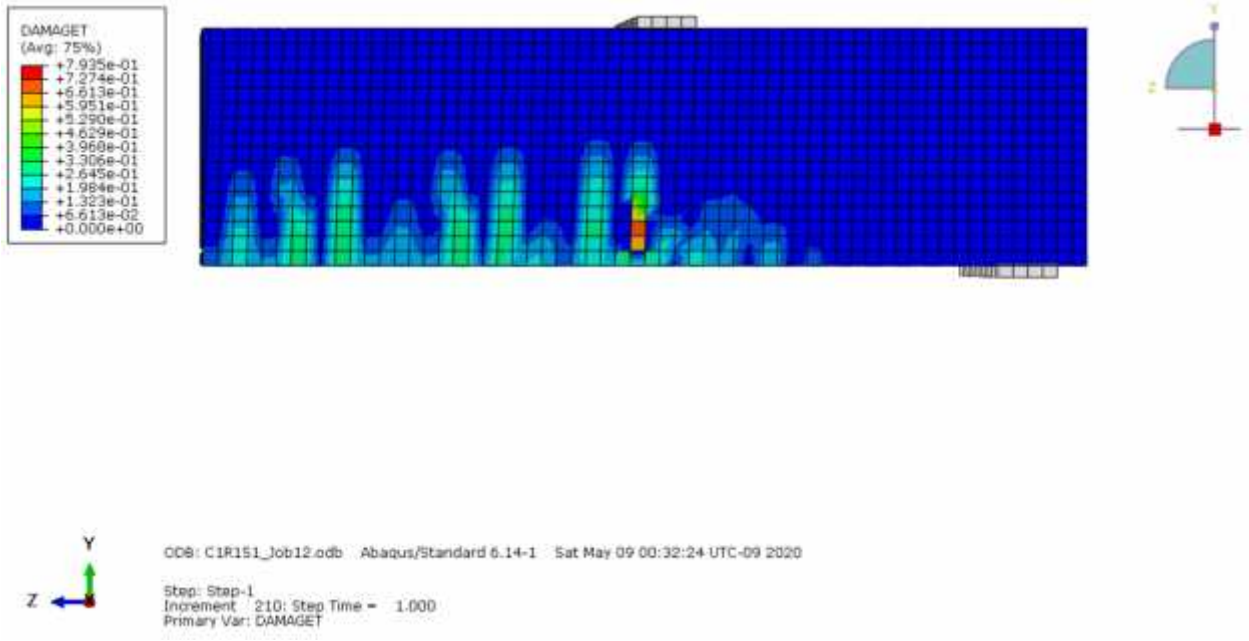

Figure E.1 Crack pattern of C1R1S1

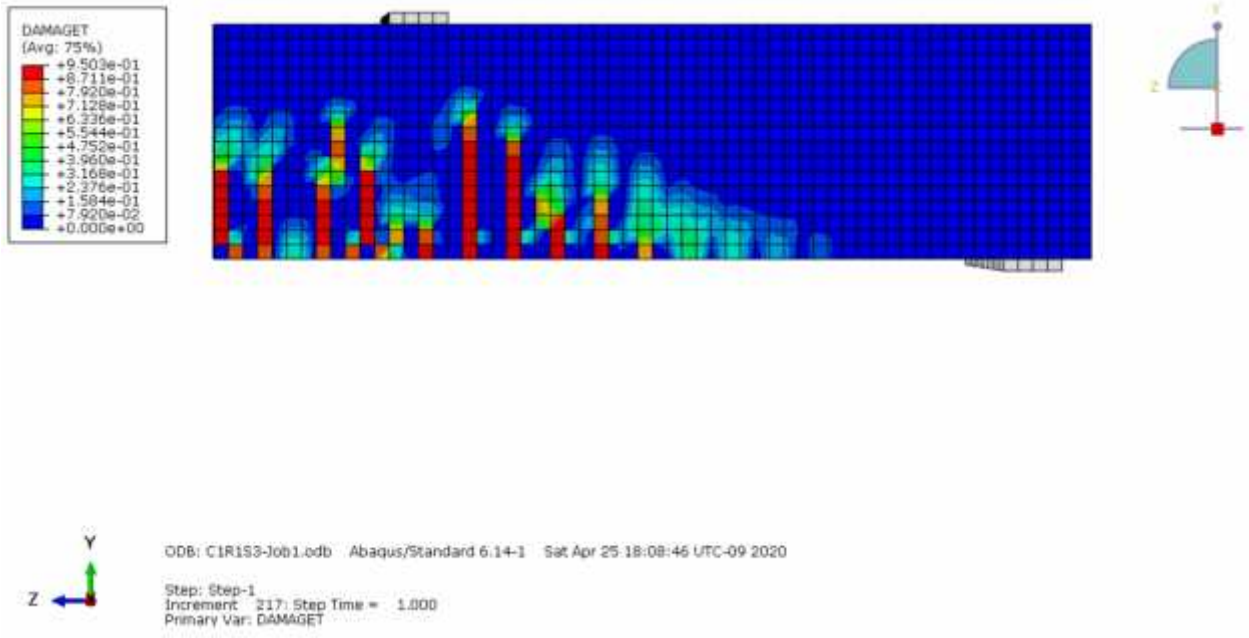

Figure E.2 Crack Pattern of C1R1S3

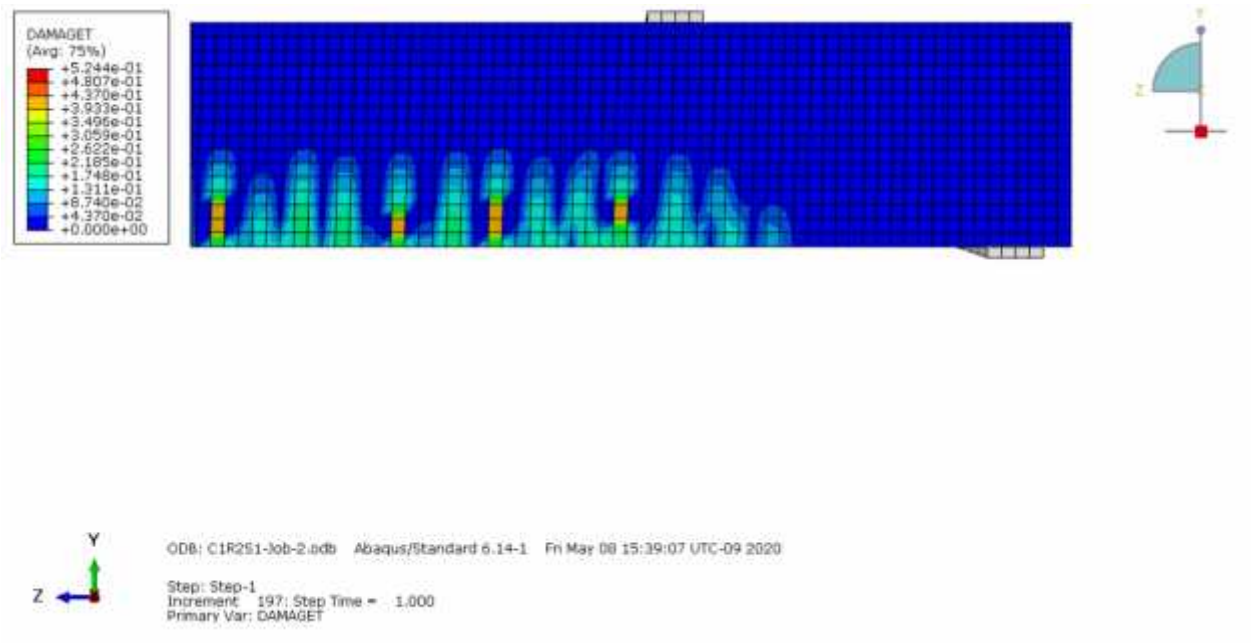

Figure E.3 Crack pattern of C1R2S1

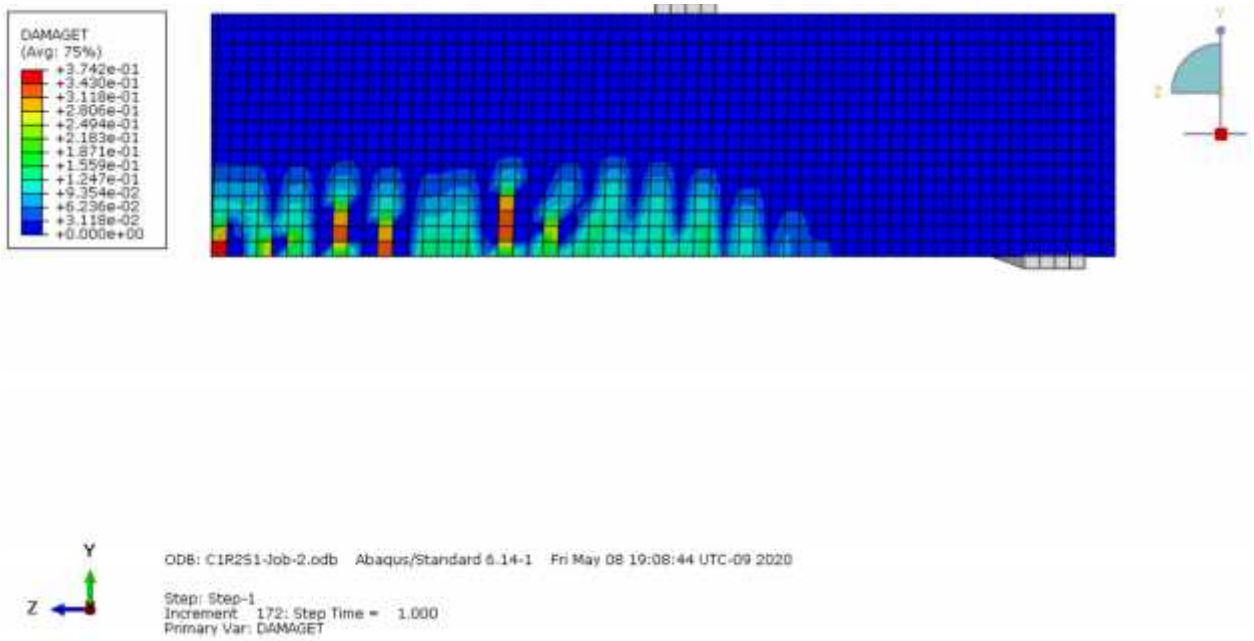

Figure E.4 crack pattern of C1R3S1

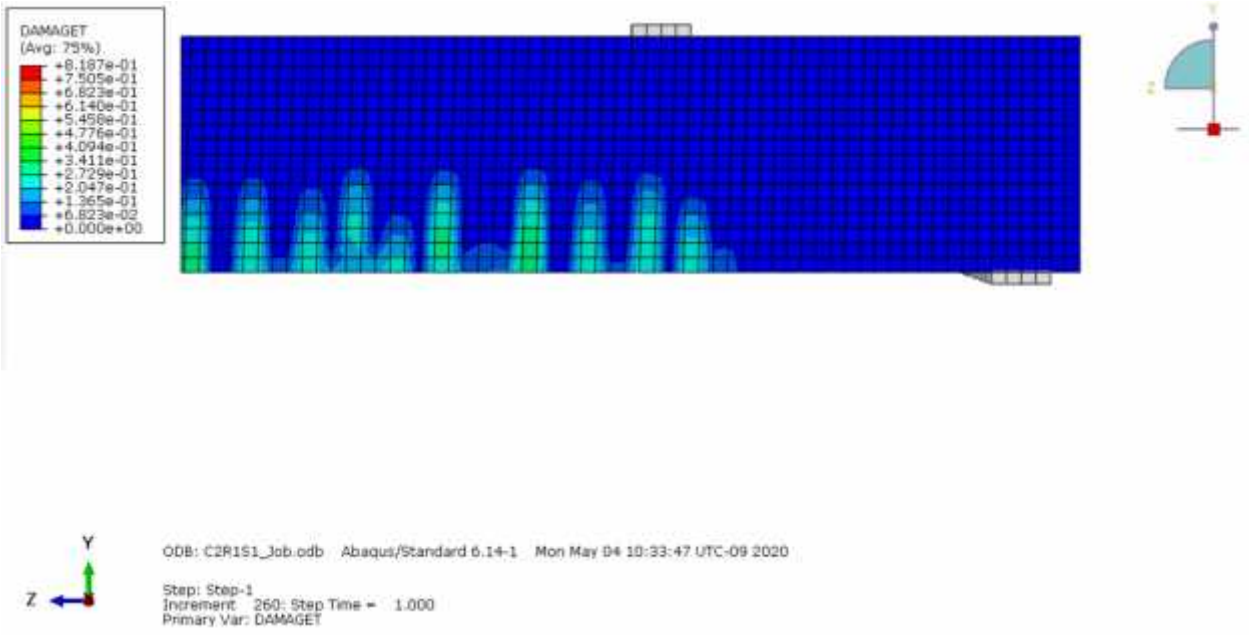

Figure E.5 Crack pattern of C2R1S1

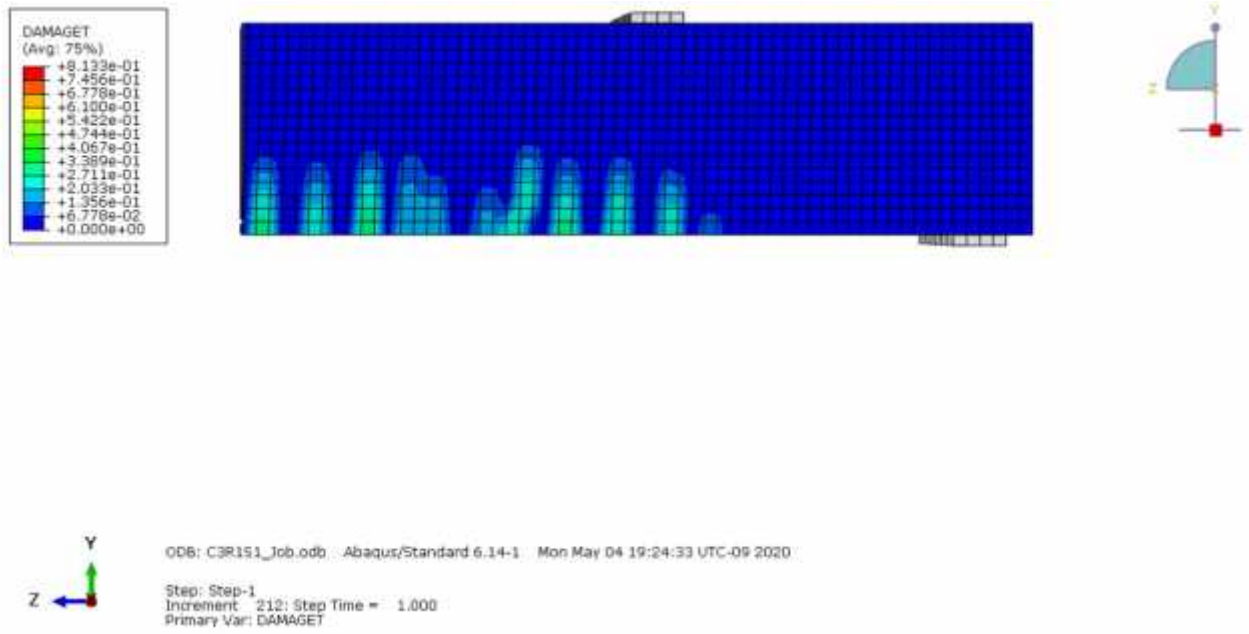

Figure E.6 crack pattern of C3R1S1

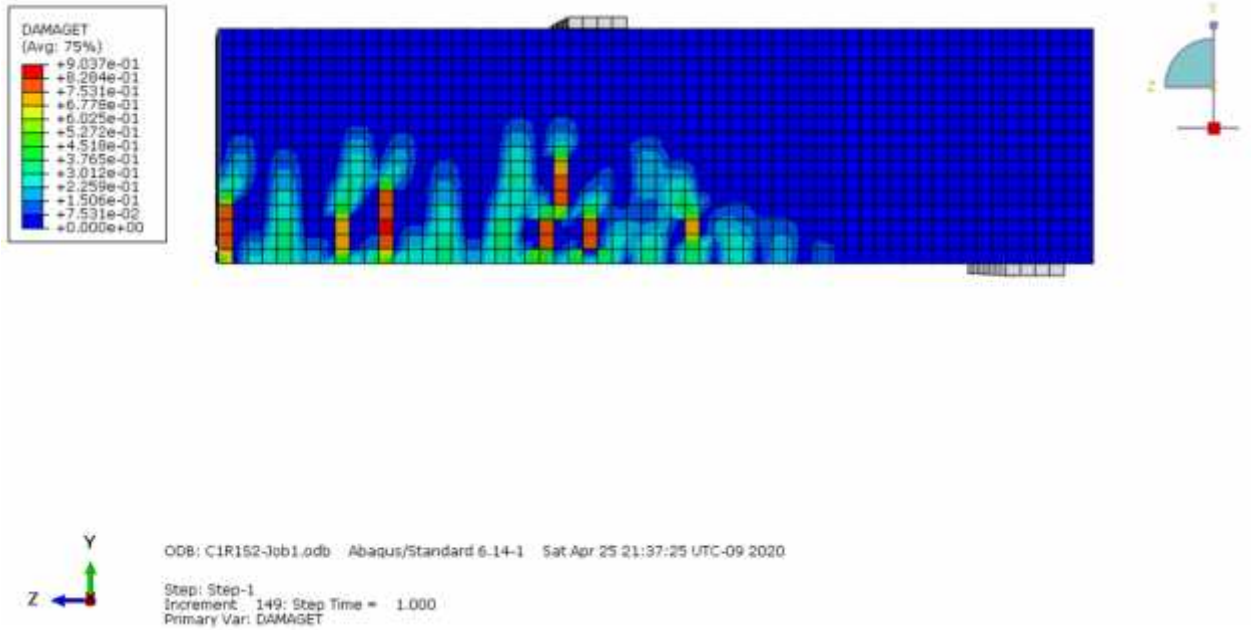

Figure E.7 crack pattern of C1R1S2

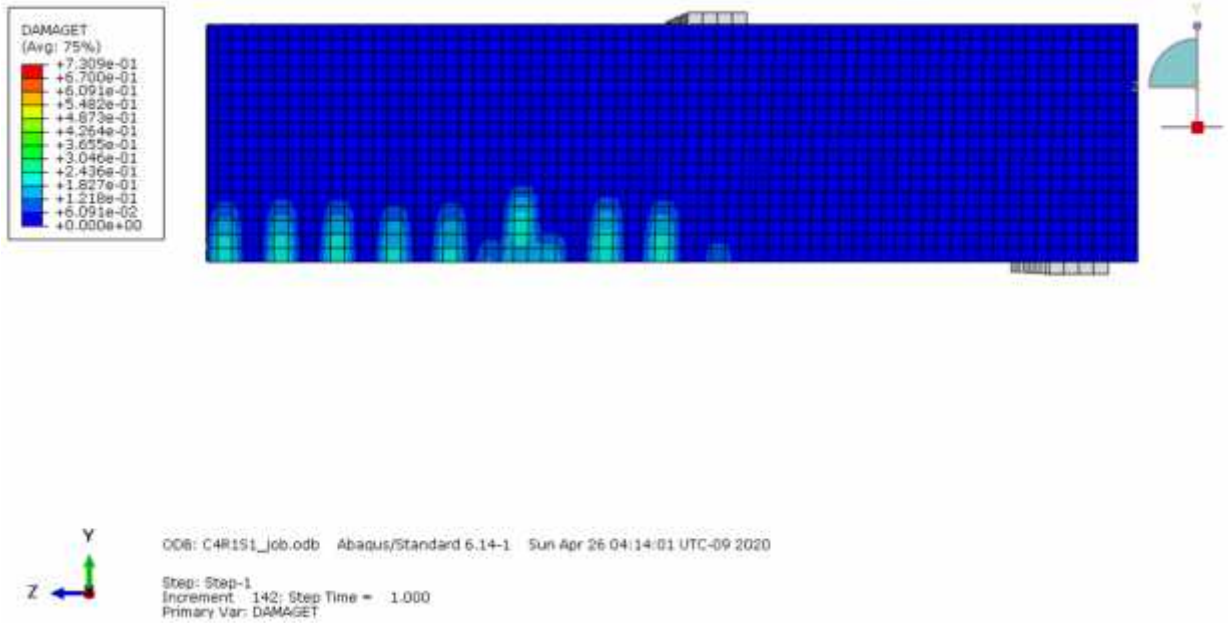

Figure E.8 Crack pattern of C4R1S1